Cable-supported bridges

(Hänge-, Spannband- und Schrägseilbrücken)

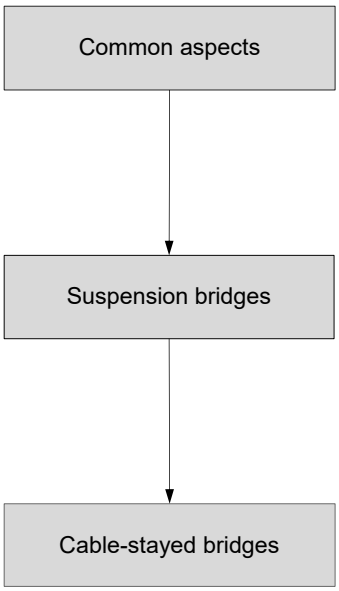

Typologies

Historical Perspective

Cable types

Static analysis of cables

Dynamic effects

Cable-supported bridges

Common aspects – Typologies

Cable-supported bridges – Common aspects: Typologies

- The typology of cable-supported bridges is related to the configuration of cable system and the deck girder which, in turn, determine the loading of the cables.
- Accordingly, the following basic types of cable-supported bridges can be distinguished:
  - → Suspension bridge: Sagging main cables (f/l = 1/9…1/11) spanning between towers / pylons. Main cables loaded laterally by hangers connecting the suspended deck girder to the main cables.
  - → Suspended bridge / Stress-ribbon: Slightly sagging main cables, spanning between abutments without towers. Cables loaded laterally by the deck girder. The deck follows the cable profile in elevation. ("stress ribbon" commonly used for suspended bridges with prestressed concrete deck)
  - → Cable-stayed bridge: Virtually straight cables connecting the deck girder to one or more pylons / towers. Cables loaded axially (primarily).
  - → Stayed suspension bridge: A "hybrid" combination of suspension bridge and cable-stayed bridge.

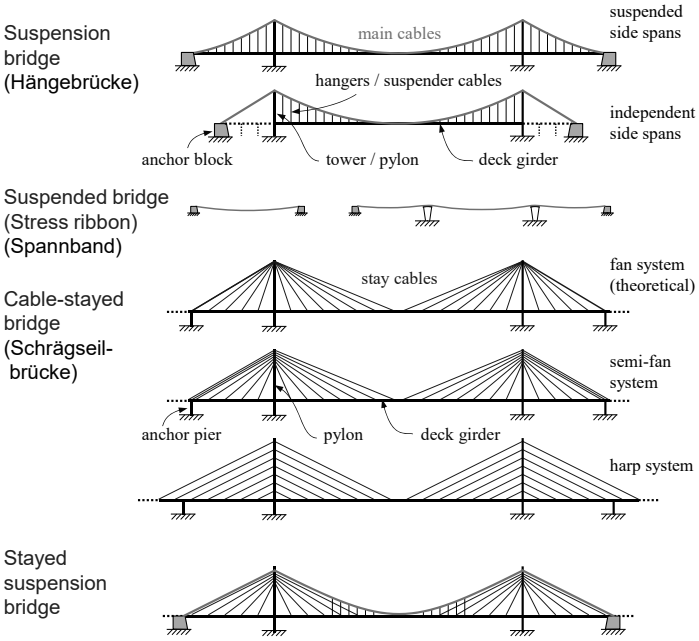

Note that the stayed suspension bridge illustrated schematically shows a modern cable configuration, such as used in the Third Bosporus Crossing (Sultan Yavuz Bridge)) Older stayed suspension bridges (as designed by J. Roebling) used hangers over the entire suspended span, combined with stays.

Cable-supported bridges

Common aspects – Historical perspective

Cable-supported bridges – Common aspects: Historical perspective

Similar to arches, suspension bridges have been built for centuries (some sources see notes):

- More than 2 millennia ago (ca. 65 n.Chr.), the first iron chain footbridge is said to have been built in Yunnan, China.
- The Incas are said to have built grass rope suspension footbridges since the 12th century, with a network of ca. 200 bridges around 1600. These bridges required regular maintenance and replacement of the ropes every 1-3 years (top photo).
- A Twärrenbrücke (“Querbrücke” = footpath along a canyon wall, suspended by means of chains) is known to have been part of the Gotthard route around 1218.
- In 1616, Faustus Verantius in a publication included a project – or rather, a vision – for a chain-supported bridge (bottom illustration).

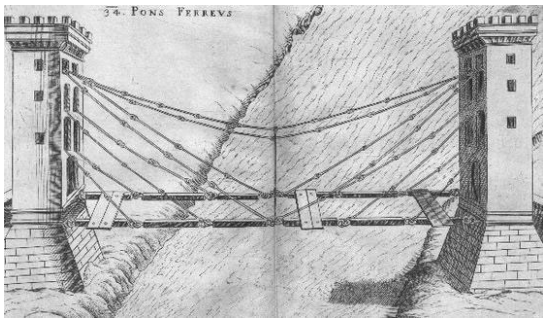

Top: Q’eswachaka bridge, Apurimac river, Peru (origins ca. 1500, renewed yearly). Grass rope suspension footbridge, span ca. 45 m. Unesco World Heritage since 2013. Photo © J. Heimsath, National Geographic

Bottom: Iron bridge project, F. Verantius, 1616 © Deutsches Museum

Sources:

- Tom F. Peters (ed.). Die Entwicklung des Grossbrückenbaus. ETH Zürich, 1979
- https://www.nationalgeographic.com/travel/destinations/south-america/peru/inca-grass-rope-bridge-qeswachaka-unesco/

Cable-supported bridges – Common aspects: Historical perspective

(continued, some sources see notes)

- Thangtong Gyalpo, a Buddhist yogi known as Chakzampa (the Bridge Builder), built 58 iron chain suspension bridges throughout the Himalayan region, with spans up to 100 m, in the 15th century (top illustrations).
- James Finley built suspension bridges in the U.S., using similar chains as T. Gyalpo, already in 1796 (bottom illustrations).
- While stone arches are virtually imperishable unless their foundations are destroyed (e.g. by floods), suspension elements are much less durable and hence, hardly any of these early cable-supported bridges have survived.
- In the following, merely some milestones in the development of suspension bridges are highlighted. For a more complete overview, refer to literature.

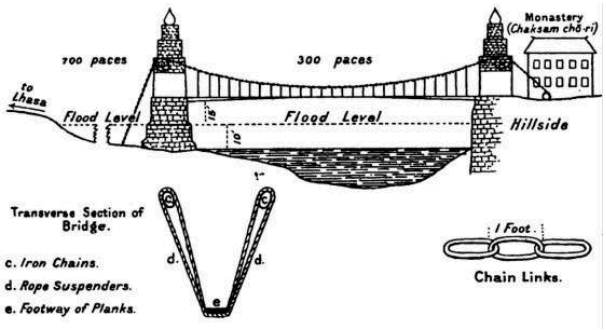

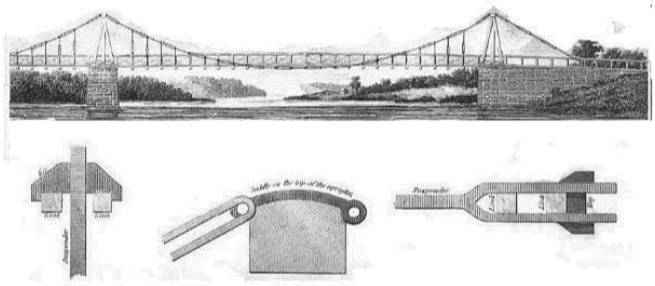

Top : Diagram of one of the earliest known suspension bridges in the world, built in 1430, at Chushul, south of Lhasa in Tibet. The sketch was taken by an Indian spy working for the Survey of India in 1878, and published by Waddell in 1905. The Chushul Chakzam ("iron bridge“) designed by Thangtong Gyalpo was a suspension footbridge, span 140 m, deck width 0.30 m, 4.5 m above river.

Bottom: Probably the Chain Bridge at Falls of Schuylkill, James Finley (1801). Chain suspension bridge, span ca. 60 m. Illustration © *The Port Folio* vol. 3, no. 6 (Philadelphia: Bradford & Inskeep, June 1810), p. 441.

Sources:

- L. Austine Waddell. Lhasa and Its Mysteries. With a Record of the Expedition of 1903-1904. E.P. Dutton, New York, 1905. Charles Stewart Drewry: A Memoir on Suspension Bridges. Longman, Rees, Orme, Brown, Green & Longman, 1832.
- Tom F. Peters (ed.). Die Entwicklung des Grossbrückenbaus. ETH Zürich, 1979.

Cable-supported bridges – Common aspects: Historical perspective

- The Passerelle Saint Antoine in Geneva (1823-1850, spans 33+23 m), designed by Guillaume-Henri Dufour (based on a proposal by Marc Séguin) was the first permanent wire cable suspension bridge, see illustration at right.
- G. H. Dufour General of Swiss Army in 1847 / 1849 / 1856 / 1859) realised two further wire-cable suspension bridges in Geneva (Pont des Pâquis 1827-…., Pont des Bergues 1834-1881) and designed several others bridges.
- Marc Séguin and his brothers designed and built several further suspension bridges, e.g. the Pont de Tournon (1825, main spans 2x89 m) and the Pont d'Andance (1827, spans 2x90, oldest suspension bridge still in use in continental Europe, see photos).

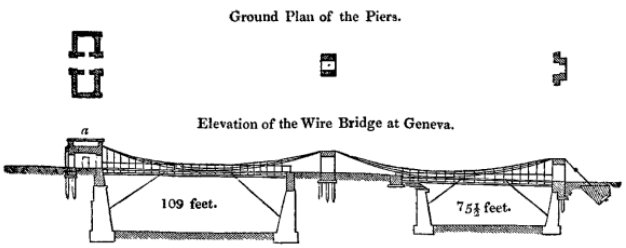

Illustration: Pont Saint Antoine, Genève, Guillaume-Henri Dufour (1823). Wire-cable suspension bridge, spans 33+23 m, width 2 m. © Charles Stewart Drewry: A Memoir on Suspension Bridges. Longman, Rees, Orme, Brown, Green & Longman, 1832.

Photos: Pont d'Andance, Andance-Andancette, Séguin brothers (1927). Wire-cable suspension bridge, spans 2 x 90.4 m, no backstay cables. © https://en.ardeche-guide.com/pont-marc-seguin-502885 .

Cable-supported bridges – Common aspects: Historical perspective

- The chain-stayed Saalebrücke in Nienburg (l = 80 m, Christian Gottfried Heinrich Bandhauer, 1825, top figure) was a precursor of cable-stayed bridges, though not very successful.
- The bridge collapsed on the 6.12.1825, only four months after inauguration, due to overload, faulty chains and / or oscillations caused by singing public during the celebration of St. Nikolaus. 55 people died.
- Bandhauer's design was very innovative, despite that he probably knew Claude Louis Marie Henri Navier's "Mémoire sur les ponts suspendus" (published 1823), where similar schemes were depicted (bottom figure; Navier's project for a suspension bridge over the Seine in Paris, the Pont des Invalides with 170 m span, also part of this publication, was never finished).
- A further highlight was the bascule opening at midspan, allowing large ship masts to pass.

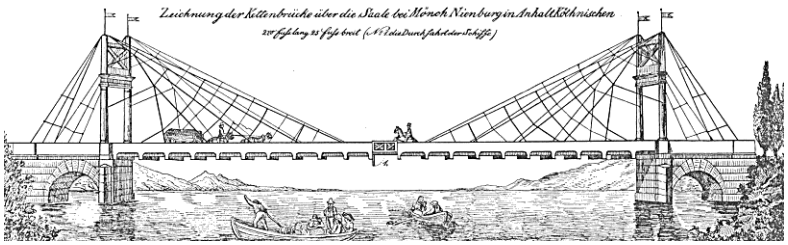

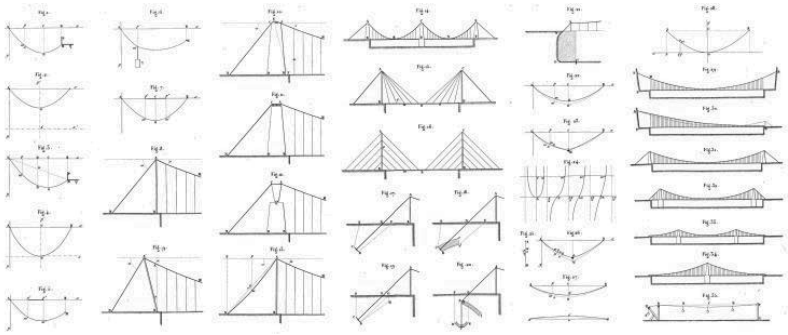

Top: Saalebrücke in Nienburg, Christian Gottfried Heinrich Bandhauer (1825). Chain-stayed bridge, span ca. 80 m. © Museum Schloss Bernburg.

Bottom: Claude Louis Marie Henri Navier, Rapport à Monsieur Becquey et Mémoire sur les ponts suspendus, 1823 (https://doi.org/10.3931/e-rara-45062).

Cable-supported bridges – Common aspects: Historical perspective

- The Menai Strait suspension bridge (1826, span 176 m), designed by Thomas Telford, is commonly recognised as the first major suspension bridge (photo).
- Earlier plans included straight backstays and a different tower design (bottom drawings).
- Telford opted for chains rather than wire cables, because he was more familiar with this type of structural element. While chains were used in several early suspension bridges (particularly in the UK), the more economical wires soon became the standard.
- The bridge initially had a lightweight timber deck, which was merely 7.4 m wide, without stiffening girders or trusses. It was highly unstable in the wind and seriously damaged in 1839.
- The deck was strengthened in 1840 and in 1893, a steel deck was installed. Major repairs were also carried out in 1999.

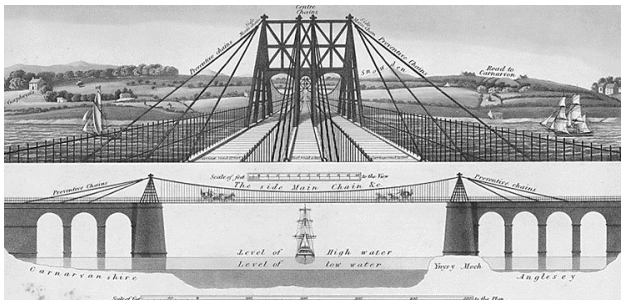

Menai Suspension Bridge, Menai Strait, Bangor, UK, Thomas Telford (1826). Wrought iron chain suspension bridge, main span 176 m, width 7.3 m.

Illustrations: Top letstourengland.com, bottom The National Library of Wales.

Cable-supported bridges – Common aspects: Historical perspective

- Suspension bridge chains were commonly eyebar chains, usually with direct connection by pins.
- The Menai suspension bridge originally had cast iron chains with indirect connection (bottom left photo). These were replaced by steel chains with direct connection in 1939.

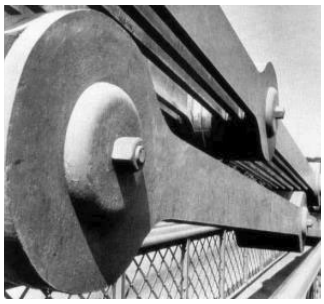

Menai Suspension Bridge, Menai Strait, Bangor, UK, Thomas Telford (1826). Wrought iron chain suspension bridge, main span 176 m, width 7.3 m.

Top Photo © Bencherlite, Wikimedia commons.

Bottom photos © Leonardo Fernández Troyano. Bridge Engineering – A Global Perspective. Thomas Telford, 2003 (originally published in Spanish: Tierra sobre el agua, 1999).

Cable-supported bridges – Common aspects: Historical perspective

- The Clifton suspension bridge (1863, span 214 m), designed by Isambard Kingdom Brunel, also used eyebar chains.
- Other relevant bridges were built before (see next slide). The Clifton bridge is mentioned here, right after the Menai straits bridge, because of the chains, and also because it should have been finished much before its opening in 1864 (see notes).
- Other than the Menai straits bridge, there are no hangers in the side spans in the Clifton bridge.

Clifton Suspension Bridge, Avon river, Bristol UK, Isambard Kingdom Brunel, revised by W. H. Barlow and J. Hawkshaw (1864). Wrought iron chain suspension bridge, main span 214 m.

Construction based on Brunel's drawings started in 1836 but was interrupted in 1843 after building the towers due to lack of funds. It only restarted in 1862, using the chains of Brunel's Hungerford Bridge across the Thames in London, that was replaced in 1860.

Cable-supported bridges – Common aspects: Historical perspective

- The Grand Pont Suspendu in Fribourg (1834, span 273 m, world record until 1849), designed by Joseph Chaley, was the longest suspension bridge worldwide for many years.
- Inspired by the bridges designed by the Séguin brothers, wires cables were used.
- Each of the four main cables was composed of more than 1000 wires, grouped in 20 strands.

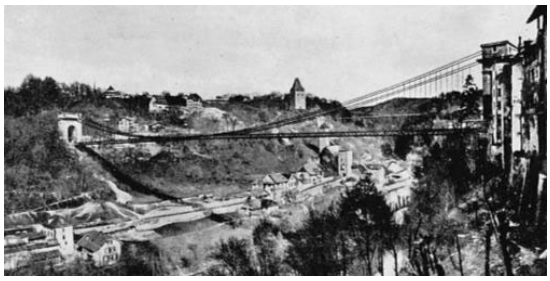

Grand Grand Pont Suspendu across the Sarine, Fribourg, Joseph Chaley (1834, replaced 1926). Suspension bridge, 4 main cables consisting of 1056 wires “No. 18”. main span 273 m, 54 m above river. Record span until 1849 (Wheeling Bridge).

Top photo © J. Brunner. Beitrag zur geschichtlichen Entwicklung des Brückenbaus in der Schweiz. Dissertation, Bern, 1924

Bottom photo © La Liberté

Cable-supported bridges – Common aspects: Historical perspective

- The Grand Pont Suspendu in Fribourg (1834, span 273 m, world record until 1849), designed by Joseph Chaley, was the longest suspension bridge worldwide for many years.
- Inspired by the bridges designed by the Séguin brothers, wires cables were used.
- Each of the four main cables was composed of more than 1000 wires, grouped in 20 strands.

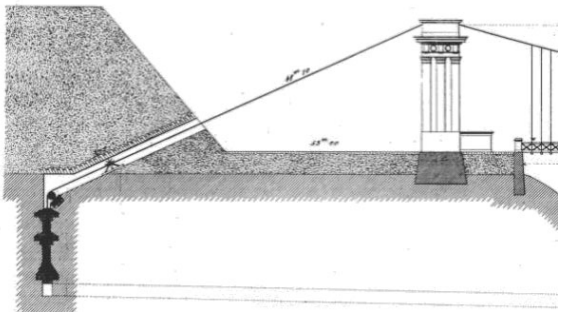

Grand Grand Pont Suspendu across the Sarine, Fribourg, Joseph Chaley (1834, replaced 1926). Suspension bridge, 4 main cables consisting of 1056 wires “No. 18”. main span 273 m, 54 m above river. Record span until 1849 (Wheeling Bridge).

Photo © https://grandfribourg.ch/

Illustration © structurae.net

Cable-supported bridges – Common aspects: Historical perspective

- Joseph Chaley also designed the Pont du Gottéron in Fribourg (1842, 151 span with only one tower)
- This bridge had a shorter span, but only one tower.
- The bridge was severely damaged in a storm in 1895 and had to be strengthened.
- It became famous in 1919 when a truck damaged the deck and fell from the bridge (bottom right photo).

Pont du Gottéron, across Gottéron and Sarine, Fribourg, Joseph Chaley (1842, replaced 1960). Suspension bridge, main span 151 m, width 4.8 m, height 76 m above river. Only one tower, cables anchored in rock.

After the bridge had already been almost destroyed in a storm in 1895, it was renovated and strengthened with two additional cables. An overloaded truck destroyed the deck in 1919, falling off the bridge. Again, the bridge deck was repaired, and the bridge remained in use until 1960.

Photo: Peter & Jeanne Schaller.

Cable-supported bridges – Common aspects: Historical perspective

- The Wheeling suspension bridge (1849, span 308 m, record until 1866), designed by Charles Ellet Jr., is the oldest suspension bridge still serving vehicle traffic.
- However, it had to be reconstructed after collapsing in 1854 due to wind-induced oscillations apparently similar to the Tacoma Narrows Bridge (see behind).
- In 1886, under guidance of J. Roebling, stays similar to the Brooklyn Bridge (see behind) were installed. Further strengthening was provided in 1922 and 1930.

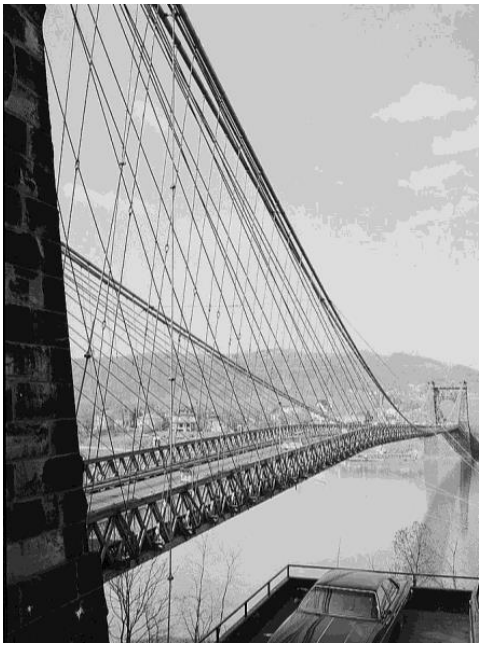

Wheeling suspension bridge across Ohio river, Wheeling, West Virginia, Charles Ellet Jr. (1849). Suspension bridge, main span 308 m, longest span until 1866.

The bridge was severely damaged in 1854 due to torsional-vertical wind-induced oscillations and was reconstructed (by Ellet, not Roebling as stated by some articles). It was strengthened under the guidance of W. Roebling only in 1886 by additional stays and moving the cables outside the walkways. It was further stiffened in 1922 and 1930.

Photos: http://www.historic-structures.com/

Cable-supported bridges – Common aspects: Historical perspective

- The Niagara Falls Suspension Bridge (1855-1896, span 250 m), designed by John August Roebling, was the world's first cable-supported railway bridge. It is also the first bridge with air-spun wire cables.
- Ch. Ellet Jr. had been in charge of building the bridge and had already erected a footbridge, but was forced to leave due to delays and technical concerns regarding his project. Roebling used Ellet's bridge as falsework / scaffolding.
- The bridge's original timber deck decayed rapidly and was replaced with stronger steel and iron versions by 1886. In 1897, the entire bridge was replaced by a steel arch bridge, capable of carrying heavier trains.

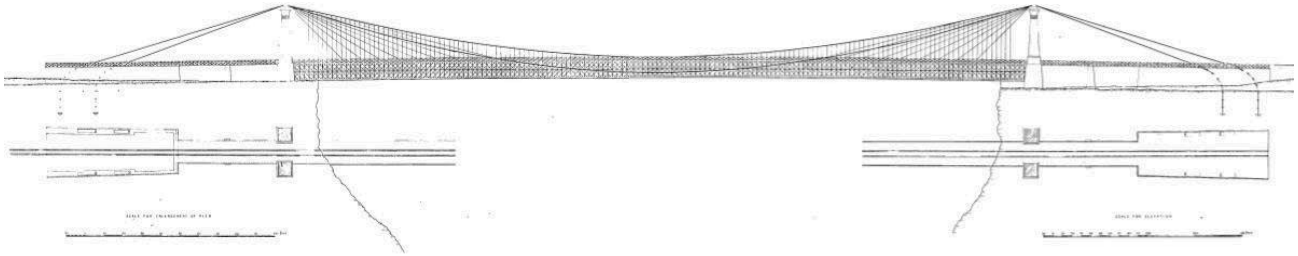

Niagara Falls suspension bridge across Niagara river, Niagara Falls Ontario (CA-U.S.), J. Roebling (1855). Combined suspension and cable-stayed bridge. Main span 250 m, 70 m above river, double deck.

The upper deck was 7.3 m wide, carrying the railway (accommodating three different gauges); the lower deck had a width of 4.6 m and was used by carriages and pedestrians. Roebling provided additional stays from deck to ground for dynamic stability (avoid train-induced oscillations).

Top illustration: Hand-coloured lithograph from 1857, Charles Parsons © United States Library of Congress's Prints and Photographs

Elevation: John Roebling. Memoir of the Niagara Falls and International Suspension Bridge. In *Papers and practical illustrations of public works of recent construction, both British and American*. John Weale, London, 1856.

Further reading: S.G. Buonopane. "The Roeblings and the stayed suspension bridge: Its development and propagation in 19th century United States." In *Proceedings*, The Second International Congress on Construction History, pages 441-460, Cambridge, England, 2006. Construction History Society.

Cable-supported bridges – Common aspects: Historical perspective

- Traffic loads on railway bridges are significantly higher than on road bridges, which is a particular challenge for suspension bridges (see structural response). Furthermore, the dynamic loads may cause vibration problems.
- Roebling mastered the challenge by designing a combination of suspension and cable-stayed bridge (though the latter designation was unknown at the time), further stiffened by a truss girder. This combination became characteristic for his bridges.
- In the Niagara Falls Suspension Bridge, Roebling designed a particularly stiff deck girder (double deck forming a tube similar to Britannia bridge, but with railway on top) and provided stays running from deck to ground to reduce oscillations.

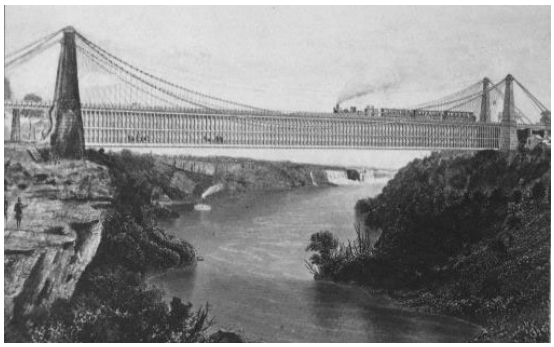

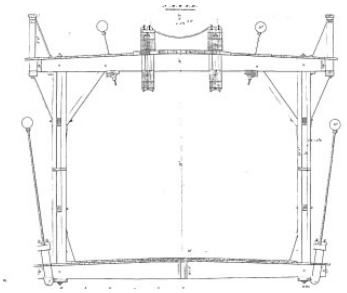

Niagara Falls suspension bridge across Niagara river, Niagara Falls Ontario (CA-U.S.), J. Roebling (1855). Combined suspension and cable-stayed bridge. Main span 250 m, 70 m above river, double deck.

The upper deck was 7.3 m wide, carrying the railway (accommodating three different gauges); the lower deck had a width of 4.6 m and was used by carriages and pedestrians. Roebling provided additional stays from deck to ground for dynamic stability (avoid train-induced oscillations).

Photo: © Swedish Technical Museum. Stereobild av "Niagara Suspension Bridge“, https://arkivkopia.se/sak/digmus-tek-TEKA0112400

Cross-section: John Roebling. Memoir of the Niagara Falls and International Suspension Bridge. In *Papers and practical illustrations of public works of recent construction, both British and American*. John Weale, London, 1856.

Further reading: S.G. Buonopane. “The Roeblings and the stayed suspension bridge: Its development and propagation in 19th century United States.” In *Proceedings*, The Second International Congress on Construction History, pages 441-460, Cambridge, England, 2006. Construction History Society.

Cable-supported bridges – Common aspects: Historical perspective

- Almost at the same time, Robert Stephenson designed the Britannia Bridge, carrying railway traffic across the Menai Strait (1850, spans 70+140+140+70 m).
- In order to control deformations and oscillations, Stephenson provided a “monster tube” cross section, consisting of riveted wrought iron plates (following contemporary shipbuilding practices), inside which the trains were running.
- Originally, Stephenson’s intention was to use the steel girder primarily for stiffness, and provide suspension cables or stays to carry a large portion of the self-weight.
- However, experiments by William Fairbairn to verify the buckling stability of the top chords indicated that they needed to be strengthened. Further experiments on stiffened plates (see cross-section photo) then led to a design that was stiff and strong enough to carry the entire load without any need for cables.
- While the bridge was seen as a “triumph of science” at the time, hardly any tubular bridges were built later (Conwy Railway bridge and Pont Victoria in Montreal, both designed by Stephenson).
- Unfortunately, the bridge had to be replaced after a fire in 1970, and the new design only maintained the piers.

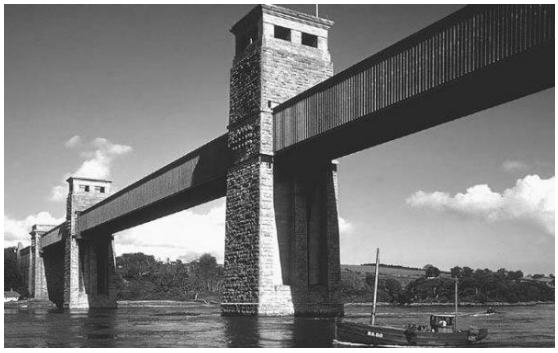

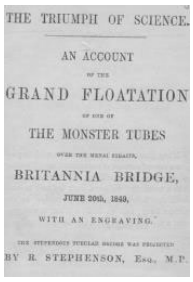
THE TRIUMPH OF SCIENCE.

AN ACCOUNT

GRAND FLOATATION

THE MONSTER TUBES

BRITANNIA BRIDGE,

WITH AN ENGRAVING.

BY R. STEPHENSON, Esq., M.P.

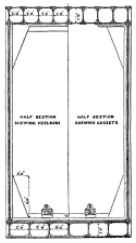

Britannia Bridge, Menai Strait, Robert Stephenson (1850). Girder bridge, wrought iron box girder, spans 70+140+140+70 m, variable depth h=9.14 m (centre) … 6.93 m (abutments), h/l = 1/10…1/15, width ca. 4.3 m.

Photo credits:

top: Godden Collection, Earthquake Engineering Research Center, University of California, Berkeley

bottom left: National Library of Wales

bottom centre: Encyclopedia Britannica, 1911

bottom right: Wrought iron section of original Britannia Bridge. Public Domain. www.structurae.net

Cable-supported bridges – Common aspects: Historical perspective

- In the John A. Roebling Suspension Bridge (1866, until 1983 Covington and Cincinnati Suspension Bridge, span 322 m) over the Ohio River, Roebling used the same concept as in the Niagara Falls suspension bridge, albeit with
  - → a less stiff truss girder since the bridge had to carry only carriages and pedestrians
  - → suspended side spans
- The Covington-Cincinnati bridge held the span record until 1868, when the Niagara-Clifton bridge was built (Samuel Keefer, stayed suspension bridge, span 384 m). However, that bridge collapsed in a hurricane in 1889.
- In 1896, the Covington-Cincinnati bridge was widened and provided with a second set of cables. Currently, it is still used, with a weight limit of 11 t.

John A. Roebling Suspension Bridge (until 1983 Covington and Cincinnati Suspension Bridge) over River Ohio, Cincinnati, John A. Roebling (1866). Stayed suspension bridge, main span 322 m, longest span until 1883.

Photo: The bridge after widening, ca. 1907. © United States Library of Congress's Prints and Photographs division, digital ID det.4a22289.

Cable-supported bridges – Common aspects: Historical perspective

- The Brooklyn Bridge (1883, until 1915 “New York and Brooklyn Bridge” or “East River Bridge”, span 486 m, record suspension span until 1903) is certainly the most prominent bridge designed by John A. Roebling.
- Roebling again used the same concept as in the Covington-Cincinnati and Niagara bridges, combining suspension cables, stay cables and a stiffening truss.

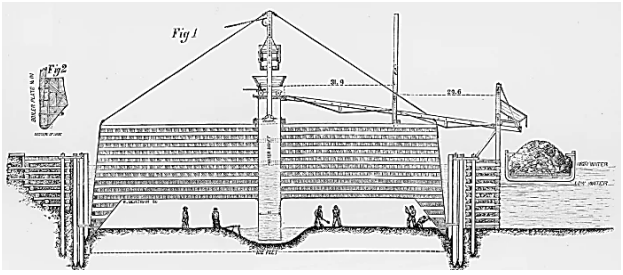

Brooklyn Bridge over East River, New York, John A. Roebling (1866). Stayed suspension bridge, main span 486 m, longest suspension bridge span until 1903.

Top: Caisson foundation of Brooklyn Bridge © Getty images.

Bottom: © http://cdn.history.com/sites/2/2013/11/brooklyn-bridge-2-H.jpeg.

Cable-supported bridges – Common aspects: Historical perspective

- Since the bridge is wider, it has four large-diameter main cables, each consisting of 5’282 wires. The cables were air-spun as in the Niagara bridge, but for the first time bundled in individual strands (19 @ 278 wires each) before assembling them.
- The truss girder is supported by 1’520 hangers (US: “suspender cables”) and 400 stays radiating from the towers.
- John A. Roebling died after an accident shortly after construction had started.
- His son, Washington Roebling, took over but became paralysed after staying in a pneumatic foundation caisson that caught fire. Washington’s wife Emily Warren Roebling subsequently led the works on site.
- The bridge today carries 6 lanes of road traffic (until 1950 8 lanes), with a weight limit of 6’000 lb (2.7 t).
- Since the opening ceremony in 1883, the upper pedestrian deck tends to be overcrowded (more than 150’000 people crossed the bridge on the first day, and six days after opening, 12 people were killed in a stampede).

Brooklyn Bridge over East River, New York, John A. Roebling (1866). Stayed suspension bridge, main span 486 m, longest suspension bridge span until 1903.

Photos: https://bloggingandthings.com/2018/09/25/new-york-fashion-guide/brooklyn-bridge/

Cable-supported bridges – Common aspects: Historical perspective

- As mentioned, the Brooklyn Bridge was the longest span suspension bridge until 1903. However, the Forth Bridge, a cantilever steel truss bridge, designed by John Fowler and Benjamin Baker, was the world's longest span bridge after opening in 1890, with a main span of 520 m, followed by the similar Québec Bridge (1918, rebuilt after having collapsed in construction 1907) with a span of 549 m.
- Suspension bridges only returned to be the longest span typology with the Ambassador Bridge (1929, span 564 m), whose span was soon almost doubled by the George Washington Bridge (1931, 1067 m).

Longest span bridges (all typologies)

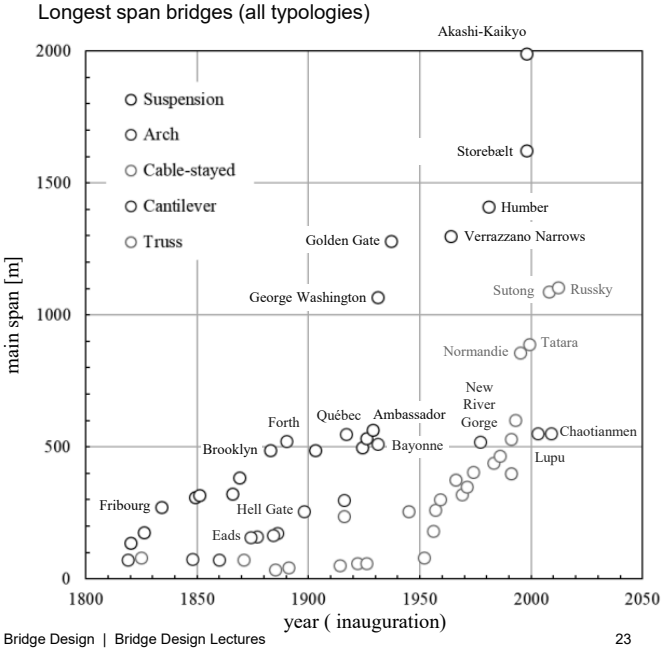

Graph based on date compiled by https://aiimpacts.org/historic-trends-in-bridge-span-length.

Photo © http://www.myhighlands.de/wp-content/uploads/2016/01/Forth-Bridge-Zug.jpg

Cable-supported bridges – Common aspects: Historical perspective

- The history of suspension bridges is closely linked to the development of theories for their analysis and design – and, unfortunately, bridge failures.
- The design of early suspension bridges (e.g. Telford's Menai Straits Suspension Bridge) was primarily based on the catenary curve (Kettenlinie), known since the end of the 17th century (Hooke, Leibniz, Huygens, Johann Bernoulli), experimental tests (see Drewry's quote in notes), and intuition.
- Navier's Theory of Suspension Bridges, published in 1823, served as a basis of suspension bridge design for the next five decades. While Navier already accounted for changes in the shape of the chains or cables (under a point load at midspan), he did not account for the effect of a stiffening girder nor cable elongations.
- In early suspension bridges, lightweight narrow timber decks were standard, and traffic loads were limited to pedestrians and carriages. Hence, most of the load consisted of the chain or cable self-weight, and the deck stiffness was indeed negligible.
- However, bridge decks became wider, and traffic loads kept increasing – up to the point where neglecting the traffic loads, nor deck girder stiffness, could no longer be justified.

Pont des Invalides, 1823 (Navier, never completed)
(timber deck on iron cross-beams)

Menai Strait Suspension Bridge, 1826
(original cross-section with timber deck)

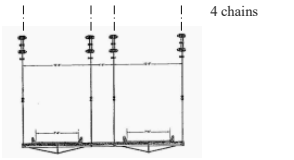

Brooklyn Bridge, 1883
(original cross-section)

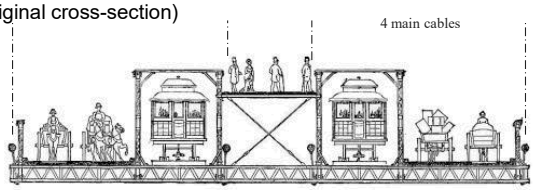

Ch. Drewry summarised the "stat-of-art" in suspension bridge design before Navier's seminal publication (Claude Louis Marie Henri Navier, Rapport à Monsieur Becquey et Mémoire sur les ponts suspendus, 1823) was generally accepted as follows: *"There is, in fact, considerable difference in opinion and practice among engineers, as to the proper strength to be given to suspension bridges. Several of the bridges described in this work do not possess half the strength that would be assigned as proper for them by the foregoing rule; and others, again, exceed it, while they have all stood unimpaired hitherto, and have sufficed for their appointed work." (*Charles Stewart Drewry: A Memoir on Suspension Bridges. Longman, Rees, Orme, Brown, Green & Longman, 1832).

Further reading (available as e-resources at ETH Library):

Karl-Eugen Kurrer. Geschichte der Baustatik. Auf der Suche nach dem Gleichgewicht, 2., stark erw. Auflage, Ernst & Sohn, Berlin 2016 (Karl-Eugen Kurrer and Werner Lorenz. The History of the Theory of Structures. Searching for Equilibrium. Construction History Series/Edition. Ernst & Sohn, Berlin 2018)

Illustrations:

top Claude Louis Marie Henri Navier, Rapport à Monsieur Becquey et Mémoire sur les ponts suspendus, 1823

middle D.P. Billington and G. Deodatis, "Performance of the Menai Straits Bridge Before and Aft er Reconstruction," in *Restructuring: America and Beyond* (American Society of Civil Engineers, 1995), 1536–1549.

bottom F. Giggs, "Brooklyn Bridge, Part 2," Structure Magazine (structuremag.org)

Cable-supported bridges – Common aspects: Historical perspective

- Many early suspension bridges suffered from excessive oscillations, and several collapsed.
- Being aware of these problems, Roebling – as already mentioned – provided stays and stiffening truss girders in his suspension bridges to increase their stiffness. Hence, his designs combined three load-carrying elements:
  → suspension cables
  → stay cables
  → stiffening girder
- However, at the time, there was no theory to analyse such a complex structure. Based on his engineering judgment, Roebling (except in his earlier bridges, where the stays were merely “activated” as stiffening against oscillations, for more details see reference in notes)
  → converted all actions to a uniformly distributed load
  → assigned most of the load to the suspension system
  → assigned the remaining part of the load to the stays
  → in most cases did not assign any loads to the stiffening truss
- Assuming that the truss is capable of transforming the applied loads to a uniform load, he thus implicitly used an equilibrium solution.

Further reading on Roebling’s design approaches:

S.G. Buonopane, D.P. Billington, “Theory and History of Suspension Bridge Design from 1823 to 1940,” ASCE Journal of Structural Engineering, Vol. 119, No. 3, March, 1993, pp. 954-977.

S.G. Buonopane. “The Roeblings and the stayed suspension bridge: Its development and propagation in 19th century United States.” In *Proceedings*, The Second International Congress on Construction History, pages 441-460, Cambridge, England, 2006. Construction History Society

Photo: Andreas Feiniger. New York in the Forties, New York 1978

Cable-supported bridges – Common aspects: Historical perspective

- Rankine had published a suspension bridge theory in 1858, where he indeed used the stiffening truss to convert arbitrary loads to uniform loads in a suspension bridge (the latter carried by the cable system). However, this theory did not find much application.
- Rather, at the end of the 19th Century, the “Elastic Theory” of suspension bridges was established, among others by Maurice Lévy and Josef Melan. This theory, equivalent to the elastic theory for arches, allows accounting for the load distribution between suspension cables and stiffening girder, satisfying equilibrium and compatibility (bending stiffness of girder, axial stiffness of cables).
- However, since the theory is based on small deformations (equilibrium is formulated in the undeformed state), it does not account for the capability of cables to carry non-uniform load by adapting their shape to the load configuration).
- Hence, in designs using this theory – analogous to a a stiffened arch – stiffening girders need to resist all non-uniform load, as well as bending moments caused by deflections due to elastic cable elongation. As a result, long-span suspension bridges designed using this theory require very stiff deck girders, as illustrated by the Williamsburg Bridge designed by Leffert L. Buck (1903, span 488 m, longest suspension span until 1924).

Williamsburg bridge, East River, New York, Leffert L. Buck (1903). Main span 488 m, longest span suspension bridge until 1924. Designed using “elastic theory”, h/l = 1/37.5. Traffic load: 8 lanes, 2 railway tracks.

Photo credit: U.S. Library of Congress.

Cable-supported bridges – Common aspects: Historical perspective

- In 1888 (refined version 1906), Josef Melan published the “Deflection Theory” of suspension bridges (Formänderungstheorie der Hängebrücken).
- This theory accounts for the beneficial effect of large cable deformations (second order deformations) in the load distribution among suspension cables and stiffening girder.
- As a result, much more slender stiffening girders could be used in bridges designed using this theory.
- Leon Moisseiff first applied the Deflection Theory in the design of the Manhattan Bridge (1909, span 448 m).
- The difference between the Manhattan bridge and the Williamsburg bridge, built only 6 years earlier and carrying even less traffic load with a similar span, is striking both visually (compare photos) as well as numerically (Slenderness h/l = 1/37.5 vs 1/56).

Williamsburg bridge, East River, New York, Leffert L. Buck (1903). Main span 488 m, longest span suspension bridge until 1924. Designed using “elastic theory”, h/l = 1/37.5. Traffic load: 8 lanes, 2 railway tracks.

Bottom: Manhattan bridge, East River, New York, Leon Moisseiff (1909). Main span 448 m. Designed using the Deflection Theory, h/l = 1/56. Traffic load: 7 lanes, 4 railway tracks.

Photos: Wikimedia Commons

Cable-supported bridges – Common aspects: Historical perspective

- When applying the Deflection Theory, structural safety can be guaranteed without stiffening girder. The required girder stiffness is thus essentially governed by the limits on deflections under traffic loads – which become smaller as the self-weight of the bridge increases.
- Consequently, very slender deck girders are sufficient in large span suspension bridges with a relatively large self weight (cables + deck girder).
- Othmar H. Ammann made use of this in his incredibly slender design (h/l = 1/351, more than six times higher slenderness than in the Manhattan bridge) of the George Washington Bridge (1931, span 1067 m, record span until 1937).
- The George Washington Bridge was disruptive regarding span, but also slenderness (see notes).

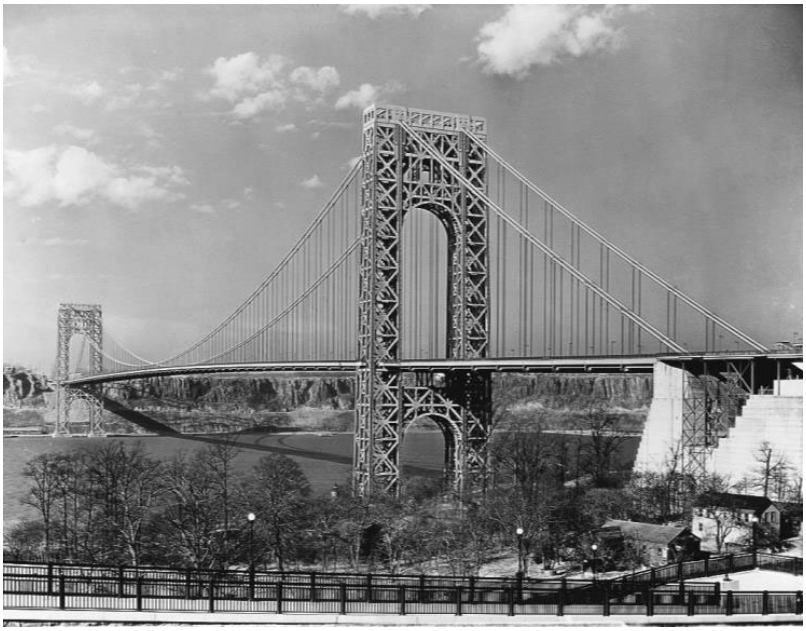

George Washington Bridge, Hudson River, New York City, Othmar H. Ammann, 1931. Span 1067 m, record until 1937.

Fritz Stüssi, Professor (Steel Structures) at ETH Zurich, commented: “It is reckless of this Ammann in America to build such a large suspension bridge without stiffening girders” (J. Scheer, Failed Bridges: Case Studies, Causes and Consequences, 2011). Although the George Washington Bridge never showed any vibration problems, one might argue that Stüssi was not completely wrong, since the George Washington Bridge’s success opened the way for a development – ever more slender bridges – that eventually lead to the collapse of the Tacoma Narrows Bridge.

Photo: © Encyclopedia Btitannica
https://www.britannica.com/technology/bridge-engineering/Suspension-bridges#/media/1/79272/408

Cable-supported bridges – Common aspects: Historical perspective

- In 1962, a second deck was added to the George Washington Bridge, increasing its capacity from 8 to 8+6 = 14 lanes of traffic.
- The slenderness was reduced to h/l = 1/120, yet the bridge still is and looks very slender.

George Washington Bridge, Hudson River, New York City, Othmar H. Ammann, 1931. Span 1067 m, record until 1937.

Photos:

right https://www.pinterest.com/twenty50nj/george-washington-bridge/;

bottom left https://media.gannett-cdn.com/

Cable-supported bridges – Common aspects: Historical perspective

- The Golden Gate Bridge was promoted by Joseph B. Strauss, who is commonly given credit for its design. However, Strauss' initial design was unsatisfactory, and the bridge finally built was designed by Clifford E. Paine, Irving F. Morrow and Charles A. Ellis (with Othmar Amman as consultant). It set a new span record in 1937 (l = 1281 m), which would hold for almost 30 years.
- It was not as slender as the George Washington Bridge, but still much more slender than earlier bridges (h/l = 1/168). A lower deck lateral bracing was installed in 1953/54 after a storm shook the bridge strongly in 1951.
- Othmar H, Ammann himself designed further very slender suspension bridges, such as the Bronx-Whitestone Bridge (1939, span 701 m, h/l = 1/210).
- After the Tacoma Narrows Bridge Collapse (see behind), the bridge was stiffened with stays and additional truss girders, reducing the slenderness to h/l = 1/91). In 2003, aerodynamic fairings were installed and the trusses removed, recovering the initial elegance.

Golden Gate Bridge, San Francisco, Clifford E. Paine, Irving F. Morrow and Charles A. Ellis (promoted by Joseph B. Strauss), 1937. Span 1281 m, record span until h/l = 1/168, record span until 1964. A lower lateral deck bracing was added in 1953-54 after a storm shook it strongly in 1951. Photo © https://cdn.getyourguide.com/img/location_img-3624-230665892-148.jpg

Bronx-Whitestone Bridge, New York City, Othmar H. Ammann, 1939. Span 701 m, h/l = 1/210. Stays added and stiffened with additional trusses in 1947 (h/l = 1/91 after stiffening). In 2003, aerodynamic fibreglass fairings were installed and the trusses removed, recovering the initial slenderness. Photo © Wikimedia Commons.

Animated photos: New York City Metropolitan Transportation Authority MTA / structurae.de / https://mapio.net/pic/p-46531632

Information on MTA website: *After performing a series of experiments* [after the Tacoma Bridge Collapse, kfm] *on the bridge's design, Ammann concluded that additional measures to stiffen the Whitestone Bridge were unnecessary. Even so, the public was scared by the fact that the two bridges were similar in design* [and according to some sources there were undesirable oscillations, kfm]*, and this led to a belief that the Whitestone Bridge might be unstable, as Moses later related. On both sides of the deck, 14-foot (4.3 m)-high steel trusses were installed to weigh down and stiffen the bridge in an effort to reduce oscillation. The stiffening project was completed in 1947. In 2003, the MTA restored the classic lines of the bridge by removing the stiffening trusses and installing fiberglass fairing along both sides of the road deck.[99][10] The lightweight fiberglass fairing is triangular in shape, giving it an aerodynamic profile that allows crosswinds to flow through the bridge rather than hit the trusses. The removal of the trusses and other changes to the decking reduced the bridge's weight by 6,000 tons, accounting for some 25% of the mass suspended by the cables, In addition, with the truss removals, the Bronx–Whitestone Bridge was able to withstand crosswinds of up to 150 miles per hour (240 km/h), whereas the trusses could resist crosswinds of no more than 50 miles per hour (80 km/h).*

Cable-supported bridges – Common aspects: Historical perspective

- Several suspension bridges with slender decks built in the late 1930s experienced excessive oscillations and had to be stiffened for this reason.
- Documented examples include the Thousand Islands Bridge (1937, span 240 m) and the Deer Isle Bridge (1939, span 329 m), both designed by the renowned engineer David B. Steinman.
- The Thousand Islands Bridge was stiffened with “truss” stays shortly after the opening, due to excessive oscillations in wind. The Deer Isle Bridge was retrofitted with “truss” stays even before opening, since similar oscillations as in the Thousand Islands Bridge had been observed during construction.
- Despite these obvious problems, and the knowledge about wind-induced collapses of several early suspension bridges without stiffening girder, ultra-slender suspension bridges kept being built.

Right side: Deer Isle Bridge Bridge, Maine, U.S., David B. Steinman, 1939. Span 329 m. Stiffening “truss” stays added before commissioning. Photos © historicbridges.org

Bottom left: Thousand Islands Bridge , St. Lawrence river, New York, U.S. – Ontario, Canada, D. Steinman, 1937. Span 240 m. Stiffening “truss” stays added shortly after inauguration. Photo ©https://www.pinterest.ch/pin/130956301634519888/

Cable-supported bridges – Common aspects: Historical perspective

- On November 7, 1940, the unimaginable happened: The Tacoma Narrows Bridge (span 853 m), designed by Leon Moisseiff, collapsed after oscillating in steady wind with a velocity of merely ca. 68 km/h.
- Moisseiff was one of the leading suspension bridge designers of the time. He had extended the deflection theory for lateral load, i.e. wind, and used it in his Tacoma Narrows design (see notes).
- Therefore, the bridge was extremely slender not only vertically (h/l = 1/355, ≈ George Washington Bridge with one deck), but also transversally (b/l = 1/72, compared to b/l = 1/47 in the Golden Gate Bridge and b/l = 1/33 in the George Washington Bridge).
- The Bridge had experienced large vertical oscillations under modest wind already during construction. Frederick B. Farquharson at the University of Washington had therefore carried out wind tunnel tests already in 1939. He recommended several measures, but most of them failed. Finally, the installation of aerodynamic fairings along the deck was decided, but the bridge collapsed less than a week later – leaving the question open if these fairings would have helped.
- The collapse was investigated by a commission including Othmar Ammann and Theodore von Kármán. Prof. Jakob Ackeret carried out wind tunnel experiments in this context at ETH Zurich.

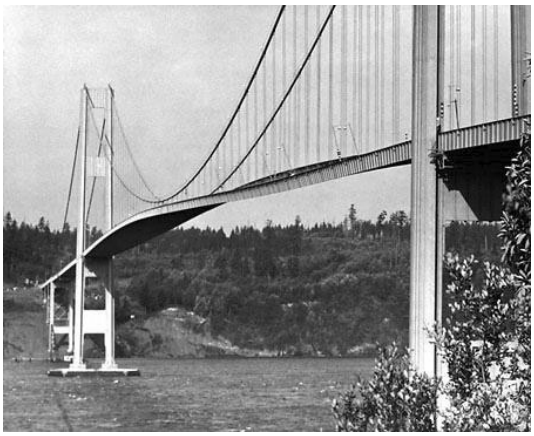

Tacoma Narrows Bridge, Puget Sound, Washington state, Leon Moisseiff, 1940. Span 853 m. Collapsed on 7.11.1940.

Video: Barney Elliott; The Camera Shop - Screenshot taken from 16MM Kodachrome motion picture film by Barney Elliott (extract)

Photo: Farquharson (Ed.), Aerodynamic stability of suspension bridges with special reference to the Tacoma Narrows Bridge; a report of an investigation, University of Washington, Structural Research Laboratory, Report No. 116, 1949-1954.

Comment (based on exchange with David Goodyear, one of the most eminent bridge designers, and familiar with the historic documents: *Considering the historical context and circumstances, it would be all too easy and even unfair to blame Leon Moisseiff alone for the collapse. Moisseiff was the lead engineer for what we would today call a peer review committee for the design, and prior to the collapse, a representative of the client even claimed to be the designer of the bridge. As the bids for the Washington Department of Highway's original design – which had a wider traditional truss than the final design – were high, the client asked Moisseiff to figure out how to save money, which is when he proposed the plate girder that was finally built. The question of adding aerodynamic fairings was also delayed for cost reasons. It could well be that the failure would not have occurred were it not for the money pressures imposed to Moisseiff by the client, who did not assume any responsibility for the disaster.*

Lesson to be learnt: Engineers are all too often subject to pressures to save money. We should think twice and resist such pressures if they entail excessive risks. Unfortunately, this is much easier said than done (engineers may even have to withdraw from a design contract in such cases).

Cable-supported bridges – Common aspects: Historical perspective

- Some highschool physics textbooks erroneously use the Tacoma failure as example for resonance. This would imply a periodic excitation by an external force (such as vortex shedding or buffeting).
- However, the bridge collapsed due to torsional flutter ("torsional galloping" in older textbooks), see section *wind-induced oscillations*:
  → self-exciting divergent aeroelastic phenomenon, where aerodynamic forces on the bridge deck couple with its motion
  → if the energy input by aerodynamic forces per cycle is larger than that dissipated by the bridge's damping, the amplitude of oscillations grows
  → if continued for some time, this leads to collapse
- Flutter is related to "resonance" insofar as in coupled flutter, a coupling of aerodynamic forces and deck motion occurs if the relevant vertical and torsional eigenfrequencies (nearly) coincide.
- The collapse marked a turning point in bridge design, particularly for cable-supported bridges:
  → Aerodynamic effects, which had received little attention before, became a major concern in long-span bridge design on that very day
  → Today, wind tunnel testing on long-span and/or slender bridges is common, and computational fluid mechanics is increasingly used.

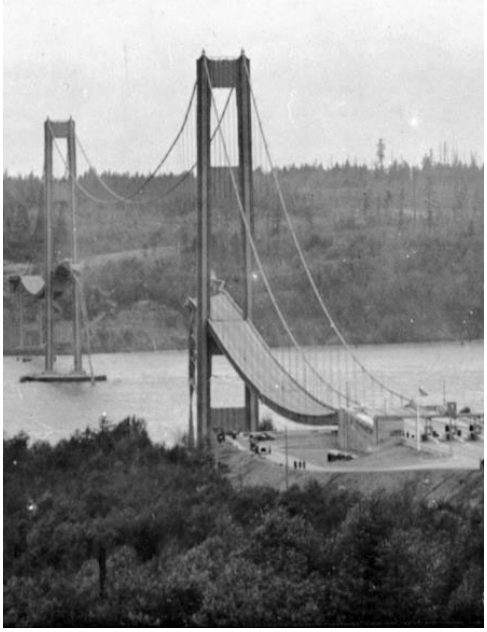

Tacoma Narrows Bridge, Puget Sound, Washington state, Leon Moisseiff, 1940. Span 853 m. Collapsed on 7.11.1940.

Video: Barney Elliott; The Camera Shop - Screenshot taken from 16MM Kodachrome motion picture film by Barney Elliott (extract)

Photo: Farquharson (Ed.), Aerodynamic stability of suspension bridges with special reference to the Tacoma Narrows Bridge; a report of an investigation, University of Washington, Structural Research Laboratory, Report No. 116, 1949-1954.

Cable-supported bridges – Common aspects: Historical perspective

- The Tacoma Narrows bridge was rebuilt in 1950, with a much deeper and wider stiffening girder, (h/l = 1/87 vs. 1/355, b/l = 1/46 vs. 1/72, truss box girder with high torsional stiffness vs. open cross-section).
- The towers had suffered severe damage, being deflected almost 4 m towards the shore after collapse of the main span. Only the cable anchorages, tower pedestals and foundations could be re-used. The steel (cables, deck, towers) was sold as scrap.
- In 2007, a second bridge was added, with equal span.

Cross-section of collapsed bridge (1940)

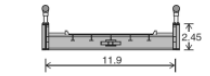

Cross-section of rebuilt bridge (1950)

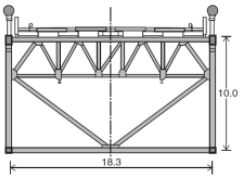

Current Tacoma Narrows Bridges, Puget Sound, Washington state; Westbound bridge Charles E. Andrew, 1950. Eastbound bridge Bechtel Infrastructure and Kiewit Construction, 2007. Span 853 m.

Cable-supported bridges – Common aspects: Historical perspective

- The Verrazzano Narrows Bridge was the last bridge designed by Othmar H. Ammann (1964, span 1298 m, longest until 1981, h/l = 1/170).
- The bridge is named after Giovanni da Verrazzano, Italian explorer who discovered the entrance to the Hudson River in 1524. It was misspelled (“Verrazano”) until 2018, when the name of the bridge was officially changed under Governor Andrew Cuomo.
- Like all suspension bridges built after the Tacoma Narrows bridge collapse, the Verrazzano Narrows bridge was subjected to scale-model tests in a wind tunnel and has a torsionally stiff cross-section to avoid flutter: The box truss section (depth 7.30 m between top and bottom chord axis) was provided from the beginning, though the bridge initially carried only one deck (unlike in the George Washington Bridge).
- Seasonal contractions and expansions of the suspension cables cause a seasonal variation of the deck elevation at midspan of 3.60 m.

Verrazzano Narrows Bridge, New York City, Othmar H. Ammann, 1964. Span 1298 m, longest until 1981. Lower deck added in 1969 (had been planned for 1975 when the bridge was built)

Photo credits:

top Brooklyn Media Group

bottom Robert Wash

Cable-supported bridges – Common aspects: Historical perspective

- In the Severn Bridge (1966, main span 978 m), the designers of Freeman, Fox & Partners introduced two revolutionary concepts:
  → an aerodynamic, slender, closed steel box-girder cross-section (streamlined “airfoil”), providing the torsional stiffness required to prevent flutter at much smaller drag forces than present in truss box girders (optimised based on wind tunnel tests)
  → slightly inclined hangers to increase stiffness and energy absorption under vertical displacements and thereby increasing the damping.
- As a result, an extremely slender and elegant bridge could be built (h/l = 1/326) without oscillation problems.
- Streamlined box girder cross-sections have been used in many subsequent cable-supported bridges (typically with an orthotropic steel deck); the inclined hangers were repeated in the Humber Bridge.
- Since 2018, the Second Severn Bridge is operative, about 6 km downstream of the First Severn Bridge (cable-stayed bridge, main span 456 m).

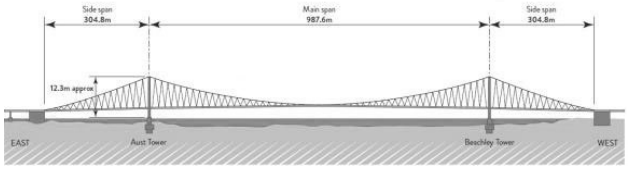

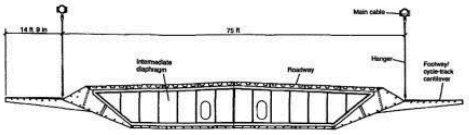

Severn Bridge, Severn River, UK, Freeman, Fox & Partners (now Arcadis), 1966. Main span 978 m.

Photos:

top: http://www.bristol-business.net/wp-content/uploads/2014/01/Severn-Bridge-6web.jpg

middle: https://www.newcivilengineer.com/technical-excellence/suspension-surgery-severn-bridge/10014750.article

bottom: severnbridges.org

Cable-supported bridges – Common aspects: Historical perspective

- In the Humber Bridge (1991, main span 1410 m, record until 1998, h/l = 1/313), Freeman, Fox & Partners again used a streamlined steel box girder with orthotropic steel deck, as well as the slightly inclined hangers.

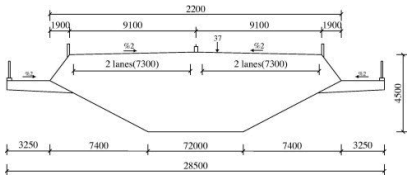

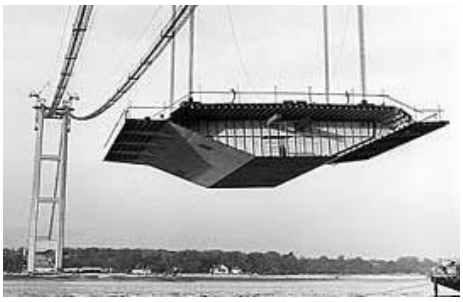

Humber Bridge, Kingston upon Hull, UK, Freeman, Fox & Partners (now Arcadis), 1981. Main span 1410 m.

Photos:

Top: https://upload.wikimedia.org/wikiped

Bottom: left http://www.engineering-timelines.com / right Thomas Vogel

Cable-supported bridges – Common aspects: Historical perspective

- The Storebælt East Bridge (1998, main span 1624 m, h/l = 1/380), designed by a team led by COWI, has conventional vertical hangers.
- The very slender steel box girder, again with orthotropic deck, is equipped with guide vanes in the main span (photo below, bottom edges) to enhance aerodynamic stability.
- The box girder is uncoated inside (corrosion protection by dehumidification).

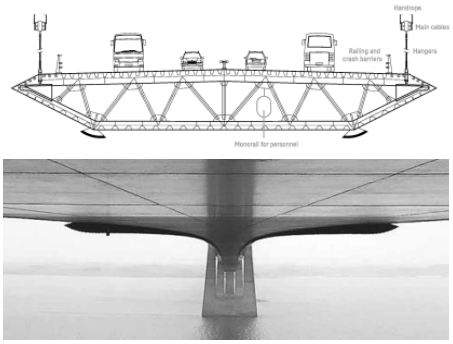

Storebælt East Bridge, Sjælland.Fyn, Denmark, COWI (with Ramboll and Dissing and Weitling),1998. Span 1624 m (never was the longest span, Akashi-Kaikyo Bridge opened 3 months earlier the same year).

Photos:

right side: Storebaelt.dk

left side: The link across Storebælt - Two bridges and a tunnel. Sund & Bælt Holding A/S, 2017.

Cable-supported bridges – Common aspects: Historical perspective

- The Akashi-Kaikyo Bridge (1998, main span 1990 m) is the currently longest span bride in service worldwide. It was designed by Satoshi Kashima at the Japan Bridge Engineering Centre
- It was designed for very high wind speed (286 km/h) and earthquakes (magnitude 8.5).
- Other than in the recent European long-span suspension bridges, its cross-section is a steel truss box girder, which is considerably less slender (h/l = 1/136) than in the Severn (1/326), Humber (1/313) and Storebaelt (1/380) bridges, but provides aerodynamic stability at very high wind velocities.

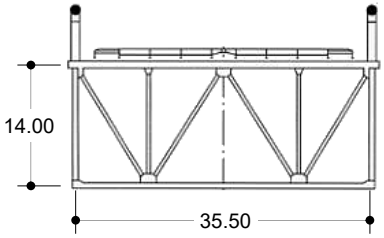

Akashi-Kaikyo Bridge, Akashi Strait, Japan, Satoshi Kashima / Japan Bridge Engineering Centre, 1998. Main span 1990 m (1992 m since Kobe Earthquake), current record span (until 2022/23).

Photos

top right: Wikimedia Commons

bottom right: https://somejapan.com/maikos-akashi-kaikyo-bridge-the-longest-suspension-bridge-in-the-world/

Cable-supported bridges – Common aspects: Historical perspective

- The two main cables, with a diameter of 1.12 m, were fabricated using prefabricated parallel wire strands (PPWS)
- Each main cable consists of 290 PPWS with 127 wires Ø5.23 mm, totalling 36’830 wires per cable (see *Cable Types* section).

Akashi-Kaikyo Bridge, Akashi Strait, Japan, Satoshi Kashima / Japan Bridge Engineering Centre, 1998. Main span 1990 m (1992 m since Kobe Earthquake), current record span (until 2022/23).

Photos:

right: broer.no

bottom left http://www.pref.oleft saka.lg.jp/en/attraction/industry/manufacture/img/topWire.jpg

Cable-supported bridges – Common aspects: Historical perspective

- The Çanakkale Bridge, crossing the Dardanelles Strait with a main span of 2023 m, will be the longest span bridge from its commissioning in 2022/23. Designers are Pyunghwa (South Korea, basic design) and COWI (Denmark, detailed design).

- Currently, 91 suspension bridges with spans above 600 m exist worldwide (Wikipedia, April 2020). Out of these, 41 are located in China.
- Despite the tremendous evolution of cable-stayed bridges towards longer spans (see following slides), many suspension bridges are currently under construction, primarily in China (21 of the 25 currently under construction).

Suspension bridges with main span ≥ 600 m

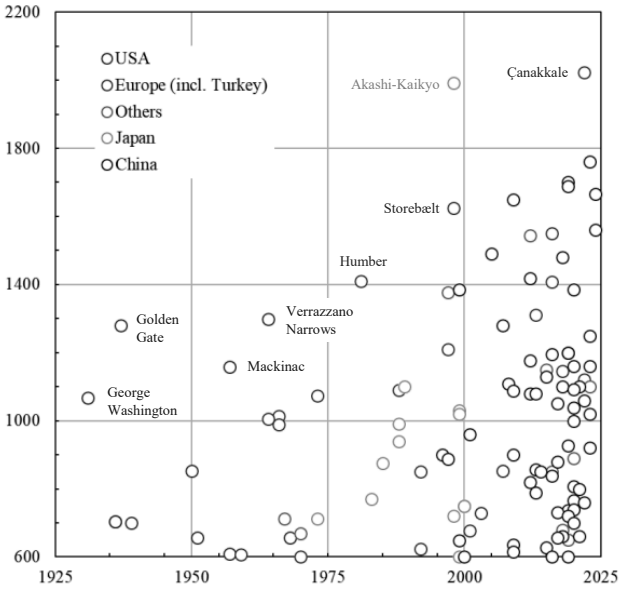

Cable-supported bridges – Common aspects: Historical perspective

- While suspension bridges are still the most economical solution for very long spans, cable-stayed bridges are increasingly being considered for longer spans as well.
- This is illustrated by the fact that since 1990, 67 cable-stayed bridges with spans above 500 m have been built, (47 in China), and a further 29 are currently under construction, mainly in China (Wikipedia, April 2020).
- The Changtai Yangtse Bridge connecting Taixing and Changzhou in China will be the longest span cable-stayed bridge from its commissioning (2024, main span 1’176 m, designed by the China Railway Major Bridge Reconnaissance and Design Institute (BRDI).

Cable-stayed bridges with main span ≥ 500 m

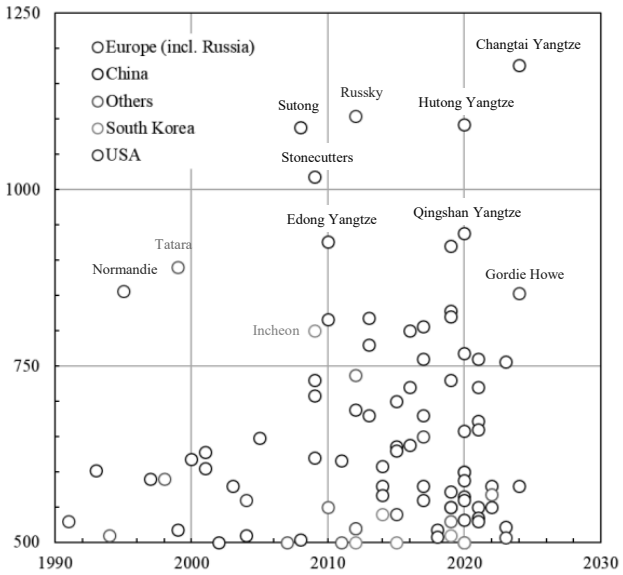

Photo: https://english.jschina.com.cn/23261/201911/t20191125_6418285.shtml

Cable-supported bridges – Common aspects: Historical perspective

- Hybrid cable systems, such as in the third Bosporus crossing designed by Michel Virlogeux and Jean-Francois Klein (2016, span 1’408 m) are viable alternatives for long spans:
  - → combination the structural efficiency of (relatively short and steep) stay cables near pylons and suspension system at midspan
  - → efficient and fast erection (stayed cantilevering from pylons can start before, and continue while suspension cables are being installed).

Third Bosporus Crossing (Yavuz-Sultan-Selim-Bridge), Istanbul, Jean-Francois Klein (T Ingénierie, Genf), 2016, l = 1408 m

Photos: left and right top www.t-ingenierie.com / right bottom www.aecom.com

Cable-supported bridges – Common aspects: Historical perspective

- Hybrid cable systems, such as in the third Bosporus crossing designed by Michel Virlogeux and Jean-Francois Klein (2016, span 1’408 m) are viable alternatives for long spans:
  - → combination the structural efficiency of (relatively short and steep) stay cables near pylons and suspension system at midspan
  - → efficient and fast erection (stayed cantilevering from pylons can start before, and continue while suspension cables are being installed)

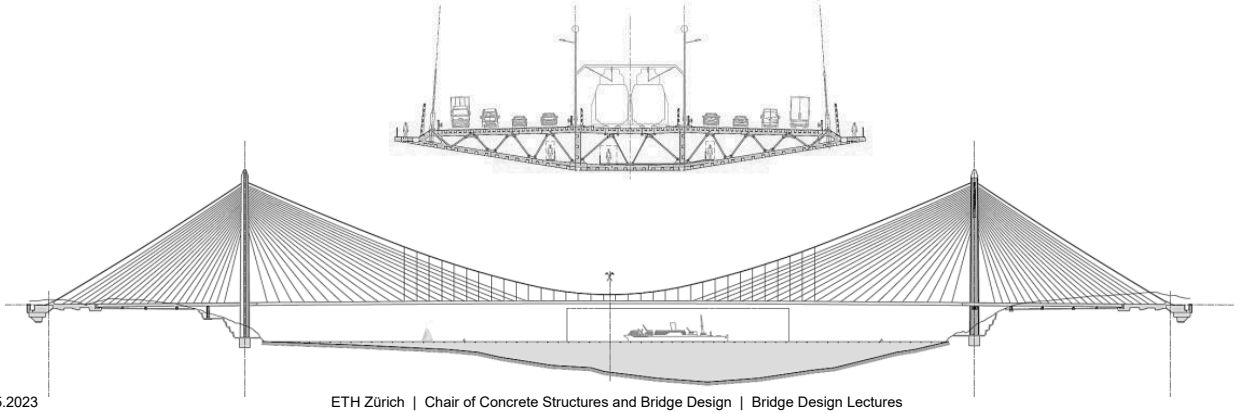

Third Bosporus Crossing (Yavuz-Sultan-Selim-Bridge), Istanbul, Jean-Francois Klein (T Ingénierie, Genf), 2016, l = 1408 m

Figures: Jean-Francois Klein, Michel Virlogeux, Thierry Delémont, Vincent de Ville de Goyet: “Third Bosporus bridge – a masterpiece of sculptural engineering,” Structural Concrete in Switzerland, fib Swiss National Group, 2018.

Cable-supported bridges – Common aspects: Historical perspective

- So far, the historical perspective has focused on suspension bridges (including the Roeblings' stayed suspension bridges).
- It is completed in the following by highlighting some major steps in the development of cable-stayed bridges.
- Among the first major cable-stayed bridges were the Albert bridge in London (1873, span 122 m) and the Stefanik Bridge in Prague (1868-1949, span 100 m), both designed by Rowland Ordish.
- Similar as John Roebling, Ordish used a combination of stays and suspension system (rods), but the stays carried most of the load in his designs.

Albert Bridge, London, U.K., Rowland Mason Ordish, 1873. Main Span 122 m. Photo Wikimedia Commons, David Iliff / Iridescent

Wikipedia: *The bridge acquired the nickname of "The Trembling Lady" because of its tendency to vibrate, particularly when used by troops from the nearby Chelsea Barracks. Concerns about the risks of mechanical resonance effects on suspension bridges, following the 1831 collapse of the Broughton Suspension Bridge and the 1850 collapse of Angers Bridge, led to notices being placed at the entrances warning troops to break step (i.e. not to march in rhythm) when crossing the bridge; Although the barracks closed in 2008, the warning signs are still in place.*

Štefanik Bridge (Franz Joseph Bridge), Prague, Czech Republic, Rowland Mason Ordish, 1868. Main span 100 m, demolished 1949. Photo Wikimedia Commons, Tlust'a

Wikipedia: *Much like its London counterpart, the Franz Joseph Bridge featured a combination of stay and suspension rods. The latter formed a cable which held the diagonal stay rods. The main span was 100 metres (330 feet) long and 9.76 metres (32.0 feet) wide, while the entire structure was over 240 metres (790 feet) long. The bridge was gradually strengthened and rebuilt in the 1890s.*

Cable-supported bridges – Common aspects: Historical perspective

- A similar, hybrid solution with predominant stay action was used e.g. by Albert Gisclard in the Pont de Cassagne (1908, main span 158 m).

Pont de Cassagne, Planes, Pyrenees-orientales, France, Albert Gisclard, 1908. Main Span: 156 m. Steel deck, narrow-gauge train bridge.

Photos structurae.de, Nicolas Janberg

Cable-supported bridges – Common aspects: Historical perspective

- The following bridges are often referred to as the first “modern” cable stayed bridges:
  - → Concrete: Pont de Donzère-Mondragon (Albert Caquot, 1952, span 81 m, concrete deck girder)
  - → Steel: Strömsund Bridge (Franz Dischinger, 1956, span 183 m, steel girders with orthotropic steel deck)

Pont de Donzère-Mondragon, Pierrelatte, France, Albert Caquot, 1952. Main span 81 m, length 160 m. Cable-stayed bridge with concrete deck. Fan stay arrangement .

Photo Structurae.net, N. Janberg

Strömsund Bridge, Strömsund, Sweden, Franz Dischinger, 1956. Main span 183 m, steel girders with orthotropic steel deck. Fan stay arrangement (16 stays in total).

Photo Wikimedia Commons, Lars Falkdalen Lindahl

Cable-supported bridges – Common aspects: Historical perspective

- In the first cable-stayed bridges, few massive stays (in many cases even only one stay per span) were used. In German, such bridges are commonly referred to as “Zügelgurtbrücken”.
- Using single stays facilitated analysis and design, as the stays could be treated as “flexible supports” (replacing a pier)
- A pioneer of this typology was Riccardo Morandi, who designed several similar bridges like the Lake Maracaibo Bridge (1962, 5 main spans @ 235 m, total length 8.7 km. built in record time, stays exchanged due to corrosion in 1982).
- To increase the stiffness of the stays, Morandi later replaced the bare cables by prestressed concrete ties.
- Morandi’s concept of prestressed concrete ties was adopted by many other designers due to its high efficiency, see bottom example (Donaubrücke Metten, 1981, span 145 m).

Lake Maracaibo Bridge (Puente General-Rafael-Urdaneta), Venezuela, Riccardo Morandi, 1962. Main spans 5x235 m (6 towers), total length 8’678 m. First major multi-span cable stayed bridge. Stay cables exchanged in 1982 due to corrosion damage.

Photo: https://de.wikipedia.org/wiki/General-Rafael-Urdaneta-Br%C3%BCcke

Donaubrücke Metten, Herbert Schambeck, 1981. Main span 145 m. Photo

Cable-supported bridges – Common aspects: Historical perspective

- Riccardo Morandi had used prestressed concrete ties in a number of his bridges, among which the Viadotto del Polcevera in Genova (1967, main spans 208 m).
- In this bridge, the prestressed concrete ties were roughly 5 times stiffer than the bare steel would have been. In addition, as long as the concrete was uncracked, it protected the steel from corrosion.
- The causes of this tragic collapse are still uncertain. However, the most plausible failure cause is the rupture of a stay due to corrosion, which is supported by the following:
  - Severe corrosion of the stays was detected before the accident
  - Failure of a stay would trigger the collapse of an entire span (as structural analysis based on the available data clearly shows)
- As mentioned, the failure cause is still unclear, and the above is thus merely speculative. However, independently of the true cause, one may conclude that single stay bridges lack robustness. Therefore, modern cable-stayed bridges are designed such that failure of a single cable will not cause collapse.
- When judging Morandi's design, it must be kept in mind that robustness was not a design goal at the time (not only in bridges: for example, cars did not have dual brake circuits in the 1960s).

Viadotto Polcevera, Genova, Italy, Riccardo Morandi, 1967. Main spans 208 m, total length 1182 m. Collapsed in 2018.

Photos:

https://it.wikipedia.org/wiki/Viadotto_Polcevera

After collapse https://cdn-media.rtl.fr/online/image/2018/0814/7794424826_000-18d2qs.jpg

Cable-supported bridges – Common aspects: Historical perspective

- The Theodor Heuss Brücke (1958, span: 260 m) and the (Rhein-)Kniebrücke (1969, span 319 m), both located in Düsseldorf and designed by Fritz Leonhardt, underline the leading role of German engineers in the development of cable-stayed bridges.
- Both bridges share a harp arrangement of the stays, in the case of the Kniebrücke combined with anchor piers at all back stays, enabling a very slender deck girder in the main span.

Theodor Heuss Brücke, Düsseldorf, Germany, Fritz Leonhardt, 1958. Main Span: 260 m. Twin steel box girders and orthotropic steel deck. Cables: harp arrangement (24 stays in total)

Photo
https://de.wikipedia.org/wiki/Datei:Oberkasseler_Bruecke_bridge_Rhine_river_Oberkassel_Pempelfort_Duesseldorf_Germany.jpg

Kniebrücke, Düsseldorf, Germany, Fritz Leonhardt, 1969. Main Span 319 m. Twin steel box girders and orthotropic steel deck - Cables: harp arrangement (16 stays in total) - All back stays are anchored to piers

Photo
https://de.wikipedia.org/wiki/Datei:Oberkasseler_Bruecke_bridge_Rhine_river_Oberkassel_Pempelfort_Duesseldorf_Germany.jpg

Cable-supported bridges – Common aspects: Historical perspective

- One of the first cable-stayed bridges with multiple number of stays was the Rheinbrücke Bonn Nord (1967, span 280 m), designed by Hellmut Homberg.
- This was also among the few early cable-stayed bridges with only one suspension plane, requiring a high torsional stiffness of the deck girder.

Rheinbrücke Bonn Nord (Friedrich-Ebert-Brücke), Bonn, Germany, Hellmut Homberg, 1967. Main span 280 m, steel deck, 80 stays. One of the first bridges with central suspension and high torsional rigidity of the deck girder.

Photo: http://www.karl-gotsch.de/Bilder/Bonn_Friedrich-Ebert1.jpg (from below) / Wikipedia, Jan Arne Petersen (overview)

Cable-supported bridges – Common aspects: Historical perspective

- The Puente de Rande, designed by Fabrizio de Miranda and Florencio del Pozo (1978, widened in 2011, span 401 m, second longest span at time of erection) was another early multi-stay cable-stayed bridge.
- The Barrios de Luna bridge (1983, span 440 m) is an early example of a bridge with closely spaced cables, enabling a very slender deck girder.
- The designers Carlos Fernández Casado and Javier Manterola took advantage of computing power to analyse the highly statically indeterminate system.

Puente de Rande, Ría de Vigo, Pontevedra, Spain, Fabrizio de Miranda / Florencio del Pozo, 1978 (widened in 2011). Main Span 401 m.

Photo Wikimedia commons, Juantiagues

Barrios de Luna (Puente Ingeniero Carlos Fernández Casado), León-Oviedo, Spain, Carlos Fernández Casado / Javier Manterola, 1983. Main Span 440 m, Concrete deck. First truly modern cable-stayed bridge - took advantage of computing power to analyse the closely spaced cables.

Photo Carlos Fernández Casado S.L.

Cable-supported bridges – Common aspects: Historical perspective

- With the Pont de Normandie (1994, span 856 m), designed by Michel Virlogeux, the span range of cable-stayed bridges was greatly increased.
- The Stonecutters Bridge (2009, span 1018 m), designed by Arup, COWI and Buckland & Taylor, was the first cable-stayed bridge with a span exceeding a kilometre.
- Clearly, with such long spans, aerodynamic effects are as important in cable-stayed bridges as in suspension bridges.
- The progress of cable-stayed bridges towards longer spans and more slender decks clearly benefitted from the experiences with aerodynamic effects in long-span suspension bridges. For example, the twin deck of the Stonecutter's bridge was chosen primarily for aerodynamic reasons.

Pont de Normandie, Le Havre, France, Michel Virlogeux / SETRA, 1994. Main Span 856 m, Steel deck in centre span, concrete deck in back span and portions of main span near pylons - Cables: Multi-strand, sheaths eliminate rain-wind oscillations, wind ties

Stonecutters Bridge, Hong Kong, Arup, COWI and Buckland & Taylor, 2009. Main Span 1018 m. Twin steel box girder decks - Cables: hybrid arrangement

Cable-supported bridges

Common aspects – Cable types

Cable-supported bridges – Common aspects: Cable types

- Cables in modern cable-supported bridges mostly consist of
  - → high-strength steel wires (commonly cylindrical)
  - → f_{pk} = 1770…1860 MPa (as in post-tensioning strands)
  - → Ø5.0… 5.5 mm in suspension bridges
  - → Ø7 mm in stay cables (parallel wire strands).
- Several wires are often shop-assembled to form prefabricated strands.
- The simplest form of strands are seven-wire strands, as used for post-tensioning tendons. The same strands may be used for cable-supported structures:
  - → 7 wires Ø5 mm, nominal diameter 15 mm = 0.6”-strand, A_p = 150 mm^2 (140 mm^2 in older strands)
  - → moderate reduction of stiffness compared to the straight wire (Ep ≈ 195 GPa)
- Note however that standard strands will not generally pass the fatigue and ductility tests required for stay cables (elevated demand, performance generally controlled by anchorages).

Seven-wire strand

Stress-strain relationships

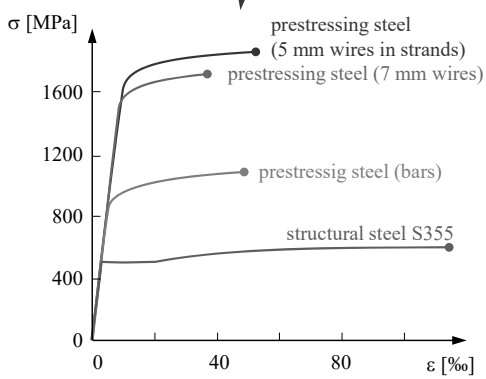

Cable-supported bridges – Common aspects: Cable types

- Multi-wire helical bridge strands (“spiral strands”, offene Spiralseile) consist of
  - → successive layers of cylindrical wires
  - → spinning in alternating direction around a straight core
  - → ca. 10% reduction of ultimate load due to twisting
  - → more pronounced stiffness reduction than in 7-wire-strands ($E \approx 160$ GPa, nominal modulus, referred to steel cross-section)
  - → wires are often galvanized for corrosion protection

Multi-helical bridge strand
(spiral strand)

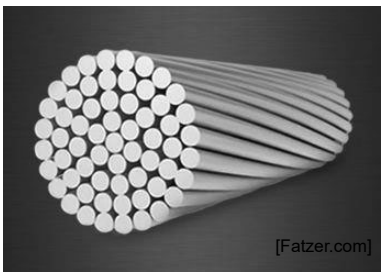

- Helical strands are compacted at first loading
  - → irreversible elongation at first loading
  - → pre-stretching common (characteristic design load +10…20%) to ensure elastic behaviour in service
  - → no need to wrap or apply bands to hold the wires together

Lillebaelt Bridge
multi-helical strand exhibit

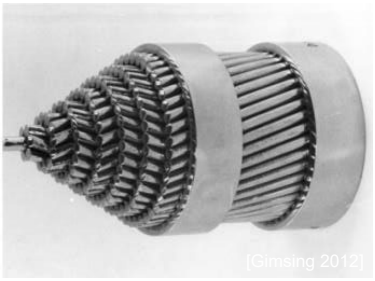

Illustrations: Top © www.fatzer.com / bottom Gimsing, Cable Supported Bridges.

Source and further reading: Niels J. Gimsing, Christos T. Georgakis. Cable Supported Bridges – Concept and Design, Wiley, 1983 (3rd edition, 2012).

Further information on strands:

- Pfeifer tension members , https://www.pfeifer.info/out/assets/PFEIFER_TENSION-MEMBERS_BROCHURE_EN.PDF
- Fatzer Brugg structural ropes https://fatzer.com/seilbau-architekturseile/
- Bridon steel ropes for beidges https://www.bridon-bekaert.com/en-au/steel-and-synthetic-ropes/bridges

Cable-supported bridges – Common aspects: Cable types

- Locked coil strands (vollverschlossene Spiralseile) consist of two types of twisted wire:
  - → core = helical strand, surrounded by outer layers = Z-shaped, interlocking wires spinning in alternating directions around the helical strand core (→ subject to irreversible elongation at first loading)
  - → tight surface, small void ratio (only ca. 10%), reduced sensitivity to transverse pressure (saddles, anchorages)
  - → slightly lower strength of wires (f_{pk} = 1370…1570 MPa), additional 10% reduction of ultimate load due to twisting
  - → moderate stiffness reduction ($E_{eq} \approx$ 180 GPa)
  - → usually galvanized, combined only with surface coating (little extra weight)
  - → always manufactured in full length and cross-section (Ø40…180 mm), including sockets, delivered pre-stretched to site on reels
  - → main use:
    … single, large-diameter locked coil strands: stay cables
    … multiple smaller diameter locked coil strands as bundle (for suspension bridges and stay cables, obsolete)

Locked coil strand

Locked coil strand section

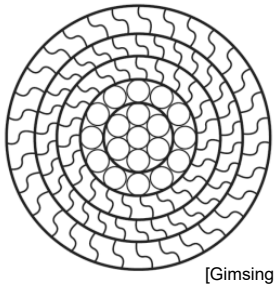

[Gimsing 2012]

Illustrations: Top © www.fatzer.com / bottom Gimsing, Cable Supported Bridges.

Cable-supported bridges – Common aspects: Cable types

- Parallel-wire main cables, consisting of a large number of individual wires, have been used since the early days of suspension bridges.
- Until the 1960s, the main cables of all major suspension bridges (including George Washington Bridge, Golden Gate Bridge, …) were fabricated on site by the air-spinning method:
  - → wires are drawn across the spans one by one (later several at a time) by spinning wheels, travelling between end anchorages
  - → after a certain number of wires is installed, they are bundled to hexagonal strands (to minimise voids when assembling them)
  - → all strand bundles are finally compressed into a dense packed cylinder (using a travelling hydraulic press) and wrapped with wires
- This process is simple, but weather sensitive, time consuming and very labour intense. In smaller suspension bridges, rather than individual wires, prefabricated strands were therefore hauled from one end anchorage to the other already in early bridges. In such cases, until the 1960s, helical strands were used (reasons see next slide), with the related disadvantages (higher void ratio, smaller stiffness, initial elongation requiring pre-stretching).

Main source Gimsing, Cable Supported Bridges.

Photo: daelim.co.kr

Cable-supported bridges – Common aspects: Cable types

- Pre-fabricated parallel-wire strands PPWS (Paralleldrahtkabel)
  → require neither reducing strength nor stiffness compared to the individual wires, which is clearly an advantage over helical strands, but they
  → were not used until the 1960s due to concerns about reeling (curving the undistorted section of a large parallel wire strand causes high stresses in the inner- and outermost wires)
- However, tests in the 1960s showed that parallel wire strands rotate when reeled (thus avoiding the excessive stresses).
- Since then, PPWS cables have largely replaced helical and locked-coil cables in short and medium span, as well as air-spun parallel wire cables in large span suspension bridges.
- Since long cables are required, the number of wires per strand is limited by transport and erection capacities. In recent suspension bridges, PPWS with up to 127 wires Ø5 mm were used, assembling the main cables from a large number of PPWS (figure: Strand reel Akashi-Kaikyo bridge, weight 85 t for a 4 km long 127-wire strand; 290 strands form each of the two main cables).
- The PPWS are hexagonal as the air-spun strands.

Prefabricated parallel wire strands

(parts of a main cable)

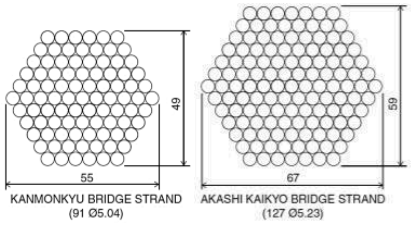

[Gimsing 2012]

Strand reel

[Gimsing 2012]

Illustrations: Gimsing, Cable Supported Bridges.

Cable-supported bridges – Common aspects: Cable types

Parallel wire cable
(Golden Gate Bridge, one of two suspension cables, *air-spun strands*)

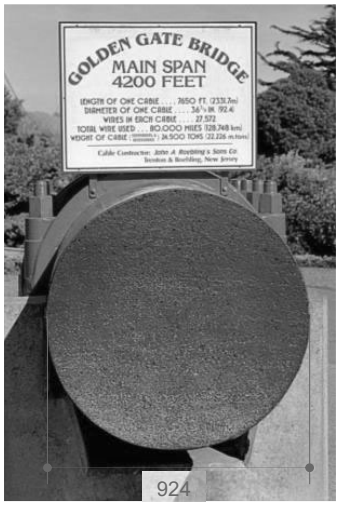

Cable detail (note outermost wires deformed by compaction)

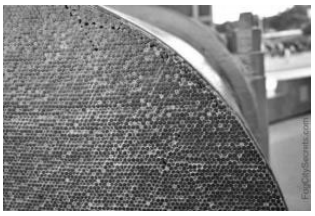

61 strands @ 452 wires Ø5 mm
(27'572 wires per cable)
4.33 t/m = 42.5 kN/m

PPWS cable
(Akashi-Kaikyo Bridge, one of two suspension cables, *prefabricated strands*)

Cable and strand dimensions [mm]

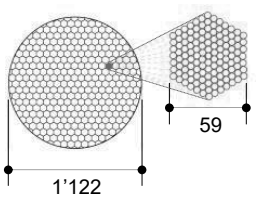

290 strands @ 127 wires Ø5 mm
(36'830 wires per cable)
6.33 t/m = 62 kN/m

Illustrations:

https://www.inside-guide-to-san-francisco-tourism.com/golden-gate-bridge-history.html

https://www.wikiwand.com/de/Drahtseil

https://awordfromjapan.files.wordpress.com/2012/07/dsc_0304.jpg

Cable-supported bridges – Common aspects: Cable types

- Larger parallel wire strands (up to 499 wires Ø7mm could be produced according to suppliers) are used for stay cables (top figure: largest stay cable of Zarate-Brazo Largo Bridges in Argentina (337 Ø7 mm wires)
- Perfectly parallel wire strands need to be held together
  - → wrapping by a spiral cable was usual in early cable-stayed bridges using parallel wire strands
  - → additional PE tube with corrosion inhibitor in void
  - → disadvantage: large diameter (wind loads) and higher dead load
- Since the 1990s, “New parallel wire strands”, developed in Japan, are being used (bottom figure). In these, the wire bundle is slightly twisted
  - → self-consolidating under tension (no need for wrapping)
  - → easier (un)reeling
  - → improved corrosion protection (cover extruded directly on wire bundle)

Prefabricated parallel wire strands

(stay cable)

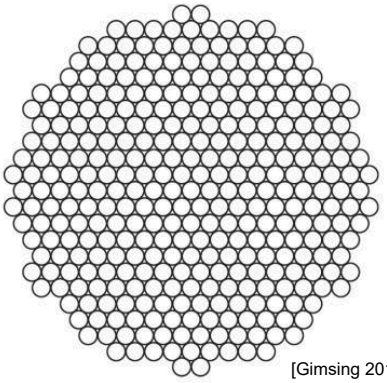

[Gimsing 2012]

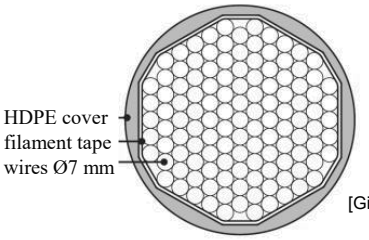

[Gimsing 2012]

Illustrations: Gimsing, Cable Supported Bridges.

Cable-supported bridges – Common aspects: Cable types

- Parallel strand stay cables consisting of 7-wire strands (up to 127 strands per cable according to suppliers) are often an economical solution today.
  - → usually installed and stressed one by one ('Isotension method'), small stressing equipment sufficient
  - → commonly made of galvanized wires today
  - → frequently each strand is protected by an extruded HDPE sheath (bottom figure)
- When using galvanized strands with individual HDPE sheaths
  - → no further corrosion protection is often provided
  - → but the stays need to be held together every 30-40 m to avoid individual oscillations of the strands
  - → cylindrical pipes are often provided to reduce drag (wind load on cables)
  - → relatively large void ratio, requiring larger diameters
- Alternatively, one may dispense of HDPE sheathing (reduced diameter), but dehumidification of the HDPE tube is then required for corrosion protection.

Parallel strand cables

(7-wire strands)

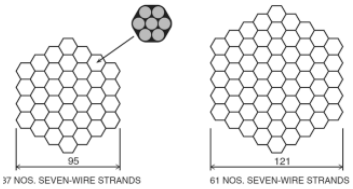

[Gimsing 2012]

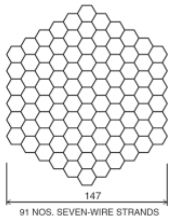

Strand detail

[tensa.nl]

Illustrations: Top Gimsing, Cable Supported Bridges, bottom Tensa.nl

Cable-supported bridges – Common aspects: Cable types

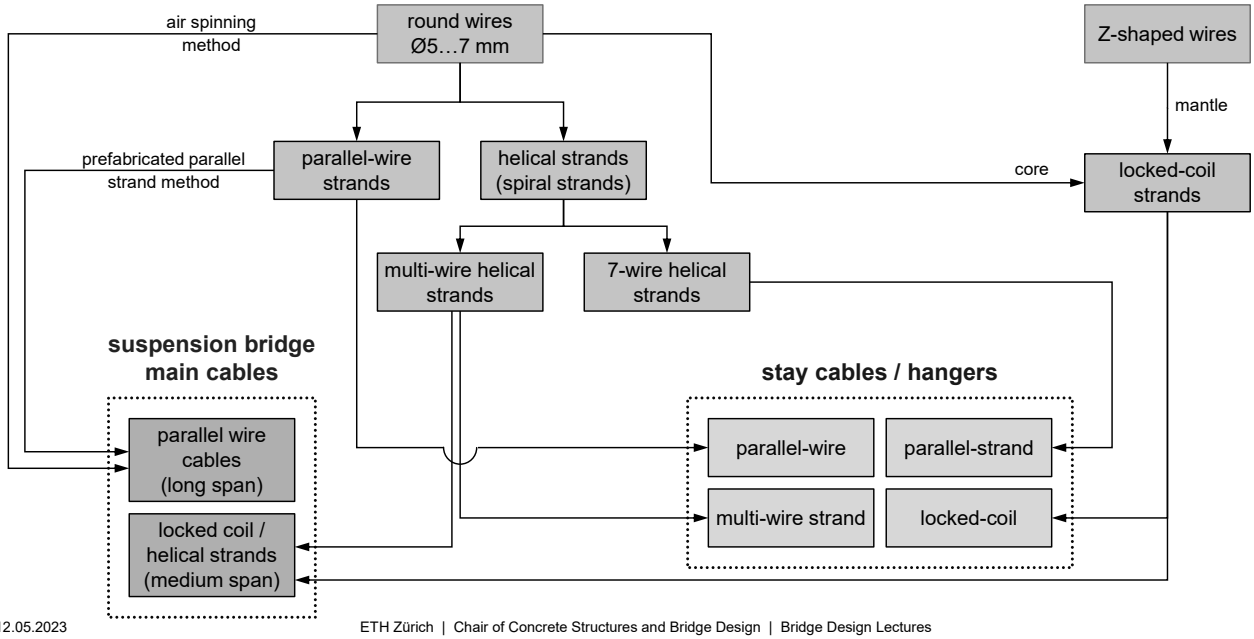

Cable-supported bridges – Common aspects: Cable types

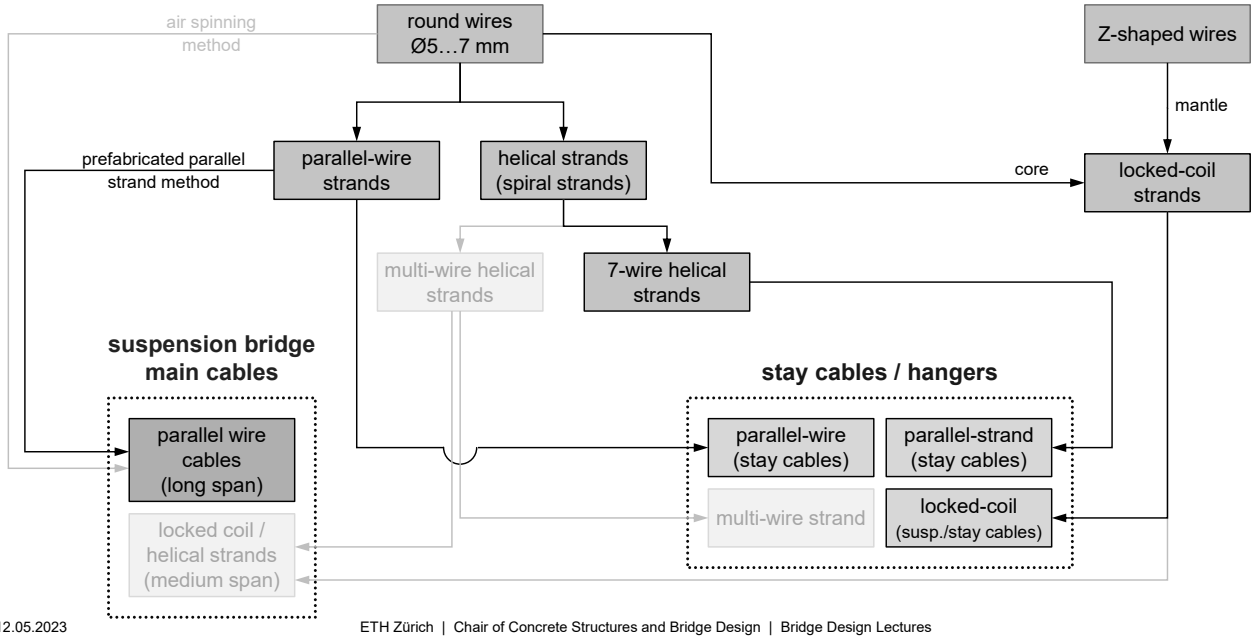

Cable-supported bridges – Common aspects: Cable types

- Modern parallel strand stay cables, including anchors, are high-tech, durable components (example see illustration)
- Using “wedge-only” anchoring, individual strands can be controlled and replaced if required (check fatigue resistance)

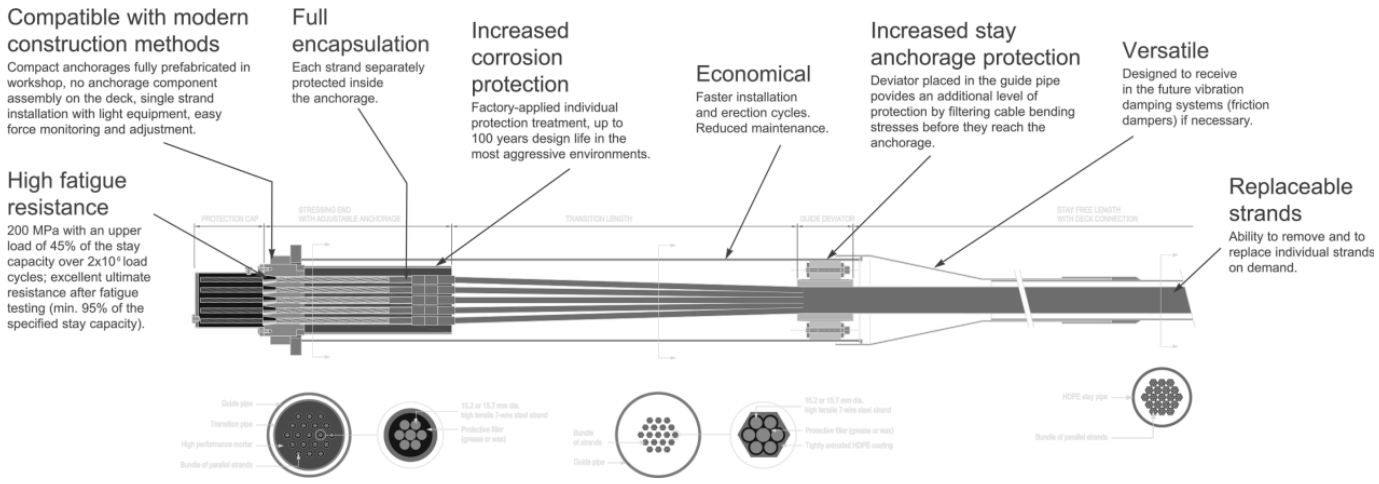

[VSL Stay Cable System 2000]

Illustration: VSL Stay cable system SSI 2000

Cable-supported bridges

Common aspects – Static analysis of cables
General cable behaviour

Cable-supported bridges – Common aspects: Laterally loaded cables

Cable-supported bridges differ significantly from girders:

- Girders as main structural component typically
  → require a relatively high amount of material
  → directly support the bridge deck
  → are supported directly on piers
  → cause only vertical reactions under vertical loads
  → extend over the length of the obstacle to be crossed
- Cables as main load-carrying element typically
  → require small quantities of structural material
  → require secondary elements (hangers) to transfer the deck loads to the cables
  → require supports (towers or pylons) much higher than the deck level
  → extend far beyond the obstacle to be crossed
  → require heavy anchor blocks to fix cables at their ends
- In spite of their high structural efficiency, cable supported bridges are therefore only advantageous if material consumption – and saving weight – is essential
  → Cable-supported bridges are economical only for long spans

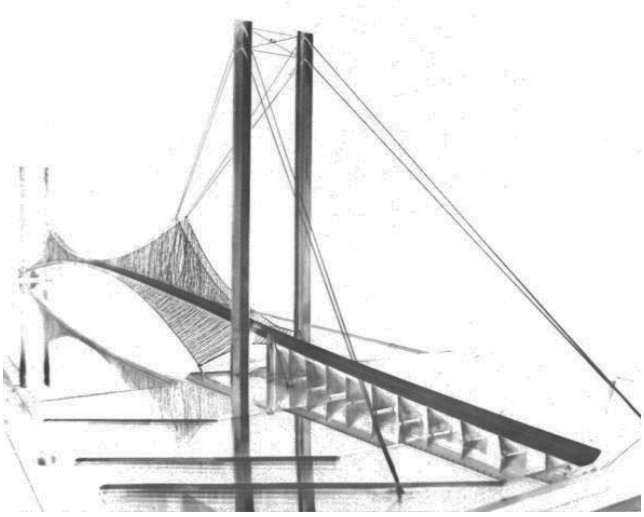

Illustration: Sergio Musmeci, Un ponte sullo Stretto di Messina: la luce più grande del mondo, 1971.

 a bridge across the Messina Straits would require a span above 3 km.

Cable-supported bridges – Common aspects: General cable behaviour

- While cables are very stiff under funicular loads (loads for which the cable's initial geometry is funicular, commonly dead load), they are considerably more flexible than girders under non-funicular load configurations.
- Hence, in the design of cable-supported structures, deformations are more of a concern than strength.
- In the detailed analysis and design of cable-supported bridges, numerical methods are used today, accounting for nonlinearities caused by large displacements, for the final layout as well as erection stages.
- If common cable configurations are used (reasonably two-dimensional cable planes), the initial geometry of the cable system may be determined using the same numerical methods, or the approximations for preliminary design outlined on the following slides.
- For complex, three-dimensional cable configurations, specialised form-finding tools may be used.

Cable profiles under non-symmetric load

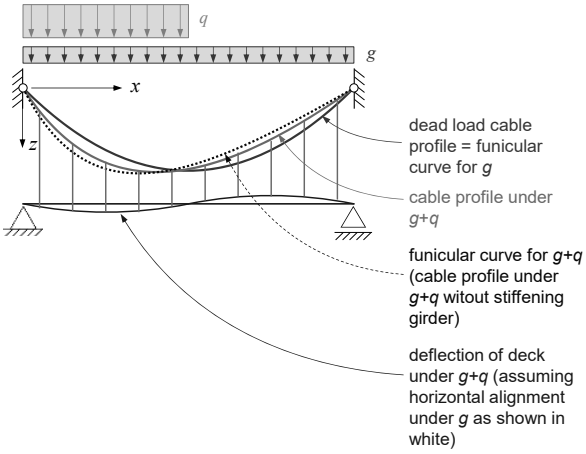

Cable-supported bridges – Common aspects: General cable behaviour

- The cable geometry under a given load can be determined iteratively, using the cable equation. This is outlined here following the lines of Marti, Theory of Structures (2012).
- Since large deformations occur, the equilibrium conditions must be formulated for the deformed system (using linear statics, a cable with $EI \to 0$ can only resist loads for which its initial geometry is funicular).
- Consider a flexible cable with constant axial stiffness but $EI = 0$ spanning between points O and A (left figure). The cable has an initial length *L*, and carries a vertical line load *q(x)* (including its self-weight).
- The cable equation is obtained formulating equilibrium of the deformed system (right figure and equations).
- The additional terms $L\alpha_T\Delta_T$ and $L\sigma_0/E$ account for possible thermal strain and cable prestress, constant along the cable length.

Static system of cable and cable element
(adapted from Marti, 2012; α = secant inclination due to anchorage height difference)

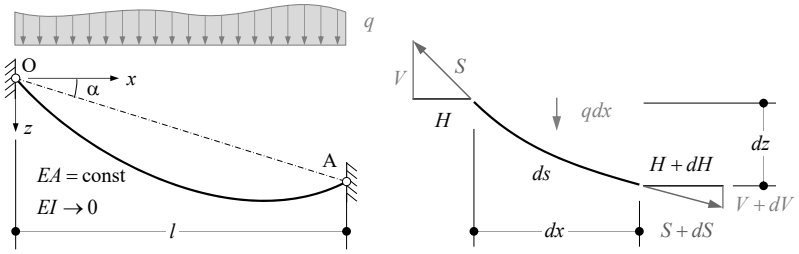

geometry: (a) $ds = \sqrt{dx^2 + dz^2} = dx\sqrt{1 + z'^2}$ $\{\text{with } z' = dz/dx\}$

equilibrium:
(b) $\Sigma F_x = dH = 0$
(c) $\Sigma F_z = qdx + dV = 0$
(d) $\Sigma M_y = Hdz - Vdx = 0$
$\rightarrow \begin{cases} H = \text{const} & \{\text{directly from (b)}\} \\ V = Hz' & \{\text{rewrite (d), with } z' = dz/dx\} \\ -Hz'' = q & \{\text{differentiate (d), insert (c)}\} \end{cases}$

cable force: (e) $S = \sqrt{H^2 + V^2} = H\sqrt{1 + z'^2}$ $\{\text{since } V = Hz', \text{ see above}\}$

deformed cable length: $\int_o^l \sqrt{1 + z'^2}\,dx = L\left(1 + \alpha_T \Delta T - \frac{\sigma_0}{E}\right) + \int_o^l \frac{S\sqrt{1 + z'^2}}{EA}\,dx$ ("cable equation")

(initial length L changes due to elastic strains S/EA, thermal strains $\alpha_T \Delta T$ and prestress σ_0)

Cable-supported bridges – Common aspects: General cable behaviour

- Using (e) and the equivalent shear force $\bar{V}$ and bending moment $\bar{M}$ in a simply supported beam subjected to q as reference (bottom figures), the rightmost term of the cable equation and the cable geometry can be expressed as:

$$\int_o^l \frac{S\sqrt{1+z'^2}}{EA}dx = \frac{H}{EA}\int_o^l \left(1+z'^2\right)dx = \frac{Hl}{EA} + \frac{H}{EA}\int_o^l \left(\tan\alpha + \frac{\bar{V}}{H}\right)^2 dx$$

$$z = x\tan\alpha + \frac{\bar{M}}{H} \qquad z' = \tan\alpha + \frac{\bar{V}}{H} \qquad z'' = -\frac{q}{H}$$

- For a given initial cable length and load, the cable geometry can be determined by (i) assuming a value of *H*; (ii) determining *z* and *z'* from the relationships above and (iii) iterating until the cable equation is satisfied, i.e.:

$$\int_o^l \sqrt{1+z'^2}\,dx = L\left(1+\alpha_T\Delta T - \frac{\sigma_0}{E}\right) + \frac{Hl}{EA} + \frac{H}{EA}\int_o^l \left(\tan\alpha + \frac{\bar{V}}{H}\right)^2 dx$$

  (note that q and hence $\bar{V}$ and $\bar{M}$ need to be adjusted to account for the cable self-weight unless this is negligible)

- In design, *L* is usually not given, but needs to be determined to achieve a certain sag = *z* at midspan → vary *L* or σ_0 until desired sag is obtained (and the cable equation satisfied).

Equivalent stress resultants for simply supported beam (adapted from Marti, 2012)

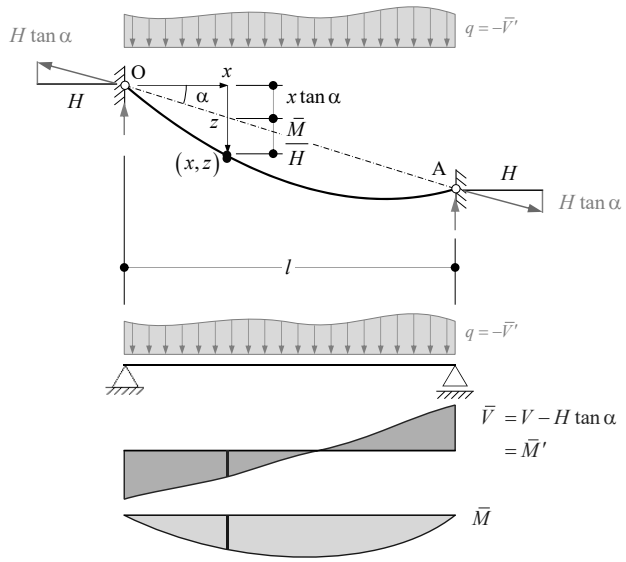

Cable-supported bridges – Common aspects: General cable behaviour

- For detailed design, numerical procedures (implemented in commercial software programs, such as e.g. Larsa 4D, Sofistik or Midas) are used.
- In preliminary design, and to determine the initial geometry in the numerical model, a uniformly distributed load (total loads span divided by span length) may be assumed.
- Under uniform load, the cable geometry is a quadratic parabola, and the integrals in the cable equation can be expressed analytically (see Marti, Theory f Structures), i.e., the length of the deformed cable under a load $\bar{q}$ is:

$$\frac{l}{2}\left[\sqrt{1+\beta^2}+\frac{\ln\left(\beta+\sqrt{1+\beta^2}\right)}{\beta}\right]=L\left(1+\alpha_T\Delta T-\frac{\sigma_0}{E}\right)+\frac{\bar{q}l^2}{2EA\cdot\beta}\left(1+\frac{\beta^2}{3}\right)$$

$$\text{where } \beta=\frac{4f}{l} \text{ and } \frac{l}{2}\left[\sqrt{1+\beta^2}+\frac{\ln\left(\beta+\sqrt{1+\beta^2}\right)}{\beta}\right]\approx l\left(1+\frac{\beta^2}{6}-\frac{\beta^4}{40}\right)$$

- Starting from a desired geometry (e,g. assuming $f \rightarrow \beta$ under dead load *g*), the initial cable length *L* is obtained. Knowing *L*, the sag *f* under any load *q* (or temperature difference) is determined by solving the equation for β.

Horizontal cable under uniform load

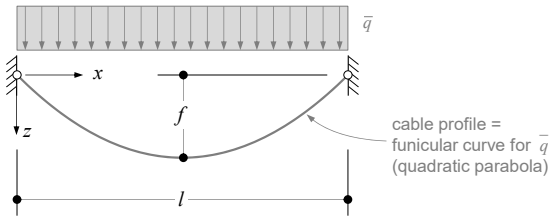

auxiliary parameter (sag/span): $\beta=\frac{4f}{l}$

hor. component of cable force: $H=\frac{\bar{q}l^2}{8f}$

maximum cable force: $S=H\sqrt{1+\beta^2}$

cable elongation ($\Delta T=0, \sigma_0=0$): $\Delta L=\frac{\bar{q}l^2}{2EA\cdot\beta}\left(1+\frac{\beta^2}{3}\right)=\frac{Hl}{EA}\left(1+\frac{\beta^2}{3}\right)$

Notes:

- Even if the cable weight is a significant part of the total weight of a suspension bridge, the errors caused by assuming a uniformly distributed load are almost exclusively due to non-uniform traffic loads; catenary and parabola nearly coincide due to the low sag/span ratio (1:9…1:11) in usual suspension bridges.

- The power series approximation (quadric function in β) of the left side of the cable equation, i.e.

$$\int_o^l\sqrt{1+z'^2}\,dx=\frac{l}{2}\left[\sqrt{1+\beta^2}+\frac{\ln\left(\beta+\sqrt{1+\beta^2}\right)}{\beta}\right]\approx l\left(1+\frac{\beta^2}{6}-\frac{\beta^4}{40}\right)$$

  is obsolete with today's computing power. It is indicated since it will be used to derive the stiffness of laterally loaded cables, and it was used as basis of many approximate formulas found in literature, e.g. in Pugsley, A.G., 1968. The Theory of Suspension Bridges. Edward Arnold, London and de Miranda, F., "Long Span Bridges", Innovative Bridge Design Handbook, Elsevier, 2016.

- In the common (except in stress ribbons) case of several spans – typically a main span and two side spans – an iterative procedure is required to match the cable forces in the different spans, involving horizontal displacements of the "supports" of each span.

Cable-supported bridges

Common aspects – Static analysis of Cables
Laterally (usually vertically) loaded cables

Cable-supported bridges – Common aspects: Laterally loaded cables

- On this and the following slides, the behaviour of suspension bridges (resp. their main cables) is investigated following the example used by Gimsing (see notes for source).
- The example is based on the following basic parameters:
  - span $l = 1'000$ m, $f_g/l = 0.1$ (100 m sag under g)
  - dead load $g = 220$ kN/m, traffic load $q = 80$ kN/m
  - cable cross-section $A = 0.56$ m² (14'551 wires Ø7 mm) (cable weight = 44.0 kN/m ≈ 20% of g, not negligible!)
- Solving the cable equation for $\beta_g = 0.4$ (dead load geometry, no thermal strain nor prestress), the initial cable length L is:

$$\frac{l}{2}\left[\sqrt{1+\beta_g{}^2}+\frac{\ln\left(\beta_g+\sqrt{1+\beta_g{}^2}\right)}{\beta_g}\right]=L+\frac{gl^2}{2EA\cdot\beta_g}\left(1+\frac{\beta_g{}^2}{3}\right)\rightarrow L=1023.474\text{ m}$$

- The full load geometry is obtained by solving for β_{g+q}:

$$\frac{l}{2}\left[\sqrt{1+\beta_{g+q}{}^2}+\frac{\ln\left(\beta_{g+q}+\sqrt{1+\beta_{g+q}{}^2}\right)}{\beta_{g+q}}\right]=L+\frac{(g+q)l^2}{2EA\cdot\beta_{g+q}}\left(1+\frac{\beta_{g+q}{}^2}{3}\right)$$

$$\rightarrow \beta_{g+q}=0.4069,\quad f_{g+q}=\frac{\beta_{g+q}l}{4}=101.726\text{ m},\quad w(q)=101.726-100=1.726\text{ m}$$

Deflection under traffic load acting over varying width *b* (adapted from Gimsing 2012)

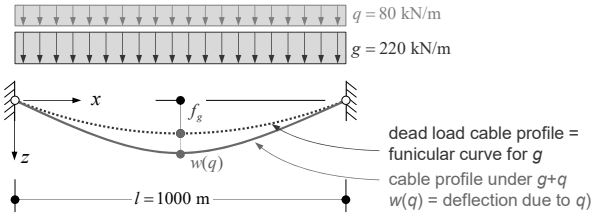

Dead load ($g = 220$ kN/m, chosen $\rightarrow f_g = 100$ m):

$$\beta_g=\frac{4f_g}{l}=0.4000 \qquad H_g=\frac{gl^2}{8f_g}=275\text{ MN}$$

$$S_g=H_g\sqrt{1+\beta_g{}^2}=296\text{ MN} \quad \sigma_g=\frac{S_g}{A_c}=491\text{ MPa}$$

Full load ($g+q = 300$ kN/m, cable equation $\rightarrow f_{g+q} = 101.726$ m):

$$\beta_{g+q}=\frac{4f_{g+q}}{l}=0.4069 \qquad H_{g+q}=\frac{(g+q)l^2}{8f_{g+q}}=368\text{ MN}$$

$$S_{g+q}=H_{g+q}\sqrt{1+\beta_{g+q}{}^2}=398\text{ MN} \quad \sigma_{g+q}=\frac{S_{g+q}}{A_c}=711\text{ MPa}$$

Source and further reading: Niels J. Gimsing, Christos T. Georgakis. Cable Supported Bridges – Concept and Design, Wiley, 1983 (3rd edition, 2012).

Note that the effect of cable inclination on the dead load has been eglected (uniform dead load) in all calculations.

Cable-supported bridges – Common aspects: Laterally loaded cables

- This slide compares the midspan deflection due to traffic load over the central part of the main span, over a varying portion *b* of the span *l*:
  → the midspan deflection under traffic load over the full span is 1.726 m, fully due to cable elongation.

  the same deflection is obtained for only ca. 10% loaded length

  → under partial length loading, the cable deflects more, with a maximum deflection of 3.12 m for a loaded length of about 40% of the span

  → only about 1/3 of the maximum deflection is due to cable elongation for 40% loaded length. The remaining deflection is due to the change of cable geometry.

  note that under uniform load (traffic load over the full span), deflections of a rigid cable are zero.

Deflection under traffic load acting over varying width *b* (adapted from Gimsing 2012)

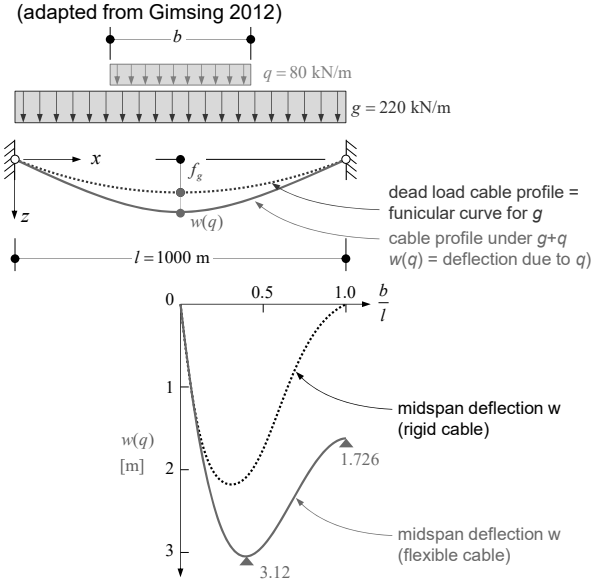

Source and further reading: Niels J. Gimsing, Christos T. Georgakis. Cable Supported Bridges – Concept and Design, Wiley, 1983 (3rd edition, 2012).

Cable-supported bridges – Common aspects: Laterally loaded cables

- As illustrated on the previous slide, starting from the fully loaded span, the midspan deflection increases if traffic loads in the outer parts are removed
- This effect, which is the opposite of what is observed in a simply supported beam, is more pronounced in slack cables (high sag/span ratio f_g/l) than in taut ones, see figure below (cable area adjusted to account for f_g/l):

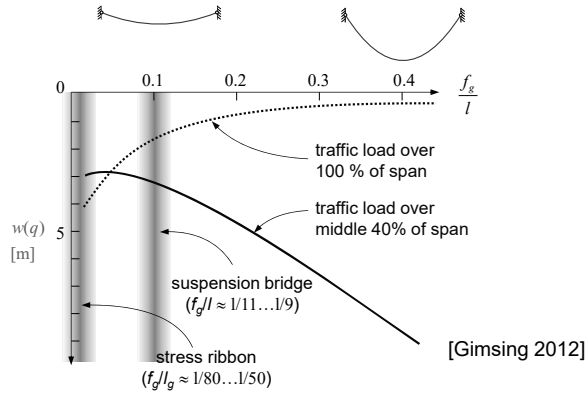

[Gimsing 2012]

Deflection under traffic load acting over varying width b (adapted from Gimsing 2012)

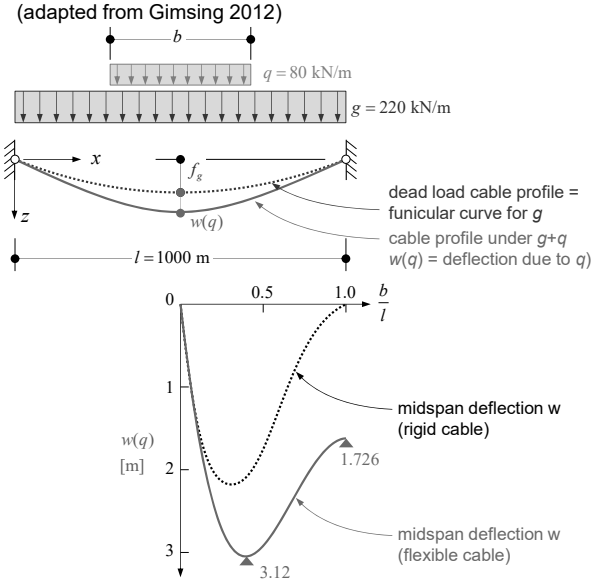

Note that the results shown here presume rigid supports. In real bridges, the tower heads deform horizontally towards the main span it loaded by traffic, causing an increase of midspan deflections. Therefore, the maximum midspan deflections typically occur at longer loaded lengths than 40% of the main span.

Cable-supported bridges – Common aspects: Laterally loaded cables

- The tension force in the cable (due to uniform load) has a stiffening effect on the deformations caused by traffic loads (the deviation from funicular load caused by the traffic load decreases with higher dead load).
- This is illustrated on this slide considering traffic load on one half of the span, and varying the dead load (same / double / half the value of previous slides):
  - → the maximum deflection under traffic load is significantly affected by the dead load
  - → modern lightweight suspension bridges (steel box girders with orthotropic steel deck) deflect much more under traffic loads than old suspension bridges with heavy steel trusses and concrete decks due to their reduced weight
  - → The bending stiffness of girders, neglected here, does not alter this conclusion, see next slides.

Deflection under traffic load in right half span, with varying self-weight *g* (adapted from Gimsing 2012)

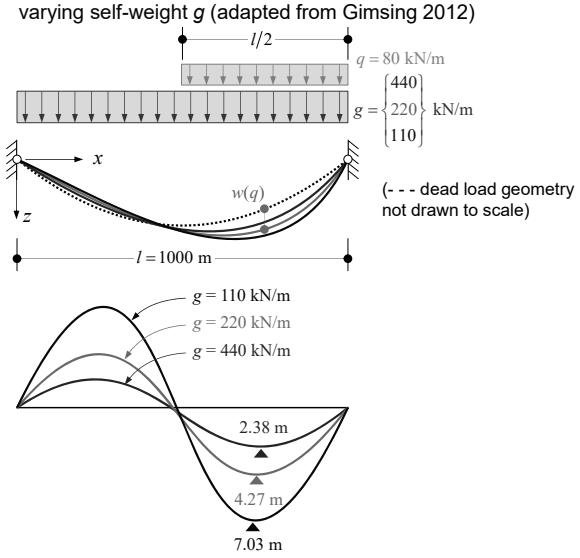

Cable-supported bridges – Common aspects: Laterally loaded cables

- Under non-symmetrical load, the points on the cable between its ends shift to the side with higher load (upper figure).
- This can be prevented, for example, by providing a prestressed guy cable (lower figure), which is connected to the middle of the main cable, see Marti (2012).
- The guy cable will cause a slight kink in the main cable at the connection, and a significantly stiffer behaviour
- In suspension bridges, a connection of suspension cables and deck girder is often used to achieve this effect.

Deflection under traffic load in right half span

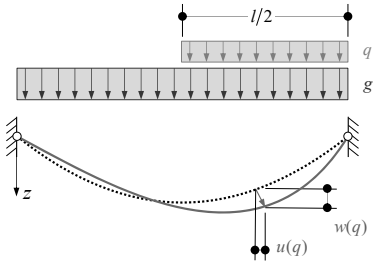

(- - - dead load geometry not drawn to scale)

Deflection under traffic load in right half span with guy cable (see Marti 2012)

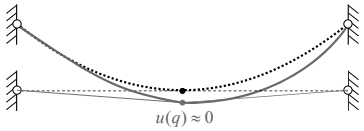

- So far, a single span with rigid supports has been assumed. On the following slides, the effect of several spans is investigated.

Cable-supported bridges – Common aspects: Laterally loaded cables

- The deformations of suspension bridges are significantly affected by the span layout. This is illustrated following (once again) an example given by Gimsing [Gimsing 2012].
- The figure compares the deflections of two three-span cables with spans of 500+1000+500 m and 250+1000+250 m, respectively, due to traffic load in the main span (other parameters as previous slides).
  - → midspan deflection in bridge with short side span is only ca. 40% of that with long side span (in a continuous beam, the midspan deflection would only decrease by ca. 20% if the side span is halved)
  - → strong influence of side span length primarily caused by horizontal displacements u_T of the tower tops (almost four times larger for long side span)
  - → horizontal displacements of the tower tops are primarily caused by sag reduction of the cables in the end spans (and not the elongation of the cable), see following slide.

Deflection under traffic load in main span, with varying side span length (adapted from Gimsing 2012)

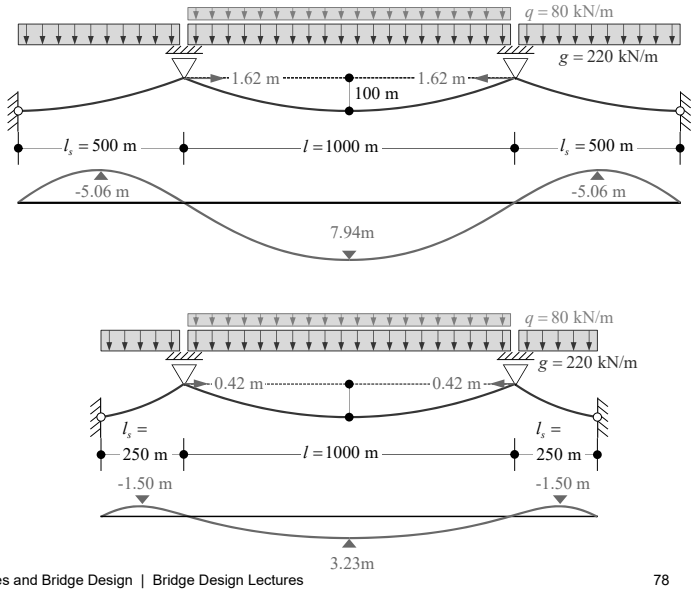

Cable-supported bridges – Common aspects: Laterally loaded cables

- Horizontal displacements of the tower tops are
  - → smaller with short side spans since the cable is initially tauter in the side spans (smaller sag required at same cable force and dead load)
  - → larger for higher dead load since the cable is initially slacker in the side spans (larger sag required at same cable force and span)

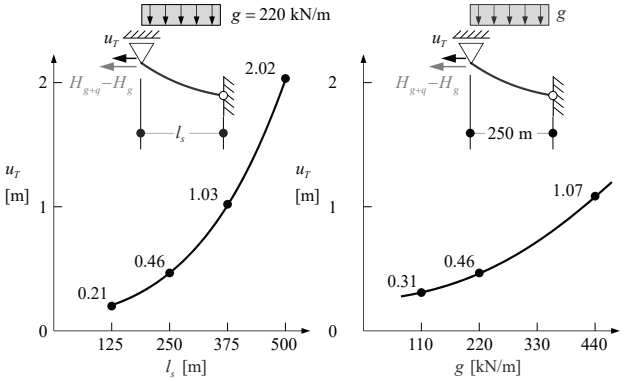

Deflection under traffic load in main span, with varying side span length (adapted from Gimsing 2012)

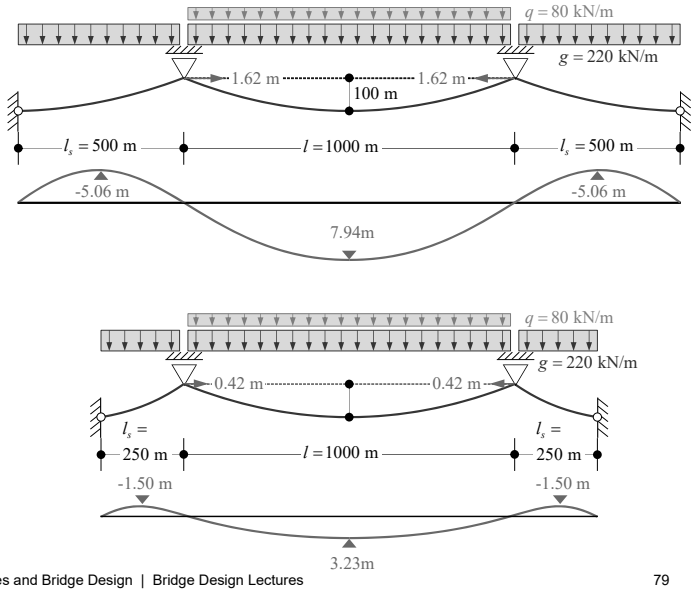

Note: Plots based on cable area corresponding to a maximum cable stress of 720 MPa under *g*+*q*.

Cable-supported bridges – Common aspects: Laterally loaded cables

- The sensitivity of cables to horizontal displacements of the supports increases with reduced sag:
  → Under equal support displacements, taut cables deflect much more than slack cables
  → Effect particularly relevant in stress-ribbons (see section on stress ribbon bridges)
- Strains imposed to the cables (temperature, creep and shrinkage in stress-ribbons) have a similar effect as horizontal support displacements.

Deflection due to horizontal support displacements

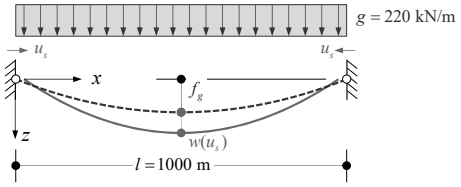

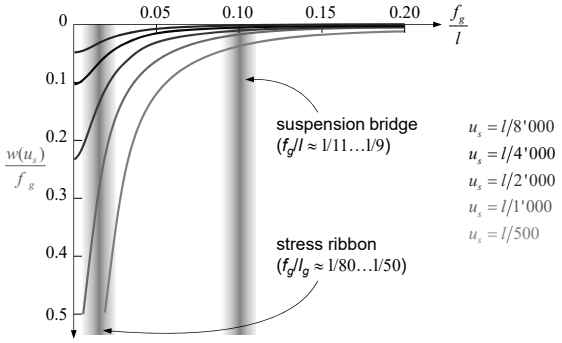

Note: Plots based on cable area corresponding to a maximum cable stress of 720 MPa under *g*+*q*.

Cable-supported bridges – Common aspects: Laterally loaded cables

- So far, it has not only been assumed that the cable acts as a rope without bending stiffness, but the stiffening effect of the deck girder has been neglected.
- This is justified in preliminary design, as illustrated by this slide comparing the deflections for the cable alone with those of suspension bridges with two different stiffening girder layouts:
  → differences negligible for traffic load over entire main span
  → differences small for traffic load over half the main span

Comparison of deflections under traffic load
(adapted from Gimsing 2012)

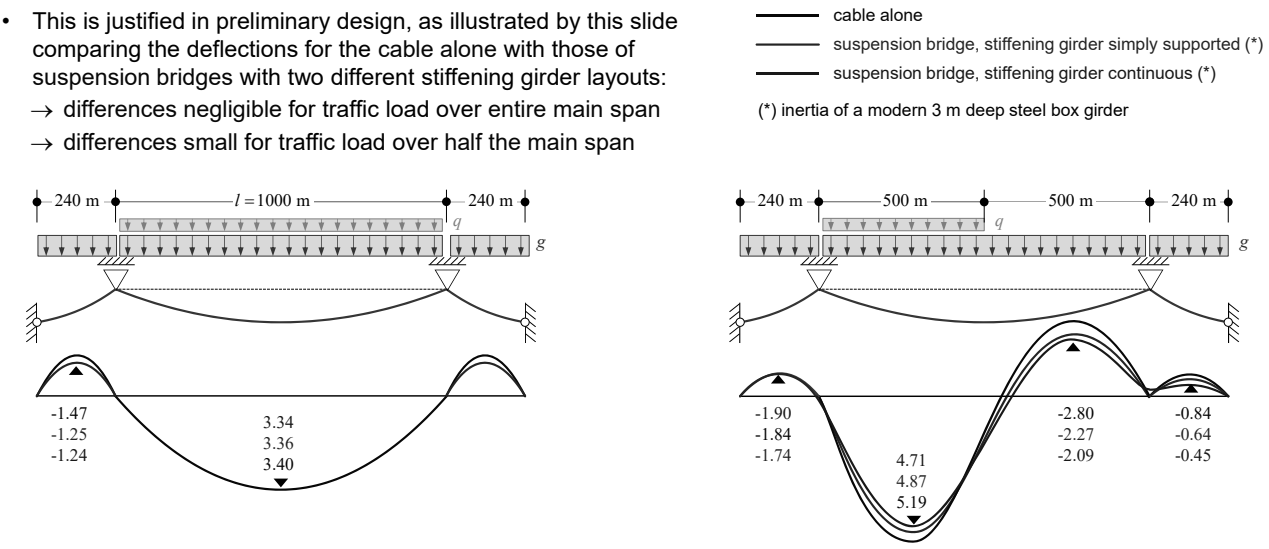

Cable-supported bridges

Common aspects – Static analysis of Cables
Axial stiffness of laterally loaded cables

Cable-supported bridges – Axial stiffness of laterally loaded cables

- The axial stiffness of laterally loaded cables is highly relevant in cable-supported structures, as illustrated on the previous slides.
- It is particularly important for long stay cables, whose axial stiffness – which directly affects the vertical displacements of the bridge girder – is reduced by the sag (photo).
- If a horizontal cable without lateral load ($q_0 = 0$) is subjected to an increase $\mathrm{d}H$ of the horizontal force H (figure), its end support B will displace to the right by:

$$du = dH \cdot \frac{l}{EA}$$

  A lateral load $q_0 > 0$ on the cable causes a sag, $q_0 l^2/(8H)$, and the displacement of support B due to dH for $q_0 > 0$ can be approximated using the cable equation (see Marti, 2012):

$$du = dH\left(\frac{l}{EA} + \frac{q_0^2 l^3}{12H^3}\right)$$

- Comparing the two results, the axial stiffness of the laterally loaded cable, idealised as straight cable with the chord length can be expressed using an idealised modulus of elasticity:

$$E_i = \frac{E}{1 + \frac{q_0^2 l^2}{12H^3} EA} \qquad \rightarrow du = dH \cdot \frac{l}{E_i A}$$

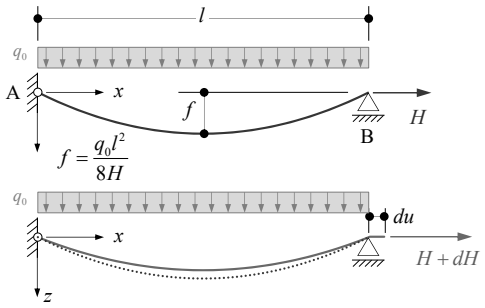

Photo: Niels J. Gimsing, Christos T. Georgakis. Cable Supported Bridges – Concept and Design, Wiley, 1983 (3rd edition, 2012).

Cable-supported bridges – Axial stiffness of laterally loaded cables

- Similarly, for a cable at an angle α to the horizontal with a total weight *G*, one gets (see Marti, 2012), with *S* = force in direction of cable chord:

$$E_i = \frac{E}{1 + \frac{G^2 \cos^2 \alpha}{12 S^3} EA} \qquad \rightarrow ds = dS \cdot \frac{l}{E_i A}$$

known as *Ernst* Equation (see notes for source and further information).

- Using the specific weight γ of the cable (total cable weight / steel volume), the idealised modulus of elasticity can be rewritten:

$$G \approx \gamma \cdot A \cdot l, \quad \sigma = \frac{S}{A} \qquad \rightarrow E_i = \frac{E}{1 + \frac{\gamma^2 a^2}{12 \sigma^3} E}; \qquad \frac{1}{E_i} = \frac{1}{E} + \frac{\gamma^2 a^2}{12 \sigma^3}$$

- As seen from the plot on the right, the axial stiffness is significantly reduced in long cables, even if they are taut (high stress levels)
- The idealised modulus of elasticity above is valid at one specific stress level (tangent modulus). For more refined analyses, the following approximate secant stiffness between two stress levels can be used:

$$E_{sec} = \frac{E}{1 + \frac{\gamma^2 a^2}{24} \left(\frac{\sigma_1 + \sigma_2}{\sigma_1^2 \cdot \sigma_2^2} \right) E}; \quad \frac{1}{E_{sec}} = \frac{1}{E} + \frac{\gamma^2 a^2}{24} \left(\frac{\sigma_1 + \sigma_2}{\sigma_1^2 \cdot \sigma_2^2} \right)$$

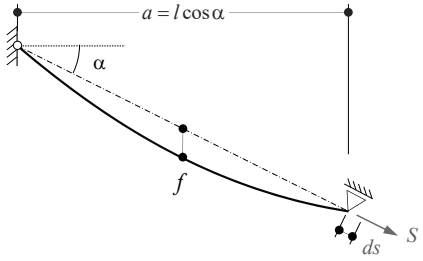

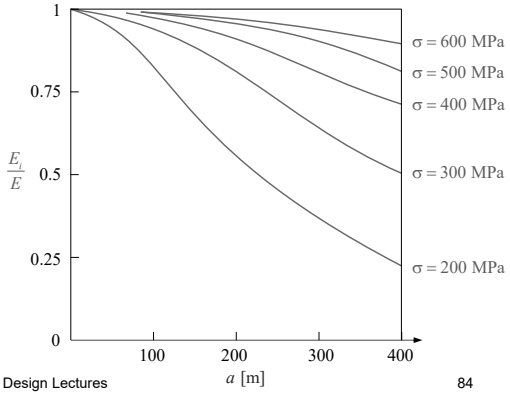

H.J. Ernst proposed the idealised elastic modulus given in the slide, as well as the secant modulus, in 1965 (Ernst, H.J., Der E-Modul von Seilen unter Berücksichtigung des Durchhanges. Bauingenieur Vol. 40, No. 2, 1965, pp. 52-55).

The Ernst equation (idealised elastic modulus) does not account for the geometric end condition at the cable anchorages, i.e., the difference between chord direction and cable inclination at the ends (obviously, the cable force is not aligned with the chord but with its direction, hence if one applies a load that is – as assumed in the derivation of the equations – aligned with the chord direction, there must be a reaction perpendicular to the latter by equilibrium). While this is negligible at normal levels of cable force (and corresponding sags) in the final bridge configuration, it is significant for construction stages with very low cable forces. In these cases, a chord model with adjusted stiffness (using the idealised elastic modulus) will overestimate the vertical stiffness, and underestimate the horizontal one. According to David Goodyear (one of the most eminent bridge designers and expert in cable-stayed bridges), neglecting this effect is the main reason why decks of cable-stayed bridges are often lower than predicted by the erection stage analysis. He recommends to use catenary elements for the cables in the FE-model at such low cable forces. If the software used does not have this option, the cable can be modelled by general nonlinear beam elements with geometric stiffness accounting for large displacements (however, such a model will take very long to solve, since several elements are needed for each cable to obtain realistic results).

Cable-supported bridges – Axial stiffness of laterally loaded cables

- As seen from the plot on the previous slide, the reduction of the idealised modulus of elasticity is pronounced for long cables working at a low stress.
- In bridges, the vertical (rather than axial) stiffness of the stays is of primary interest. Considering a single stay cable inclined at an angle α, the cable force due to a load Q and the resulting cable elongation are

$$S = \frac{Q}{\sin\alpha} \qquad ds = \frac{Q}{\sin\alpha} \cdot \frac{l}{E_i A}$$

  and assuming that the deck girder is axially rigid, the vertical displacement (using e.g. the Williot diagram) corresponds to

$$w = \frac{ds}{\sin\alpha} = \frac{Q}{\sin^2\alpha} \cdot \frac{l}{E_i A}$$

- Hence, the vertical stiffness of the stay is

$$k_z = \frac{Q}{w} = \frac{E_i A}{l} \sin^2\alpha = E_i A \cdot \frac{h^2}{l^3} \qquad \left(\frac{h}{l} = \sin\alpha\right)$$

- As the longest stays are typically also the flattest, their vertical stiffness is thus strongly reduced by the combined effect of sag (E_i), and inclination.
- The equations still neglect the difference between chord direction and cable inclination at the bottom anchorage, which is relevant for very low stress and large sag (erection), see notes on previous slide for details.

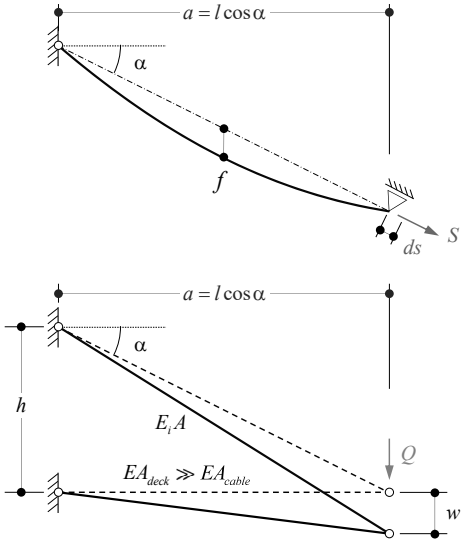

Further reading: W. Kaufmann, D. Karagiannis, K. Widmer, “Load factors for permanent actions and cable preload in cable-stayed bridges,” Structural Engineering International, IABSE, 2020.

Cable-supported bridges

Common aspects – Static analysis of Cables
Combined cable-type and bending response

Cable-supported bridges – Common aspects: Bending of cables

- When analysing the global structural behaviour of cable-supported bridges, it is usually sufficient to neglect the bending stiffness of the cables – even in the case of stress-ribbons with a relatively stiff cross-section (see section on stress-ribbons).
- However, local bending of the cables (resp. stress ribbons) needs to be considered to verify
  → fatigue stresses, particularly for stay cables
  → serviceability of stress ribbons (crack widths, durability)
- The behaviour of stress-ribbons can be analysed by accounting for the combined cable-type and bending response. As outlined by Marti (Theory of Structures, 2013, Chapter 18.9), the differential equation

$$EIw'''' - \left(H + \Delta H\right) w'' = q - g\frac{\Delta H}{H} \qquad \left(H = H(g), \Delta H = \Delta H(q)\right)$$

  with the solution

$$w = c_1 + c_2 x + c_3 \cosh(\lambda x) + c_4 \sinh(\lambda x) + w_{part} \qquad \left(\lambda = \frac{H + \Delta H}{EI}\right)$$

  covers the entire spectrum from a pure bending response only ($\lambda = 0$), to a pure cable-type response ($\lambda \to \infty$). Note that it has been assumed in the derivation of the differential equation that the dead load *g* is carried by cable tension alone.

Stress-ribbon geometry used for illustrations on next slides (typical stress-ribbon footbridge)

Elevation

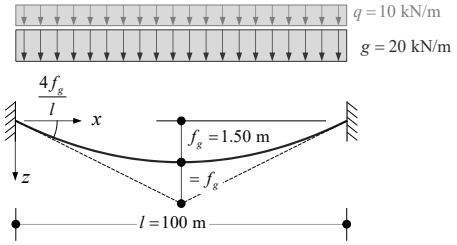

Cross-section

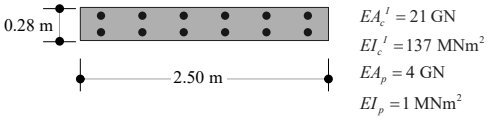

Note: Plots based on cable area corresponding to a maximum cable stress of 720 MPa under *g*+*q*.

Cable-supported bridges – Common aspects: Bending of cables

- In cables – particularly stay cables and stress-ribbons – bending moments are caused by sag variations (due to load, imposed strains or dynamic effects), since the end anchorages are commonly fixed, rather than hinged.
- Solving the differential equation given on the previous slide, one gets the following expression for the bending moments (Marti 2012, 19.9.2.2):

$$M(x) = \frac{g_c}{\lambda^2} + \left(\varphi_0 - \frac{g_c b}{2N}\right)\sqrt{N \cdot EI} \cdot \frac{\cosh\left[\lambda\left(\frac{b}{2} - x\right)\right]}{\sinh(\lambda \frac{b}{2})} \quad \left(\lambda = \sqrt{\frac{N}{EI}}\right)$$

  where b = horizontal span and φ_0 = imposed end rotation of cable. The first term on the right side can usually be neglected.

- As illustrated in the figure for $\varphi_0 = 0$, the bending moments
  → range from 5…20% of those in a clamped girder for $\varphi_0 = 0$
  → are localised near the end anchorages (particularly for low bending stiffness, as is the case in stay cables)
- If the end rotation φ_0 is set to that of a hinged cable under dead load, as usual, variable loads and end rotations still cause bending moments.

Bending moments due to dead load
(cable end rotation $\varphi_0 = 0$)

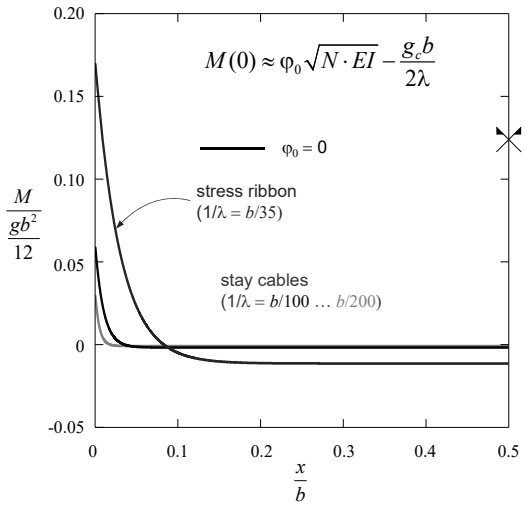

Note: Plots based on cable area corresponding to a maximum cable stress of 720 MPa under *g*+*q*.

Cable-supported bridges – Common aspects: Bending of cables

- In stress-ribbons, relevant bending moments are also caused by traffic loads. Analytical solutions are available e.g. for the cases shown on the right:
  → asymmetric traffic load on half a span (Marti 2012, 18.9.3.2)
  → concentrated load at midspan (Marti 2012, 18.9.3.3)
- The figures illustrate the bending moments for a typical stress-ribbon (cross-section see previous slides). It can be seen that the bending moments are 1-2 orders of magnitude smaller than in a beam of equal span, and also significantly smaller than in a two-hinged arch (where they would amount to $ql^2/64$ and $7Ql/128$, respectively). Due to the high slenderness of the stress ribbon, they are, however, still not negligible.
- The bending moments that would occur if only the cables were active (concrete as weight), whose values are indicated in brackets, are another order of magnitude smaller.
- For general loading, geometrically nonlinear analyses accounting for large deformations are required. Specialised software is recommended for such cases.

Bending moments under selected load configurations (normalised with M in a two-hinged arch under same load)

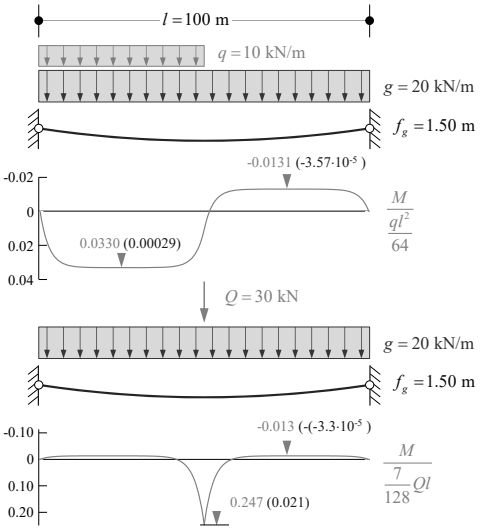

Note: Plots based on cable area corresponding to a maximum cable stress of 720 MPa under *g*+*q*.

Cable-supported bridges

Common aspects – Dynamic effects

Cable-supported bridges

Common aspects – Dynamic effects
Pedestrian-induced oscillations

Cable-supported bridges – Dynamic effects: Pedestrian-induced oscillations

- Many early suspension bridges suffered from excessive oscillations due to traffic or wind, and several unfortunately collapsed.
- For example, the following bridges collapsed due to oscillations caused by pedestrians:
  - According to some sources (Stiftung Deutsches Technikmuseum Berlin Historisches Archiv), the Saalebrücke in Nienburg (chain-stayed bridge, l = 80 m, Christian Gottfried Heinrich Bandhauer, 1825) collapsed due to rhythmic movements of the singing crowd on the bridge.
  - The Broughton chain suspension bridge (l = 44 m, S. Brown, 1826), collapsed in 1831 by a detachment of 74 soldiers marching in step. 20 soldiers were injured, six severely.
  - The Angers wire-cable suspension bridge (Pont de la Basse-Chaîne, l = 102 m, J. Chaley, 1838), presumably collapsed in 1850 by a combination of corrosion in anchor cables and resonance caused by a battalion of almost 800 soldiers crossing the bridge during a thunderstorm with strong wind (not walking in step, but involuntarily moving in tune, known as “lateral lock-in” today). 226 soldiers died.

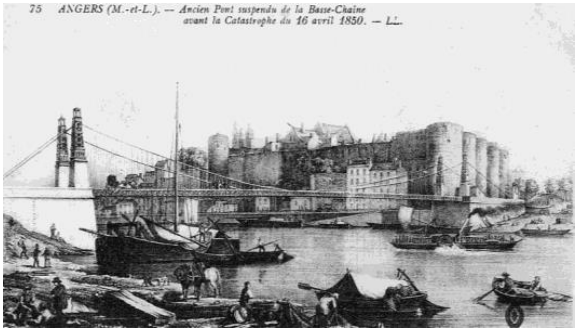

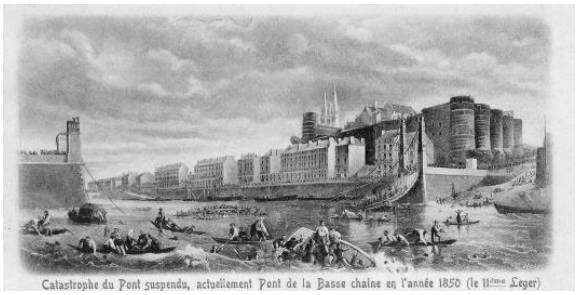

Source Broughton collapse: Anon (16 April 1831), "Fall of the Broughton suspension bridge, near Manchester". The Manchester Guardian.

On 12 April 1831, the 60th Rifle Corps carried out an exercise on Kersal Moor under the command of Lieutenant Percy Slingsby Fitzgerald […]. As a detachment of 74 men returned to barracks in Salford by way of the bridge, the soldiers, who were marching four abreast, felt it begin to vibrate in time with their footsteps. Finding the oscillations amusing, some of them started to whistle a marching tune, and to "humour it by the manner in which they stepped", causing the bridge to vibrate even more. The head of the column had almost reached the Pendleton side when they heard "a sound resembling an irregular discharge of firearms". Immediately, one of the iron columns supporting the suspension chains on the Broughton side of the river fell towards the bridge, carrying with it a large stone from the pier to which it had been bolted. The corner of the bridge, no longer supported, then fell 16 or 18 feet into the river, throwing about forty of the soldiers into the water or against the chains. The river was low and the water only about two feet deep at that point. None of the men were killed, but twenty were injured, including six who suffered severe injuries including broken arms and legs, severe bruising, and contusions to the head.

Angers collapse: Rapport de la commission d'enquête (MM. Dupuit, Mery de Contades, Hougan, Roland, Mahyer, 20 avril 1850), pour rechercher les causes et les circonstances qui ont amené la chute du pont suspendu de la Basse-Chaîne". Annales des Ponts et Chaussées: 394–411.

The failure was attributed to dynamic load due to the storm and the soldiers, particularly as they seem to have been somewhat in step, combined with corrosion of the anchors for the main cables. The cable anchorages at Angers were found to be highly vulnerable, as they were surrounded by cement, which was believed to rustproof them for the indefinite future. However, the wire strands separated from their cement surrounds. This allowed water to penetrate and corrode the wires. Citation see next slide.

Photos: Pont de la Basse-chaine before collapse. La rupture du Pont de la Basse-Chaîne à Angers en 1900. both © Wikimedia commons.

Cable-supported bridges – Dynamic effects: Pedestrian-induced oscillations

- Many lightweight bridges experience excessive oscillations under pedestrian load. Evidently, many people walking in step increase the amplitude of the vibrations.
- The Albert Bridge in London (1873) is one of many examples where troops are advised to break step to avoid problems. In Switzerland, the same rule holds e.g. for the pedestrian suspension bridge under the SBB Aarebrücke in Brugg, frequently used by soldiers in the nearby barracks.

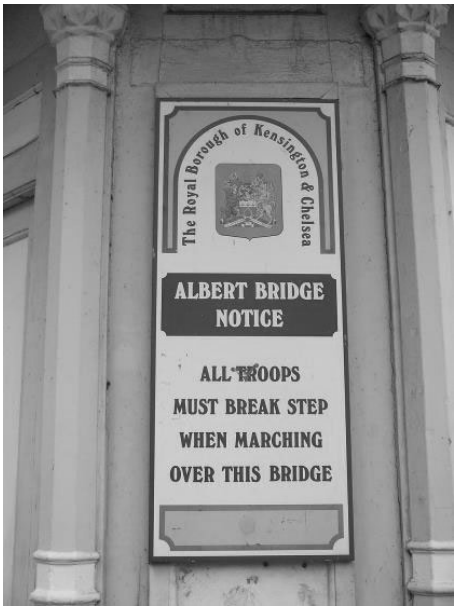

Albert Bridge, London, U.K., Rowland Mason Ordish, 1873. Main Span 122 m. Photo Wikimedia Commons, David Iliff / Iridescent

Wikipedia: *The bridge acquired the nickname of "The Trembling Lady" because of its tendency to vibrate, particularly when used by troops from the nearby Chelsea Barracks. Concerns about the risks of mechanical resonance effects on suspension bridges, following the 1831 collapse of the Broughton Suspension Bridge and the 1850 collapse of Angers Bridge, led to notices being placed at the entrances warning troops to break step (i.e. not to march in rhythm) when crossing the bridge.*

(continued from previous slide) Angers collapse: Rapport de la commission d'enquête (MM. Dupuit, Mery de Contades, Hougan, Roland, Mahyer, 20 avril 1850), pour rechercher les causes et les circonstances qui ont amené la chute du pont suspendu de la Basse-Chaîne". Annales des Ponts et Chaussées: 394–411.

Extract: *Soldiers stationed in the region frequently used the bridge, and two battalions of the same regiment had crossed earlier that day. The third battalion arrived during a powerful thunderstorm when the wind was making the bridge oscillate. When the soldiers began to cross, their bodies acted as sails, further catching the wind. Survivors reported that they had been walking as if drunk and could barely keep themselves from falling, first to one side and then to the other. As usual in crossing that bridge, the soldiers had been ordered to break step and to space themselves farther apart than normal. However, their efforts to match the swaying and keep their balance may have caused them to involuntarily march with the same cadence, contributing to the resonance. In any case, the oscillation increased. At a time when the bridge was covered with 483 soldiers and four other people (though the police had prevented many curiosity seekers from joining the march), the upstream anchoring cable on the right bank broke in its concrete mooring, three to four meters underground, with a noise like "a badly done volley from a firing squad". The adjacent downstream cable broke a second later, and the right-bank end of the deck fell, making the deck slope very steeply and throwing soldiers into the river. Many of those who fell were saved by their fellow soldiers who had not yet crossed and by residents of Angers who came to the rescue, but a total of 226 people died."*

Cable-supported bridges – Dynamic effects: Pedestrian-induced oscillations

- Pedestrian-induced oscillations are not unique to cable-supported bridges, but may occur in any lightweight structure.
- Such oscillations, including lateral oscillations, were studied intensely by Prof. Hugo Bachmann at ETH Zurich in the 1980s. In a book published by IABSE 1987 (see notes), he had recommended to avoid the following frequency ranges in footbridges (or carry out detailed vibration analyses):
  → vertical oscillations: 1.6…2.4 Hz and 3.5…4.5 Hz
  → lateral oscillations: 0.8…1.2 Hz and 1.6 …2.4 Hz
- Bachmann had also already investigated the effect of the number of people simultaneously crossing a bridge (excitation, added mass), and their potential synchronisation with movements.
- Despite this knowledge, the Millennium Bridge in London (Arup / Foster Partners / A. Caro) was built in 2000 with the first two lateral eigenfrequencies in the critical range around 1 Hz (sources see notes).
- The bridge had to be evacuated at the opening due to severe lateral oscillations. The “wobbly bridge” was then retrofitted with 37 viscous dampers and 52 tuned mass dampers (cost: ca. 5 million pounds).
- The designers launched a research programme to study this problem, that “had not yet been incorporated into the relevant bridge design codes” (see notes).

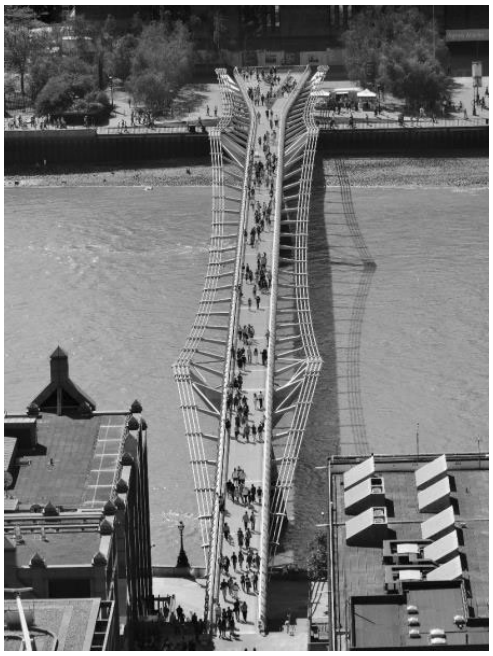

Millennium Bridge, London, Arup / Foster Partners / A. Caro, 2000. Footbridge, spans 81+144+108 m

Photo https://viel-unterwegs.de/ portrait Wikimedia Commons.

References:

H. Bachmann, W. Ammann, “Vibrations in Structures: Induced by Man and Machines. International Association for Bridge and Structural Engineering, Structural Engineering Documents, No. 3e, 1987.

Th. Wenk, “Brückenschwingungen: Einwirkung – Modellbildung – Dämpfung – Nachweise,“ SZS Brückenbautagung Stahl- und Stahlbetonverbundbau, 2016.

David E Newland: “Vibration of the London Millennium Footbridge: Part 1 – Cause,“ University of Cambridge, February 2003.

“An immediate research programme was launched by the bridge's engineering designers Ove Arup, supported by a number of universities and research organisations. It was found that some similar experiences had been recorded in the literature, although these were not well-known and had not yet been incorporated into the relevant bridge building codes. A German report in 1972 quoted by Bachmann and Ammann in their IABSE book (1987), described how a new steel footbridge had experienced strong lateral vibration during an opening ceremony with 300-400 people.”

Cable-supported bridges – Dynamic effects: Pedestrian-induced oscillations

- Current bridge design codes still primarily rely on frequency range recommendations similar to those of Bachmann, see e.g. SIA 260.
- Observing these recommendations, excessive oscillations due to pedestrian traffic are avoided, since the dominant eigenmodes of the bridge will have eigenfrequencies that differ sufficiently from the frequencies excited by pedestrians.
- These frequency ranges, particularly if higher natural frequencies are aimed at, are difficult to observe in footbridges (one might claim that any elegant footbridge is susceptible to oscillations).
- However, eigenfrequencies in the critical range need not necessarily cause problems, particularly if sufficient damping is provided – which is difficult to quantify in the design stage, though.
- Hence, as indicated in the figure (source see notes), if critical frequencies are present, it is recommended to
  - carry out dynamic analyses and (since damping is uncertain)
  - provide space for installing tuned mass dampers (Tilger) and/or viscous dampers in case oscillations should prove excessive
- For more details, see lecture *Structural Dynamics and Vibration Problems*

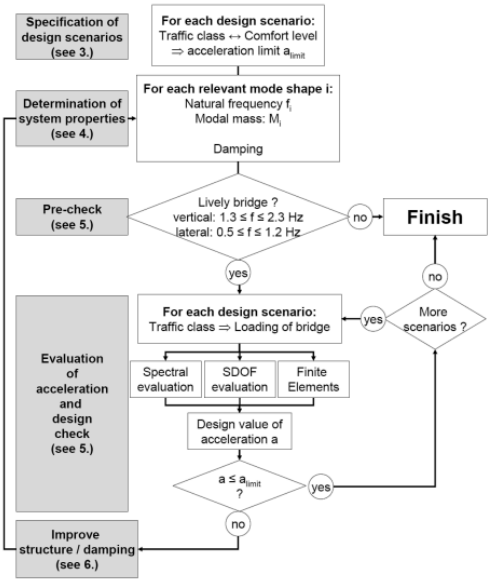

Diagram: Ch. Heinemeyer, “European design guide for footbridge vibration,” Proceedings, footbridge – Third International Conference, 2008,

Cable-supported bridges – Dynamic effects: Pedestrian-induced oscillations

- Current bridge design codes still primarily rely on frequency range recommendations similar to those of Bachmann, see e.g. SIA 260.
- Observing these recommendations, excessive oscillations due to pedestrian traffic are avoided, since the dominant eigenmodes of the bridge will have eigenfrequencies that differ sufficiently from the frequencies excited by pedestrians.
- These frequency ranges, particularly if higher natural frequencies are aimed at, are difficult to observe in footbridges (one might claim that any elegant footbridge is susceptible to oscillations).
- However, eigenfrequencies in the critical range need not necessarily cause problems, particularly if sufficient damping is provided – which is difficult to quantify in the design stage, though.
- Hence, as indicated in the figure (source see notes), if critical frequencies are present, it is recommended to
  - carry out dynamic analyses and (since damping is uncertain)
  - provide space for installing tuned mass dampers (Tilger) and/or viscous dampers in case oscillations should prove excessive
- For more details, see lecture *Structural Dynamics and Vibration Problems*

Birskopfsteg Basel (zpf Ingenieure, oscillations already anticipated in design → 2 tuned mass dampers provided)

Very slender and elegant footbridge (h/l = 1/73)

Vertical Eigenfrequencies critical (0.9/2.9/3.9 Hz)

→ tuned mass dampers planned from beginning (located inside the steel box girder):

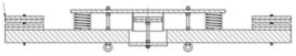

Birskopfsteg Basel, ZPF Ingenieure, 2014. Span 51+25 m, depth 0.70 m.

Photos: Th. Wenk, “Brückenschwingungen: Einwirkung – Modellbildung – Dämpfung – Nachweise,“ SZS Brückenbautagung Stahl- und Stahlbetonverbundbau, 2016.

Cable-supported bridges

Common aspects – Dynamic effects
Wind-induced oscillations

Cable-supported bridges – Dynamic effects: Wind-induced oscillations

Introduction

- As outlined in the section “Historical Perspective”, many early suspension bridges suffered from excessive oscillations also due to aerodynamic effects.
- The table on the right shows an overview of suspension bridges affected by wind-induced oscillation problems requiring stiffening measures in the best case, and leading to collapse in the worst.
- At the end of the 19th century, these problems were well known, due to the frequent problems with suspension bridges. John Roebling provided stays and stiff trusses in his suspension bridges (and retrofitted others) in order to prevent wind-induced oscillations.
- However, at the beginning of the 20th century, using the newly established deflection theory, the leading suspension bridge experts (Othmar Ammann, David Steinman, Leon Moisseiff, …) designed ever more slender suspension bridges.

Year	*Bridge*	*Span*	*Incident*
1818	Dryburgh Abbey Bridge	79	collapse
1821	Union Bridge	137	oscillations
1834	Lahnbrücke Nassau	75	collapse
1836	Brighton Chain Pier	78	collapse
1838	Montrose Bridge	131	collapse
1839	Menai Straits Bridge	176	partial failure
1852	Roche-Bernard Bridge	198	collapse
1854	Wheeling Bridge	310	collapse
1854	Queenston-Lewiston Bridge	259	collapse
1889	Niagra-Clifton Bridge	386	collapse
1895	Pont du Gottéron	151	partial failure
1937	Fyksesund Bridge	230	oscillations
1937	Golden Gate Bridge	1’280	oscillations
1938	Thousand Islands Bridge	240	oscillations
1939	Deer Isle Bridge Bridge	329	oscillations
1939	Bronx-Whitestone Bridge	701	oscillations?
1940	Tacoma Narrows Bridge	853	collapse

Cable-supported bridges – Dynamic effects: Wind-induced oscillations

Introduction

- Even before the Tacoma Narrows Bridge collapsed, severe wind-induced oscillations had been observed in several recently built, slender suspension bridges.
- Nonetheless, aerodynamic effects on bridges were only recognised and investigated in detail after the Tacoma Narrows Bridge collapse.
- Even if from today's perspective (see notes *), the mechanics of the failure were not fully understood at the time – aeroelasticity was a relatively new field of research even in aeronautics – the collapse marked a turning point in bridge design, particularly for cable-supported bridges:
  - → Aerodynamic effects, which had received little attention before, became a major concern in long-span bridge design on that very day.
  - → Today, wind tunnel testing for aerodynamic effects on long-span and/or slender bridges is common.

Top: Bronx-Whitestone Bridge, New York City, Othmar H. Ammann, 1939. Span 701 m, h/l = 1/210. Stays added and stiffened with additional trusses in 1947 (h/l = 1/91 after stiffening). In 2003, aerodynamic fibreglass fairings were installed and the trusses removed, recovering the initial slenderness. Photo © Wikimedia Commons.

Bottom: Deer Isle Bridge Bridge, Maine, U.S., David B. Steinman, 1939. Stiffening stays added before commissioning. Photo © Deer Isle Bridge historicbridges.org

(*) T. Abbas, I. Karakov, G. Morgenthal. Methods for flutter stability analysis of long-span bridges: a review. Bridge Engineering, Volume 170, 2017, Issue BE4, pp. 271-310

Cable-supported bridges – Dynamic effects: Wind-induced oscillations

Introduction

- Several slender suspension bridges from the 1930s were retrofitted after the Tacoma Narrows bridge collapse, based on the new knowledge. This and the next slides show a few examples.
- A lower deck bracing, forming a torsionally stiff truss girder, was installed in the Golden Gate Bridge (1937, span 1281 m), yet only in 1953. Comparing the slenderness with that of other bridges (particularly the Tacoma Narrows Bridge), an immediate stiffening indeed did not seem urgent:

Bridge	*width/span*	*depth/span*
Tacoma Narrows (collapsed)	1 / 72	1 / 350
Tacoma Narrows (rebuilt)	1 / 46	1 / 112
Golden Gate	1 / 47	1 / 168
George Washington, one deck	1 / 33	1 / 355
George Washington, two decks	1 / 33	1 / 120
Bronx-Whitestone	1 / 31	1 / 209

Golden Gate Bridge, San Francisco, Joseph B. Strauss, 1937. Span 1281 m, record span until h/l = 1/168, record span until 1964. A lower lateral deck bracing was added in 1953-54 after a storm shook it strongly in 1951. Photo © https://cdn.getyourguide.com/img/location_img-3624-230665892-148.jpg

Stiffening truss photos: https://www.goldengate.org/exhibits/resisting-the-twisting/

Cable-supported bridges – Dynamic effects: Wind-induced oscillations

Introduction

- The Bronx-Whitestone bridge (1939, span 701 m, right) was stiffened with stays and additional truss girders, reducing the slenderness to h/l = 1/91). In 2003, aerodynamic fairings were installed and the trusses removed, recovering the initial elegance.
- The the Fyksesund Bridge (1937, span 230 m, bottom), was stiffened by bottom stays in 1945.

Bronx-Whitestone Bridge, New York City, Othmar H. Ammann, 1939. Span 701 m, h/l = 1/210. Stays added and stiffened with additional trusses in 1947 (h/l = 1/91 after stiffening). In 2003, aerodynamic fibreglass fairings were installed and the trusses removed, recovering the initial slenderness.

Top right Photo © Wikimedia Commons, Bottom right Top photo: structurae.de

Fyksesund Bridge, Hardanger Fjord, Norway, Olaf Stang, 1937, span 230 m. Stiffened by bottom stays in 1945 (hardly visible). Photo: https://www.stamps.dk/

Bronx-Whitestone Bridge, information on MTA website: *After performing a series of experiments [after the Tacoma Bridge Collapse, kfm] on the bridge's design, Ammann concluded that additional measures to stiffen the Whitestone Bridge were unnecessary. Even so, the public was scared by the fact that. the two bridges were similar in design, and this led to a belief that the Whitestone Bridge might be unstable, as Moses later related. On both sides of the deck, 14-foot (4.3 m)-high steel trusses were installed to weigh down and stiffen the bridge in an effort to reduce oscillation. The stiffening project was completed in 1947. In 2003, the MTA restored the classic lines of the bridge by removing the stiffening trusses and installing fiberglass fairing along both sides of the road deck.[99][10] The lightweight fiberglass fairing is triangular in shape, giving it an aerodynamic profile that allows crosswinds to flow through the bridge rather than hit the trusses. The removal of the trusses and other changes to the decking reduced the bridge's weight by 6,000 tons, accounting for some 25% of the mass suspended by the cables, In addition, with the truss removals, the Bronx–Whitestone Bridge was able to withstand crosswinds of up to 150 miles per hour (240 km/h), whereas the trusses could resist crosswinds of no more than 50 miles per hour (80 km/h).*

Cable-supported bridges – Dynamic effects: Wind-induced oscillations

Wind velocities and dynamic pressure

- Design of structures against wind load is based on a reference wind speed. SIA 261 uses the peak velocity, including gusts of a few seconds, measured 10 m above ground on a free field, with a return period of 50 years. Other codes are based on different reference values, and calculation of wind loads must not be mixed.
- Due to the surface roughness, the design wind speed varies depending on the terrain conditions and increases with the height above ground z, reaching a limit value at z = 300…500 m).
- The dynamic pressure (Staudruck) q caused by a wind velocity u is:

$$q = \frac{\rho u^2}{2} \quad \left(\rho = \text{air density} \approx 1.2 \frac{\text{kg}}{\text{m}^3}\right)$$

- For static analyses, only $q(u)$ is needed. For dynamic analyses – e.g. buffeting – the wind speed needs to be decomposed into
  → a time-constant mean wind speed u of constant direction
  → a superimposed, time variable turbulence part with horizontal, transcerse and vertical components u_t v_t and w_t
- The turbulent components can be described in terms of turbulence intensity, integral length, and spectrum and are highly site-specific.

Characteristic values of dynamic pressure(SIA 261)

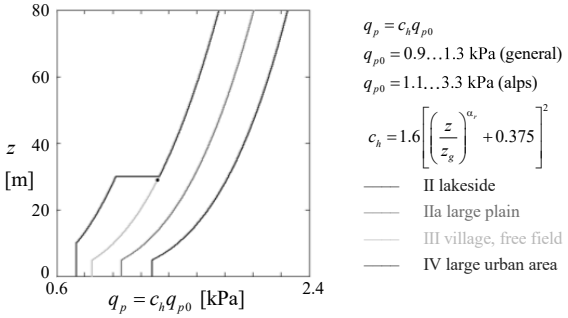

Exemplary wind spectrum (power spectral density)

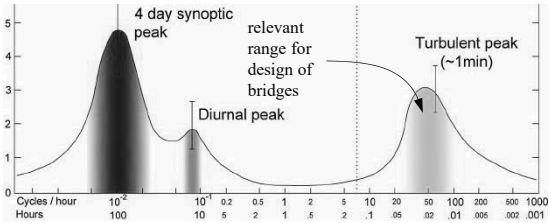

Source Wind spectrum: R.I. Harris, “The macro-meteorological spectrum—a preliminary study,” Journal of Wind Engineering and Industrial Aerodynamics 96 (2008) 2294–2307

Cable-supported bridges – Dynamic effects: Wind-induced oscillations

Aeroelasticity – Basic aspects

- Aerodynamic effects are relevant to tall, slender buildings and flexible long-span bridges.
- When studying these effects, the interaction of aerodynamic forces (→ fluid dynamics) with the static and dynamic response (→ structural mechanics) of the structure needs to be accounted for.
- This interaction is studied by aeroelasticity (Aeroelastik), a fundamental topic in aeronautical engineering.
- An in-depth treatment of aeroelasticity is beyond the scope of this lecture. In fact, even the most experienced designers of long-span bridges rely on specialised experts when designing for wind loads.
- However, some basic aspects are treated here to
  → facilitate a basic understanding and awareness of potential problems caused by aerodynamic effects
  → provide the common vocabulary required for communication with aerodynamic experts
  → provide a basis for further study of this subject

Humen Pearl River Bridge, Guangdong, China. 1997. Main span 888 m, designed for Typhoon winds (219 km/h characteristic wind speed).

Video: https://www.youtube.com/watch?v=VGjrZDNk_EQ (South China Morning Post, 5 May 2020; according to recent information, "*it is believed that the maintenance crews have altered the aerodynamic shape of the deck by erecting rows of temporary traffic barriers and have induced the deck oscillations at relatively low wind speed*").

Photo: Wikimedia Commons / hinnne

Further reading on aeroelasticity: Earl H. Dowell, A Modern Course in Aeroelasticity, Springer, 2015. https://doi.org/10.1007/978-3-319-09453-3 (digital full-text access via ETH Library)

Cable-supported bridges – Dynamic effects: Wind-induced oscillations

Aeroelasticity – Basic aspects

- Long-span bridge decks exposed to transverse wind can be analysed similarly to aircraft wings.
- This may be less obvious in the case of truss girders (bottom, Akashi-Kaikyo bridge cross-section), but is evident for streamlined modern bridge girders such as the deck of the Humber bridge (right).

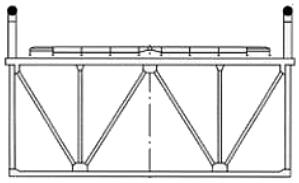

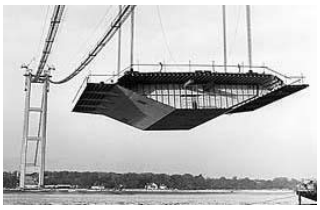

Humber Bridge, Kingston upon Hull, UK, Freeman, Fox & Partners (now Arcadis), 1981. Main span 1410 m.

Photos:

Top: https://upload.wikimedia.org/wikiped

Bottom: left http://www.engineering-timelines.com / right Thomas Vogel

Cable-supported bridges – Dynamic effects: Wind-induced oscillations

Aeroelasticity – Basic aspects

- Such streamlined girders (right: Third Bosporus Crossing) of modern long-span bridges indeed resemble airfoils (Tragflächen).
- Like the wings of an aircraft, bridge girders – as airfoils – may be damaged by torsional divergence and flutter, which are examined on the following slides.
- Further aerodynamic phenomena relevant to bridges, such as buffeting, vortex shedding and galloping are briefly outlined behind.
- Galloping is typical for bluff bodies (stumpfe Körper). Here, it has to be kept in mind that even streamlined bridge decks may become bluff by traffic on the bridge.
- Furthermore, other than in aircraft wings (where except in gliders, the air velocity is dominated by the cruise speed), wind on bridges is commonly turbulent and non-uniform in time and space.

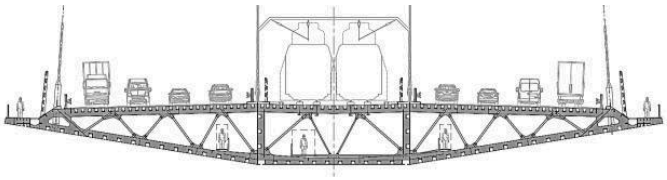

Third Bosporus Crossing (Yavuz-Sultan-Selim-Bridge), Istanbul, Jean-Francois Klein (T Ingénierie, Genf), 2016, l = 1408 m

Figures: Jean-Francois Klein, Michel Virlogeux, Thierry Delémont, Vincent de Ville de Goyet: “Third Bosporus bridge – a masterpiece of sculptural engineering,” Structural Concrete in Switzerland, fib Swiss National Group, 2018.

Cable-supported bridges – Dynamic effects: Wind-induced oscillations

Aeroelasticity – Basic aspects

- The air flowing about an airfoil exerts stresses on its surface, that are nearly perpendicular to the surface (pressure >> friction).
- Integration of the stresses yields the following aerodynamic forces (per unit length) acting on the airfoil of width *b* (“chord length”):

$f_D = c_D \cdot q \cdot b$ drag force (not referred to h as in structures)

$f_L = c_L \cdot q \cdot b$ lift force

$m_t = c_m \cdot q \cdot b^2$ aerodynamic moment (torque)

- Here, *q* is the dynamic pressure (Staudruck) corresponding to a turbulent airflow with uniform velocity *u*

$$q = \frac{\rho u^2}{2} \quad \left(\rho = \text{air density} \approx 1.2 \frac{\text{kg}}{\text{m}^3} \right)$$

and c_D, c_L and c_m are non-dimensional coefficients, depending on the angle of attack α, commonly determined from wind tunnel tests (see example in figure, for two different wing profiles).

- While aircraft wings are typically optimised to obtain high lift forces (resp. high lift/drag ratio), this is not desired in bridge girders.

Pressure (including friction) and resultant forces on an airfoil

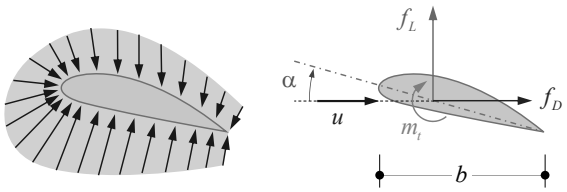

Lift and drag coefficients for standard wing profiles

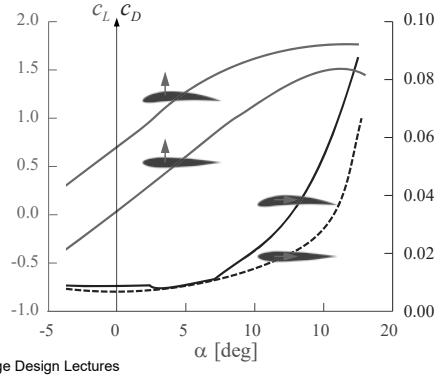

The lift and drag coefficients correspond to NACA standard profiles 0012 and 6412 and are found in various publications.

Photo: Wind tunnel testing of bridge girder section model at Norwegian Technical University NTNU. Photo by NTNU/Bartosz Siedziako.

Cable-supported bridges – Dynamic effects: Wind-induced oscillations

Typical section model

- For a basic understanding of the phenomena of torsional divergence and flutter, only the aerodynamic lift force f_L and the aerodynamic torque m_t need to be considered, and it is sufficient to consider the simplified system of a “typical section”:
  → flat plate rigid airfoil (width b) mounted on a stiff axis supported to the walls of a wind tunnel via springs representing the bending and torsional stiffness of the airfoil.
- The aerodynamic moment / torque (= coefficient c_m) depends on the position of the reference point. Commonly, the aerodynamic centre AC is chosen as reference (point about which the moment is independent of the angle of attack α) → $c_{m,AC}$ = constant.
- The total aerodynamic angle of attack α corresponds to an initial angle α_0 and the elastic twist of the axis α_e caused by the torque with respect to the shear centre. If the airfoil moves fast vertically (oscillation), α also depends on its velocity (relative velocity).
- With respect to the airfoil axis (shear centre) C, the resulting torque $m_{t,C}$ (all positive as shown in the figure) is

$$m_{t,C} = f_L \cdot e + m_{t,AC} = \left[c_L(\alpha) \cdot e + c_{m,AC} \right] \cdot b \cdot q$$

Typical section: Rigid, flat plate airfoil
(unit length section of an infinitely long wing)

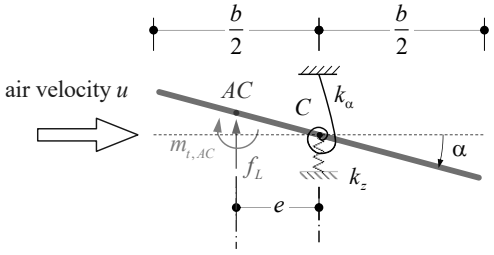

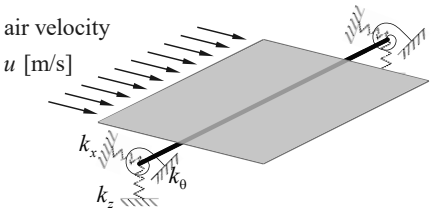

Photo: Wind tunnel testing of bridge girder section model at Norwegian Technical University NTNU. Photo by NTNU/Bartosz Siedziako.

Cable-supported bridges – Dynamic effects: Wind-induced oscillations

Torsional divergence

- For a flat plate in two-dimensional incompressible subsonic flow, the lift coefficient and the position of AC are:

  $$c_L = 2\pi \cdot \alpha \qquad e = \frac{b}{4}$$

  and the resulting torque is thus:

  $$m_{t,C} = \left(c_L \cdot e + c_{m,AC}\right) \cdot b \cdot q = \left(\pi\alpha b/2 + c_{m,AC}\right) \cdot b \cdot q$$

- This torque must be resisted by the torsional spring, i.e.

  $$m_{t,C} = \left(\pi\alpha b/2 + c_{m,AC}\right) \cdot b \cdot q \overset{!}{=} k_\alpha \cdot \alpha_e$$

- Observing that $\alpha = \alpha_0 + \alpha_e$ and solving for the elastic twist α_e one gets:

  $$\alpha_e = \frac{b \cdot q}{k_\alpha} \cdot \frac{\pi b \alpha_0/2 + c_{m,AC}}{1 - q\dfrac{\pi b^2}{2k_\alpha}}$$

- The elastic twist of the airfoil becomes infinite when the denominator is zero, i.e., for a dynamic pressure and corresponding wind speed

  $$q\frac{\pi b^2}{2k_\alpha} = 1 \;\rightarrow q = \frac{2k_\alpha}{\pi b^2} = \frac{\rho u^2}{2} \qquad \rightarrow u_D = \frac{2}{b}\sqrt{\frac{k_\alpha}{\pi\rho}}$$

Typical section: Rigid, flat plate airfoil
(unit length section of an infinitely long wing)

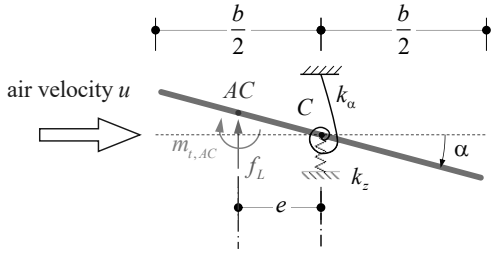

Wind tunnel test of a bridge section at NTNU

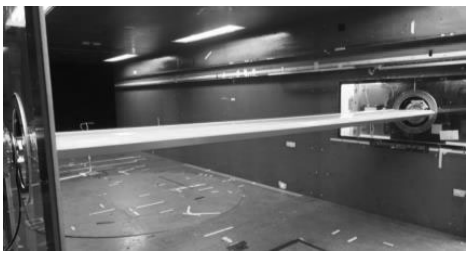

Photo: Wind tunnel testing of bridge girder section model at Norwegian Technical University NTNU. Photo by NTNU/Bartosz Siedziako.

Cable-supported bridges – Dynamic effects: Wind-induced oscillations

Torsional divergence

- Hence, at the wind speed u_D, the flat plate airfoil would fail in torsion. This phenomenon is referred to as torsional divergence.
- For a general airfoil, the lift coefficient c_L differs from $2\pi\alpha$ and is not linear in α (and the distance e varies with α). Hence, the theoretical value of u_D derived above – that can be determined without wind tunnel testing – is of little use in design.
- However, for small variations of α, it may be approximated by the first order Taylor series

  $$c_L = c_{L0} + \frac{\delta c_L}{\delta \alpha} \cdot \alpha$$

  which yields the applied torque

  $$m_{t,C} = c_{L0} \cdot b \cdot q \cdot e + \frac{\delta c_L}{\delta \alpha}(\alpha_0 + \alpha_e) \cdot b \cdot q \cdot e + c_{m,AC} \cdot b \cdot q \overset{!}{=} k_\alpha \cdot \alpha_e$$

  and the elastic twist and critical wind speed (obtained by setting the denominator in the first equation equal to zero)

  $$\alpha_e = \frac{b \cdot q}{k_\alpha} \cdot \frac{e\left(c_{L0} + \frac{\delta c_L}{\delta \alpha}\alpha_0\right) + c_{m,AC}}{1 - q \cdot \frac{\delta c_L}{\delta \alpha} \cdot \frac{be}{k_\alpha}} \quad \rightarrow u_D = \sqrt{\frac{2k_\alpha}{\frac{\delta c_L}{\delta \alpha} \cdot \rho be}}$$

Typical section: Rigid, flat plate airfoil
(unit length section of an infinitely long wing)

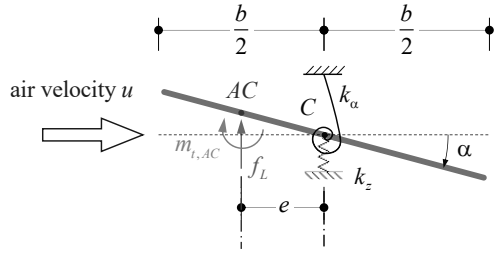

Wind tunnel test of a bridge section at NTNU

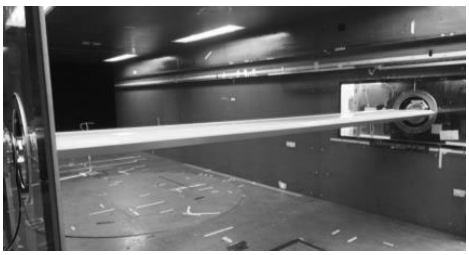

Cable-supported bridges – Dynamic effects: Wind-induced oscillations

Torsional divergence

- The distance e cannot directly be obtained from wind tunnel tests, since the coefficient $c_{m,AC}$ is unknown.
- In bridge aeroelasticity, the total aerodynamic moment coefficient c_t referred to the bridge axis (combining the above values and determined from wind tunnel tests) is thus commonly used

$$m_{t,C} = qb^2 c_t(\alpha) = \frac{\rho u^2}{2} b^2 c_t(\alpha)$$

- Using again the first-order Taylor series, and setting the denominator of the resulting equation for the elastic twist equal to zero, one gets the critical wind speed u_d for torsional divergence

$$m_{t,C} = \frac{\rho u^2}{2} b^2 \left(c_{t0} + \alpha \frac{\delta c_t}{\delta \alpha} \right) = k_\alpha \cdot \alpha_e$$

$$\rightarrow \alpha_e = \frac{\rho u^2}{2} \frac{b^2}{k_\alpha} \frac{c_{t0} + \alpha_0 \frac{\delta c_t}{\delta \alpha}}{1 - \frac{\rho u^2}{2} \frac{b^2}{k_\alpha} \frac{\delta c_t}{\delta \alpha}} \rightarrow u_D = \sqrt{\frac{2k_\alpha}{\rho b^2 \frac{\delta c_t}{\delta \alpha}}}$$

- Using plots of the coefficient c_t (and its derivative) determined from wind tunnel tests, the critical wind speed u_D can be determined.

Exemplary aerodynamic moment coefficient and derivative (including traffic effect [Pospisil et al., see notes])

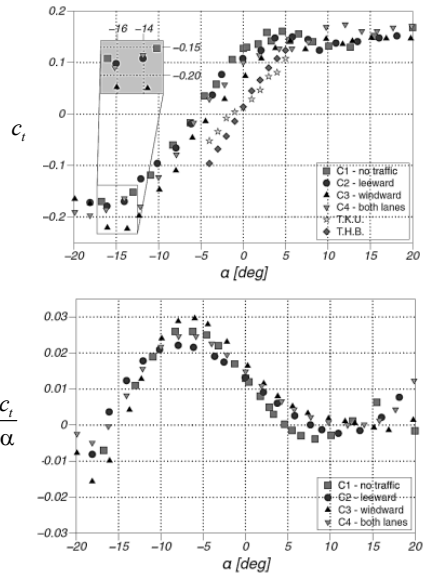

S. Pospíšil, A. Buljac, H. Kozmar, S. Kuznetsov,M. Machácek, R. Král, “Influence of Stationary Vehicles on Bridge Aerodynamic and Aeroelastic Coefficients,” ASCE Journal of Bridge Engineering, 2016.

Cable-supported bridges – Dynamic effects: Wind-induced oscillations

Coupled flutter

- Torsional divergence is usually not critical in bridges. However, the critical wind speed for torsional divergence u_D is useful for the analysis of coupled flutter as well.
- Coupled flutter, a divergent aeroelastic instability phenomenon occurring at the flutter velocity $u_f < u_D$, has the following characteristics:
  - simultaneous vertical and torsional harmonic oscillation
  - coupling of vertical and torsional oscillations due to nearly coinciding eigenfrequencies f_v and f_t
  - energy accumulation and, eventually, collapse
- The phenomenon of flutter is known in bridge engineering since the prominent Tacoma Narrows Bridge collapse by torsional flutter in 1940 (see section *historical perspective*).

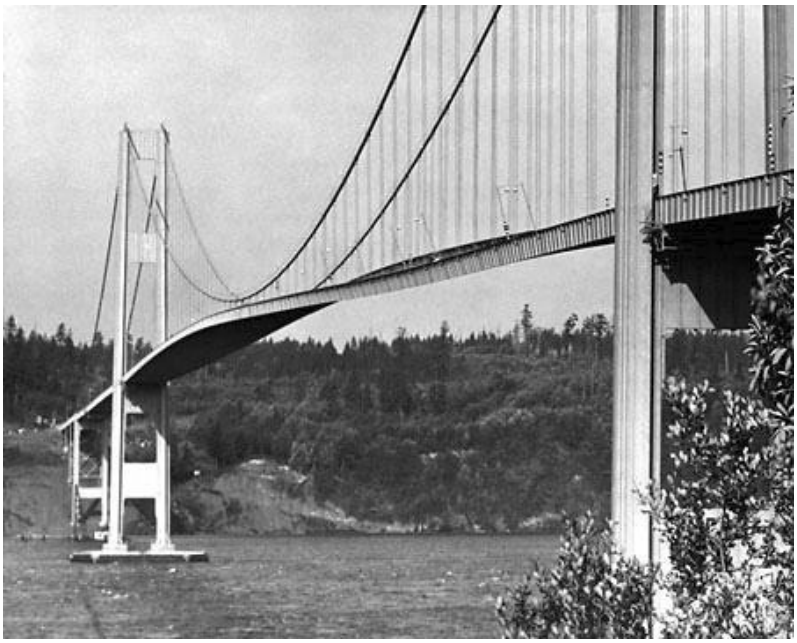

Tacoma Narrows Bridge, Puget Sound, Washington state, Leon Moisseiff, 1940. Span 853 m. Collapsed on 7.11.1940.

Photo: Farquharson (Ed.), Aerodynamic stability of suspension bridges with special reference to the Tacoma Narrows Bridge; a report of an investigation, University of Washington, Structural Research Laboratory, Report No. 116, 1949-1954.

Cable-supported bridges – Dynamic effects: Wind-induced oscillations

Coupled flutter

- Other than torsional or vertical flutter, coupled flutter (also referred to as “classic flutter”) can be understood – in a simplified manner – by considering the energy balance of a bridge deck subjected to simultaneous vertical and torsional oscillations with equal frequency (figures).
- Energy is fed into the system when the signs of
  - vertical velocity and lift force
  - angular velocity and torque

  coincide; for opposite signs, energy is extracted.
- For a phase shift of $\pi/2$ (upper figure):
  - the work done by the aerodynamic torque cancels out
  - the work done by the lift force is always positive

  $\rightarrow$ energy is accumulated in every cycle

  $\rightarrow$ amplitude of oscillations increases correspondingly

  $\rightarrow$ flutter instability
- Without a phase shift, the work done by lift force as well as torque cancel out (lower figures) $\rightarrow$ no instability

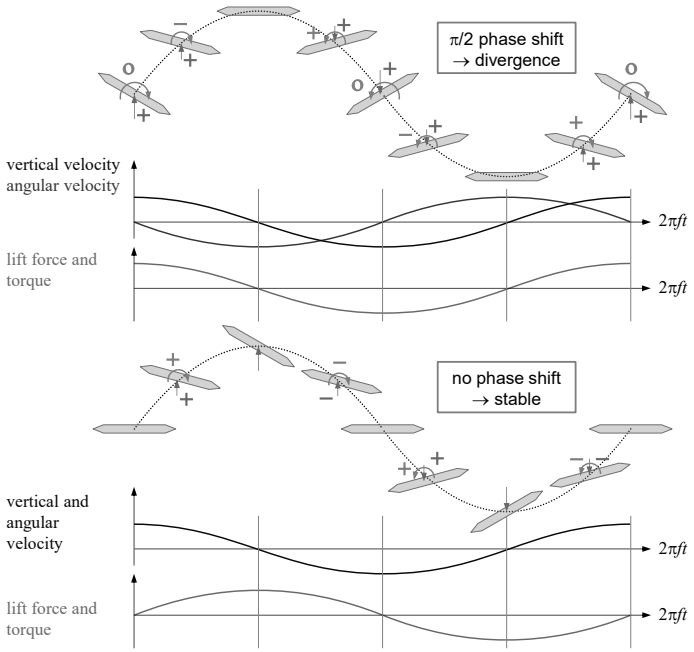

Cable-supported bridges – Dynamic effects: Wind-induced oscillations

Coupled flutter

- The torsional eigenfrequency f_t of cable-supported bridges with two cable planes is commonly larger than their vertical eigenfrequency f_v (see figure; for A-shaped pylons with inclined cable planes, the torsional frequency is even higher).
- However, the equivalent torsional stiffness, and hence f_t, is reduced by the aerostatic pressure, which increases with air velocity.
- For a flat plate airfoil, this leads to the flutter velocity

$$u_f = u_D \sqrt{1 - \frac{f_v^2}{f_t^2}} \leq u_D$$

where u_d = is critical wind speed for torsional divergence.

- The above equation is strongly simplified and neglects the dynamic nature of wind loads. A better approximation is given by Selberg's semi-empirical equation:

$$u_f = 0.52 u_D \sqrt{\left(1 - \frac{f_v^2}{f_t^2}\right) \cdot b \cdot \sqrt{\frac{m}{I_m}}} \leq u_D$$

where m is the mass of the girder per unit length and I_m is the corresponding mass moment of inertia (see figure).

Ratios of vertical and torsional eigenfrequencies for Bridges with two cable planes at their edges

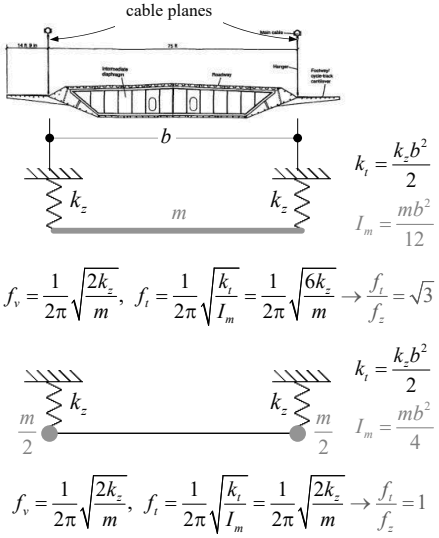

Source of flutter velocity formulas, and recommended reading: Niels J. Gimsing, Christos T. Georgakis. Cable Supported Bridges – Concept and Design, Wiley, 1983 (3rd edition, 2012).

Cable-supported bridges – Dynamic effects: Wind-induced oscillations

Coupled flutter

- Selberg's simple equation is useful for first estimations of the flutter velocity as long as $f_t/f_v > 1.5$. As illustrated in the figure, the approximation is much better for the streamlined girder ("airfoil") than the bluff variants.
- A more realistic semi-empirical approximation of the critical flutter velocity of a bridge girder, originally proposed by Scanlan and Tomko (see notes for sources) is possible based on the formulation of the equations of motion of a two-dimensional section of a symmetrical bridge deck with linear viscous damping and restoring forces:

$$m\ddot{h} + d_h\dot{h} + k_h h = L_h$$
$$I_m\ddot{\alpha} + d_\alpha\dot{\alpha} + k_\alpha\alpha = M_\alpha$$
$$m\ddot{p} + d_p\dot{p} + k_p p = D_p$$

- In the above equations, "*d*" is been used for the viscous damping coefficients and *k* for the stiffnesses, to distinguish from aerodynamic coefficients. For the remaining notation (common in aeroelastic analysis of bridges), see figure.
-

Comparison of critical wind speed determined in wind tunnel tests and flutter velocity according to Selberg
[variants for Lillebaelt bridge, taken from Gimsing 2012)

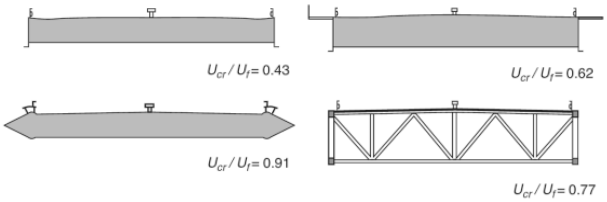

Two-dimensional bridge deck section – notation

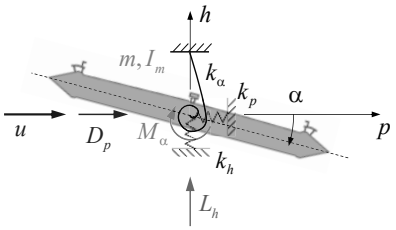

Source: Earl H. Dowell, A Modern Course in Aeroelasticity, Springer, 2015.
https://doi.org/10.1007/978-3-319-09453-3 (digital full-text access via ETH Library)

Cable-supported bridges – Dynamic effects: Wind-induced oscillations

Coupled flutter

- The aeroelastic forces can be determined using flutter derivatives, i.e., velocity-dependent force coefficients H^*_i, A^*_i and P^*_i (= relative changes of system damping and stiffness with regard to the wind speed variation) (terms in grey = lateral motions often neglected)

$$\begin{Bmatrix} L_h \\ M_\alpha \\ D_p \end{Bmatrix} = \frac{\rho u^2 b}{2} \begin{bmatrix} \lambda_R H_1^* & \lambda_R H_2^* & \lambda_R^2 H_3^* & \lambda_R^2 H_4^* & \lambda_R H_5^* & \lambda_R^2 H_6^* \\ \lambda_R A_1^* & \lambda_R A_2^* & \lambda_R^2 A_3^* & \lambda_R^2 A_4^* & \lambda_R A_5^* & \lambda_R^2 A_6^* \\ \lambda_R P_1^* & \lambda_R P_2^* & \lambda_R^2 P_3^* & \lambda_R^2 P_4^* & \lambda_R P_5^* & \lambda_R^2 P_6^* \end{bmatrix} \cdot \begin{Bmatrix} \dot{h}/u \\ b\dot{\alpha}/u \\ \alpha \\ h/b \\ \dot{p}/u \\ p/b \end{Bmatrix}$$

with the so-called reduced frequency $\lambda_R = \frac{2\pi f b}{u} = \frac{\omega b}{u}$

- Based on plots of the flutter derivatives as functions of λ_R, obtained from wind tunnel tests, the flutter equations are obtained as follows:
  - assume that h, α and p are proportional to $e^{i\omega t}$ (harmonic oscillations)
  - insert expressions for h, α and p in equation of motion (previous slide) and set the determinant of the amplitudes of h, α and p to zero

  → for each value of λ_R a complex equation in ω is obtained

  → the lowest (nearly) real solution λ_{Rc} yields the flutter velocity: $\lambda_{Rc} = \frac{\omega_c b}{u} \rightarrow u_f = \frac{\omega_c b}{\lambda_{Rc}}$

Flutter derivatives of Kao-Ping Hsi bridge [Náprstek 2015]

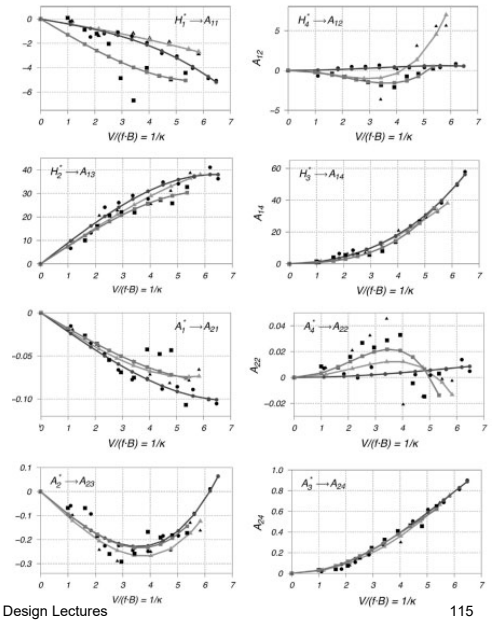

Note that the flutter derivatives have to be obtained from wind tunnel tests, using measurements performed on the oscillating, rather than the fixed body (i.e., scale model of bridge section).

Sources:

Earl H. Dowell, A Modern Course in Aeroelasticity, Springer, 2015. https://doi.org/10.1007/978-3-319-09453-3 (details on aeroelasticity in civil engineering in Chapter 6.1; digital full-text access via ETH Library)

T. Theodorsen, General theory of aerodynamic instability and the mechanism of flutter, NACA Report 496, 1965 (showing that for small oscillations the expressions for L_h and M_α are linear in h and α and their first and second derivatives).

Figure: J. Náprstek, S.Pospíšil, J.-D. Yau: “Stability of two-degrees-of-freedom aero-elastic models with frequency and time variable parametric self-induced forces,” Journal of Fluids and Structures 57 (2015) 91–107

Cable-supported bridges – Dynamic effects: Wind-induced oscillations

Flutter derivatives ↔ Potential aeroelastic problems

- The flutter derivatives are also helpful to detect other potential aerodynamic problems, e.g. single mode flutter or oscillations caused e.g. by buffeting or vortex shedding.
- Here, the sign of the flutter derivatives associated with the velocity-proportional aeroelastic forces ($\dot{h}$, $\dot{\alpha}$) is particularly relevant, as a positive sign is equivalent to negative viscous damping = excitation:
  - $H_1^* > 0$ → susceptible to vertical oscillations ($\dot{h}$) (vertical flutter / “bending type galloping”)
  - $A_2^* > 0$ → susceptible to torsional oscillations ($\dot{\alpha}$) (torsional flutter / “torsional galloping” → Tacoma Narrows collapse)
  - $H_2^* > 0$ and $A_1^* > 0$ → coupling of $\dot{\alpha}$ and $\dot{h}$, → danger of coupled flutter
- Realistic analysis of aerodynamic effects is complex and involves wind tunnel testing
  → beyond “daily business” even for experienced designers
  → consultation with experts common

Equations of motion and flutter (neglecting lateral components) and flutter derivative A_2^* for different bridge sections [Gimsing 2012]

$$\begin{Bmatrix} L_h = m\ddot{h} + d_h\dot{h} + k_h h \\ M_\alpha = I_m\ddot{\alpha} + d_\alpha\dot{\alpha} + k_\alpha\alpha \end{Bmatrix} = \frac{\rho u^2 b}{2} \begin{Bmatrix} \lambda_R H_1^* & \lambda_R H_2^* & \lambda_R^2 H_3^* & \lambda_R^2 H_4^* \\ \lambda_R A_1^* & \lambda_R A_2^* & \lambda_R^2 A_3^* & \lambda_R^2 A_4^* \end{Bmatrix} \begin{Bmatrix} \dot{h}/u \\ b\dot{\alpha}/u \\ \alpha \\ h/b \end{Bmatrix}$$

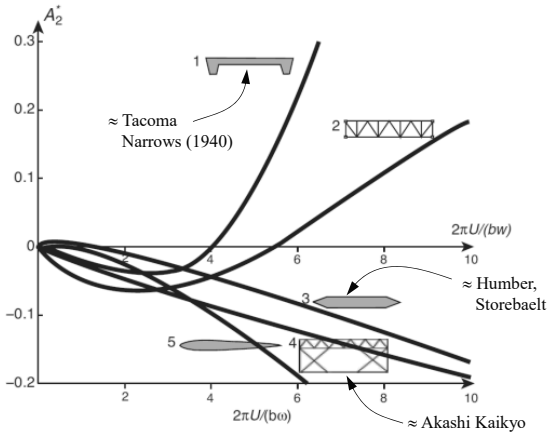

The terms “bending type galloping” and “torsional galloping” are older, but still used (e.g. by Svensson, Cable-Stayed Bridges, 40 years of experience worldwide).

Cable-supported bridges – Dynamic effects: Wind-induced oscillations

Use of flutter derivatives for aeroelastic phenomena

- Even if aerodynamic stability is satisfied – i.e., the critical velocities for flutter and torsional divergence are higher than the design wind speed – large wind-induced oscillations may not be excluded.
- The most relevant phenomena potentially causing large, albeit self-limiting oscillations are
  - buffeting
  - vortex-shedding
  - galloping
- While galloping mainly affects cables, buffeting and vortex shedding also cause oscillations of the bridge girder. As seen in the upper figure, these mechanisms occur at lower wind velocities than coupled flutter.
- All these phenomena are fairly complex and can only be approximated analytically or numerically (computational fluid dynamics), requiring wind tunnel tests in general. They will only be briefly outlined in the following. As with flutter, consulting with wind experts is recommended.

Schematic response of a slender structure under wind (adapted from [Gimsing 2012])

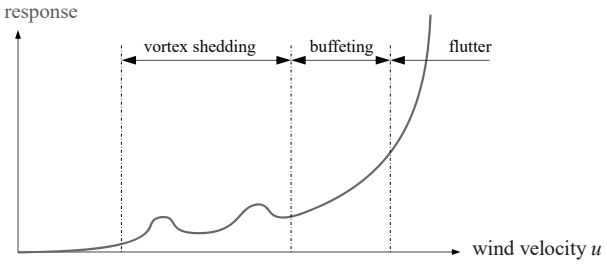

Vortex-induced oscillations on the Storebælt bridge before mounting of guide vanes [Gimsing 2012]

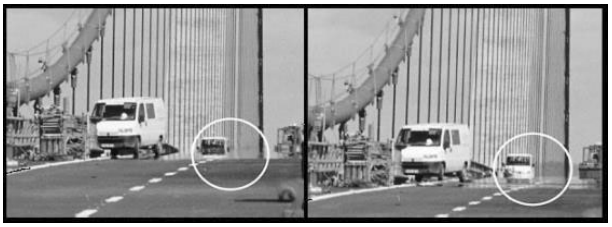

Source: Niels J. Gimsing, Christos T. Georgakis. Cable Supported Bridges – Concept and Design, Wiley, 1983 (3rd edition, 2012).

Cable-supported bridges – Dynamic effects: Wind-induced oscillations

Buffeting

- Buffeting is the forced, random vibrational response of a structure to random, turbulent wind. Turbulence can be due to topographical or structural obstructions or the bridge itself, the latter having minor importance.
- Using the horizontal and vertical turbulent wind components u_t and w_t (see *wind velocities and dynamic pressure* slide), normalised with respect to the mean wind velocity u), the buffeting forces may be expressed as

$$\begin{Bmatrix} L_{h,b} \\ M_{\alpha,b} \\ D_{p,b} \end{Bmatrix} = \frac{\rho u^2 b}{2} \begin{bmatrix} c_L & \frac{\partial c_L}{\partial \alpha} + c_D \\ c_t b & \frac{\partial c_t}{\partial \alpha} b \\ c_D & \frac{\partial c_D}{\partial \alpha} \end{bmatrix} \cdot \begin{Bmatrix} \frac{u_t}{u} \\ \frac{w_t}{u} \end{Bmatrix} \qquad \left(\frac{w_t}{u} = \tan\alpha \cdot \frac{u_t}{u} \approx \alpha \cdot \frac{u_t}{u} \right)$$

- These forces are inserted in the equations of motion of a two-dimensional section (see coupled flutter) to obtain the peak response of the structure
- The structure is then designed for the forces corresponding to the peak response (using e.g. RMS combinations of the modes).

Turbulent wind forces on bridge deck

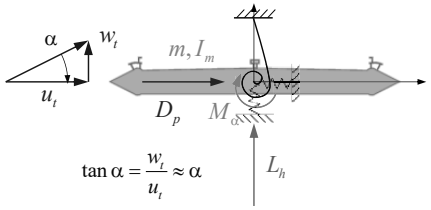

Exemplary wind spectrum (power spectral density)

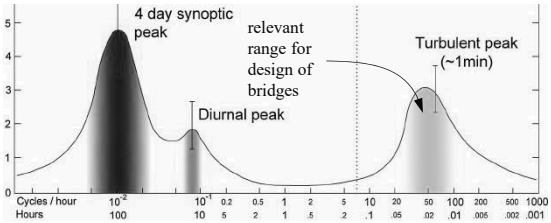

Source: W.F. Chen and L. Duan (Ed.). Bridge Engineering Handbook. Second Edition, Five Volume Set, CRC Press / Taylor and Francis, 2014 (digital full-text access via ETH Library).

Cable-supported bridges – Dynamic effects: Wind-induced oscillations

Vortex shedding

- When air flows past a bluff (= not streamlined) body, vortices are created depending on the size and shape of the body, causing vibrations of slender bodies as observed by Strouhal in 1878. The Aeolian harp (Windharfe) makes acoustic use of this phenomenon.
- The shedding of vortices in the wake of circular cylinders was studied by Bénard and also studied by von Kármán, after whom the orderly array of vortices in the wake of a cylinder has been named (von Kármán street).
- For long prismatic bodies with a transverse dimension Ø (cable diameter, girder depth), the vortex shedding frequency is

$$f_s = S_r \cdot \frac{u}{Ø}$$

  where S_r = Strouhal number.
- Generally, the Strouhal number depends on the Reynolds number, but for long cylinders, $S_r \approx 0.21$ may be used. For bridge decks, it varies greatly; according to [Gimsing 2012], $S_r \approx 0.21$ was measured for Storebælt Bridge.

Shedding of vortices in the wake of a cylinder
(animation: C. de la Rosa Siqueira)

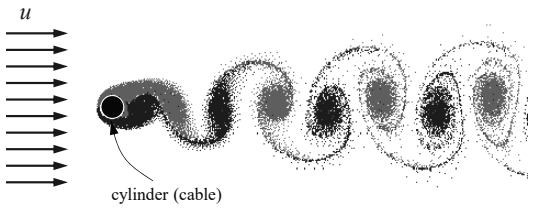

Instantaneous vorticity magnitude field of a twin deck
(CFD analysis of Stonecutters bridge, effect of guide vanes)

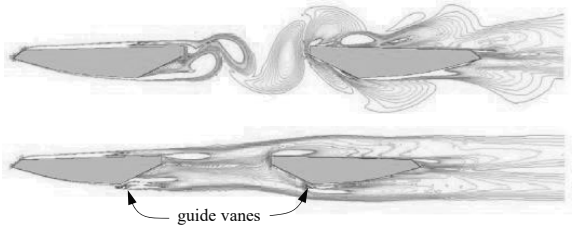

Vortex shedding GIF: Wikimedia commons, Cesareo de La Rosa Siqueira

CFD analysis: F. Nietoa, I. Kusanoa, S. Hernándeza, J.Á. Juradoa, “CFD analysis of the vortex-shedding response of a twin-box deck cable-stayed bridge,” The Fifth International Symposium on Computational Wind Engineering (CWE2010), Chapel Hill, North Carolina, USA May 23-27, 2010

Cable-supported bridges – Dynamic effects: Wind-induced oscillations

Vortex shedding

- Large oscillations may occur in case of resonance, i.e., if the vortex shedding frequency coincides with a the frequency of a dominant eigenmode of the bridge cylinder f_i . Hence, the critical velocity is

$$u_{cr} = \frac{f_i \cdot Ø}{S}$$

- Even if the critical vortex-shedding velocity u_{cr} is reached, large oscillations only occur if all following conditions are met:
  - low structural damping
  - laminar wind flow with low turbulence intensity, nearly perpendicular to the girder axis (ca. ±20°)
  - u_{cr} high enough to excite bridge, but not too high such that narrowing of the wake disrupts the creation of vortices.
- Hence, only few cable supported bridges have exhibited excessive vortex-shedding oscillations though u_{cr} is often exceeded.
- The Storebælt Bridge experienced significant vortex-induced oscillations (photo on previous slide) before guide vanes were installed. As potential problems had been detected in the wind tunnel tests, provisions had been made in design to fit these elements to the bottom corners of the deck (figure and photo).

Guide vanes preventing vortex-induced oscillations on the Storebælt bridge [Gimsing 2012]

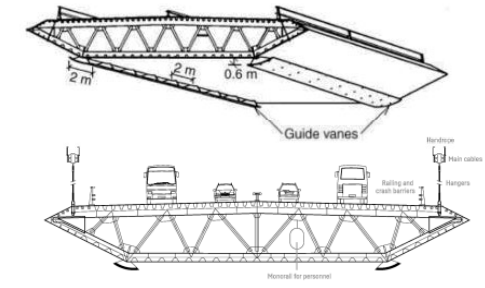

Top Illustration: Niels J. Gimsing, Christos T. Georgakis. Cable Supported Bridges – Concept and Design, Wiley, 1983 (3rd edition, 2012).

Bottom illustration and photo: The link across Storebælt - Two bridges and a tunnel. Sund & Bælt Holding A/S, 2017.

Cable-supported bridges – Dynamic effects: Wind-induced oscillations

Galloping

- Generally, two types of galloping are known: Wake galloping and across-wind galloping. The former refers to oscillations of a downstream body cylinder induced by the wake flow of an upstream cylinder. It is rarely relevant in bridges and therefore not further considered here.
- Across-wind galloping, simply referred to as galloping in the following, is a large amplitude oscillation in a plane normal to the wind flow velocity, by slender structures with bluff cross-section, such as ice-laden cables or – rarely – bridge decks (e.g. when loaded with traffic).
- The static lift and drag coefficients (c_L, c_D) as functions of the angle of attack α are sufficient for a satisfactory analytical description of galloping, but the variation of the angle of attack with the movement of the body (figure) needs to be accounted for. The equation of motion is thus

$$m\ddot{y} + d\dot{y} + ky = -\frac{\rho u^2 b}{2}\left(\frac{\partial c_L}{\partial \alpha} + c_D\right)\Bigg|_{\alpha=0} \cdot \frac{\dot{h}}{u} \qquad \left(\frac{\dot{h}}{u} = -\tan\alpha \approx -\alpha\right)$$

- The structure tends to instability if the total damping is negative:

$$d + \frac{\rho u b}{2}\left(\frac{\partial c_L}{\partial \alpha} + c_D\right)\Bigg|_{\alpha=0} \le 0 \qquad \rightarrow \left(\frac{\partial c_L}{\partial \alpha} + c_D\right)\Bigg|_{\alpha=0} \le 0$$

No movement ($\dot{h} = 0$)

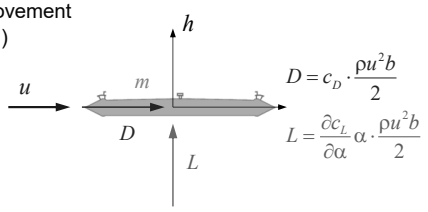

Relative velocity and forces:

Upward movement ($\dot{h} > 0$)

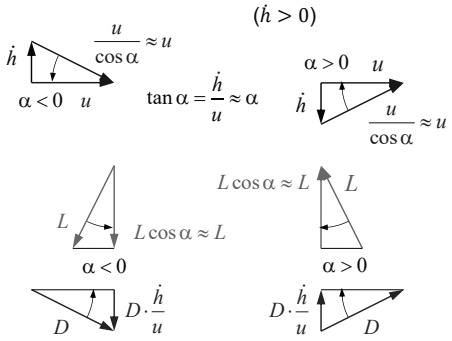

Downward movement ($\dot{h} > 0$)

Source: W.F. Chen and L. Duan (Ed.). Bridge Engineering Handbook. Second Edition, Five Volume Set, CRC Press / Taylor and Francis, 2014 (digital full-text access via ETH Library).

Cable-supported bridges – Dynamic effects: Wind-induced oscillations

Cable vibrations

- Main cables of suspension bridges are rarely suffering from large vibrations. They may e.g. be excited by oscillations of their ends (Pylon tops).
- Hangers and stay cables are more frequently affected by vibrations. These may be caused by vortex shedding or galloping, where the latter is more frequent.
- While dry galopping may also occur, rain-wind induced vibrations of stay cables are the most frequent problem. The exact mechanism is still not well understood, but it appears that the creation of water rivulets along a significant length of a cable causes an apparent modification in cable shape, leading to the initiation of galloping (video)
- Cable vibrations may cause discomfort with users, and ultimately lead to fatigue failure of a stay cable or components of the cable. Mitigation can be classified as follows:
  - aerodynamic control (surface modification e.g. to avoid rivulets)
  - structural control (modify mass or stiffness)
  - mechanical control (e.g. viscous dampers, see video)

Cross-section of stay cable with upper water rivulet

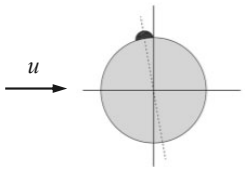

Indented HDPE stay tube (Stonecutters bridge)

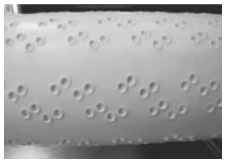

Rain-wind induced vibrations of stay cables (Franjo Tuđman Bridge, Dubrovnik)

Top: Illustrations from Gimsing (2012)

Bottom: Franjo Tuđman Bridge, Dubrovnik, 2002. Span 304.5 m. Photo Wikimedia Commons, Video: Rain-wind induced vibrations and damper installation, , source https://www.youtube.com/watch?v=SsfQN1ilcGU